The Chaffey Dam Story

Final report for CRCFE projects B.202 and B.203

Edited by Bradford Sherman, CSIRO Land & Water

Contributing authors:

Bradford Sherman	CSIRO Land and Water
Phillip Ford	CSIRO Land and Water
Pat Hatton	CSIRO Land and Water
JohnWhittington	CRCFE
Damian Green	CRCFE
Darren Baldwin	MDFRC
Rod Oliver	MDFRC
Russ Shiel	MDFRC
Jason van Berkel	Water Studies Centre, Monash University
Ron Beckett	Water Studies Centre, Monash University
Leigh Grey	University of Canberra
Bill Maher	University of Canberra

Preface

The CRC for Freshwater Ecology's Chaffey Dam Project is perhaps the most thorough interdisciplinary study of reservoir ecology yet undertaken in Australia. From the outset we have striven to integrate physics, chemistry and biology to understand the interrelationships that lead to the formation of algal blooms, especially of blue-green algae. This meant identifying and quantifying the supply of nutrients, the processes that transport them through the reservoir and the conditions that lead to their transformation into algae. Throughout the project, the emphasis has been on developing a quantitative understanding of the important processes.

To accomplish the project's goals required a program of continuous intensive monitoring that could not have been undertaken by the project scientists alone. The project owes much of its success to the support of the local community, especially the Chaffey Dam Advisory Committee (CDAC), the Department of Land and Water Conservation (DLWC), and the Tamworth Environmental Laboratory (TEL). We would especially like to thank Ian Dowling, Nick Burr, Greg Walker, Bruce Hindmarsh, Brian Parsons and Andrew Brissett (DLWC), Alan Sinclair and the members of CDAC, Dan O'Connor and the staff at TEL, and the Scofield's at the Peel Inn (our home away from home for two years). In addition, I would like to thank Steve McCord and Prof. Geoff Schladow from the University of California, Davis, for their support with regards to water quality modelling. It's been a pleasure and a privilege to work with all of you.

1 Executive Summary

Despite a significant research effort into understanding the physics of artificial reservoir destratification both overseas and in Australia, little work has been done regarding chemical and biological measures of the effectiveness of destratification. Historically, destratification systems have been designed to reduce the temperature difference between the top and bottom of the water column without specific consideration of their chemical or biological effects. Designers have implicitly assumed that a reduction in the temperature change would lead to complete mixing of the water column. This mixing commonly is assumed to produce a deeper surface mixed layer (SML) in the reservoir, and to increase dissolved oxygen concentrations in the deeper waters. Increased dissolved oxygen concentrations lead to decreased concentrations of soluble iron and manganese and decrease the release of nutrients from the sediment. However, close inspection of field data offered as proof of successful destratification (i.e. approximately uniform temperature in the vertical) invariably reveals a remnant temperature stratification near the water surface.

Artificial destratification may control blue-green algal blooms in two ways. By deepening the surface mixed layer, it reduces the amount of light available to an algal cell and hence its rate of photosynthesis. The dominant bloom-forming algal species in Chaffey Reservoir (discussed in Chapter 9), *Anabaena* and *Ceratium*, do not grow well under well-mixed, i.e. lower light, conditions and so a deeper SML may exert a selective pressure that favours other species. By reducing the amount of dissolved nutrients, especially phosphorus, in the water column, destratification can reduce the amount of algae that can exist in the reservoir. As all types of algae require phosphorus to grow, a reduction in reservoir phosphorus content will reduce the total amount of all types of algae within the reservoir without necessarily changing the distribution of algal species.

The Destratification and Water Quality project addressed several significant knowledge gaps regarding the chemical and biological responses of a reservoir, Chaffey Dam near Tamworth, NSW, as it underwent artificial destratification. Specifically, we sought to understand:

- which processes limit the supply of oxygen to the hypolimnion and sediments
- how phytoplankton respond physiologically to sudden changes in the ambient light and nutrient environments
- how sediment nutrient releases are linked to changes in the temperature and oxygen concentration at the sediment-water interface
- how phosphorus is transformed between different size fractions and chemical species
- the impact of dessication, arising from large changes in reservoir level, on sediment nutrient dynamics

- the quantities of nutrient supplied to the reservoir from internal (sediment) and external (catchment) sources

Routine field sampling took place from September 1995 to June 1997. This sampling program supplemented the existing monitoring performed by the NSW DLWC. Ten intensive field experiments of 7-10 days duration were undertaken to examine short-term effects of artificial destratification. In addition, DLWC provided its entire historical water quality database for the reservoir and catchment so that data collected by the project could be placed in a historical context.

Significant findings -

The 100 L s^{-1} destratification system at Chaffey Dam was operated on five occassions between February 1995 and April 1997. Each period was of 4 – 5 weeks duration except April 1997 when the system was turned off after 10 days because of extreme oxygen depletion near the surface of the reservoir.

The destratifier did not cause complete mixing of the water column at any time, even when the reservoir was at 20% of capacity nor did it produce a deeper surface mixing layer (SML). Despite producing a weaker temperature gradient, there was insufficient mixing energy input at the water surface via surface heat losses and wind stirring to deepen the surface layer (Section 7.2). Microstructure temperature profiles showed that temperature changes as small as 0.05 °C were sufficient to prevent downwards transport of buoyant blue-green algae.

After 14 days of compressor operation the vertical temperature distribution reached a quasi-equilibrium state after which continued operation provided little or no further reduction in the temperature change across the water column. A quasi-equilibrium oxygen distribution was established typically after 3 weeks of operation. The quasi-equilibrium condition took the form of nearly linear temperature and oxygen gradients and represented a balance between sources of heat and oxygen near the surface of the reservoir, downward transport due to large-scale destratification-induced circulation, and, in the case of oxygen, *in situ* consumption throughout the water column.

Theoretical design considerations indicate that a 5-fold increase in airflow rate (and number of plumes) would be able to destratify a full reservoir with a 16 °C temperature difference in about three weeks. However, numerical modelling results using meteorological data from the reservoir required an airflow rate of up to 1800 L s^{-1} to alter the SML sufficiently to reduce the growth of phytoplankton through light limitation. The difference between the theoretical (700 L s^{-1}) and numerically-derived (1800 L s^{-1}) design airflow rates reflects the importance of local climatological conditions which are considered only in the numerical simulations.

When commenced in spring, destratification maintained oxygen concentrations at 50-60% of saturation at the bottom of the water column. The elevated oxygen concentrations removed iron, manganese and hydrogen sulfides within a few days. As soluble iron was oxidised, dissolved phosphorus was bound to iron complexes and became unavailable to the phytoplankton. Destratification reduced the net amount of phosphorus released from the sediments to the hypolimnion by up to 85%.

The Peel River is a major source of nutrients to Chaffey Reservoir (Section 8.3.7). Delivery of nutrients from the catchment typically exceeded the observed net changes in reservoir nutrient content implying that the reservoir acts as a sink for the external nutrient load. In the Peel R., both turbidity and suspended sediment were poorly correlated with FRP and TP and reasonably well correlated with nitrate and total kjeldahl nitrogen. On average, 30% of the total phosphorus carried by the Peel River was present as filterable reactive phosphorus. The ratio of FRP:TP did not correlate significantly with gauge height.

The dominant source of the sediments (and presumably the particulate phosphorus) carried by the Peel R. is known to be the eastern catchment (Section 8.2.3). However, the source of FRP within the catchment is unknown because geochemical tracing techniques consider only particulate matter. FRP delivered by the Peel R. accounted for at least half of the observed change in total phosphorus content in the reservoir during the study period. This result implies that during normal-wet precipitation years, the catchment may supply 50% or more of the phosphorus that is subsequently converted into algal biomass.

The vast majority of dissolved phosphorus in the water column was present as orthophosphate, the most bioavailable form. Following an initial spring or early summer phytoplankton bloom which eventually sedimented out of the surface layer, concentrations of phosphorus were very low, approaching the limit of detection. Low phosphorus and nitrogen concentrations were often present but seldom reduced the cell division rate. However they did prevent the accumulation of algal biomass until autumnal deepening of the surface layer entrained hypolimnetic nutrients into the surface layer. The cell division rate determines how quickly the maximum biomass is attained. FRP accumulation in the hypolimnion was the major determinant of the following year's algal biomass but did not impact on species dominance.

The phytoplankton community was dominated (88% of the algal biomass) by either motile or positively buoyant species that remained in the surface layer. The surface layer was rarely deeper than the euphotic depth and so provided an excellent light environment for algal growth. Blue-green algae have grown in all months of the year at Chaffey Dam.

Algal management implications -

Destratification may prove to be effective in reducing the algal biomass present in the reservoir because it effectively reduces the internal phosphorus load from the reservoir's sediments. It should also reduce the amount of particle-bound phosphorus delivered by the Peel R. that is recycled into a bioavailable form. However, the inability of destratification to deepen the SML, and thereby change the light environment, makes it ineffective for the elimination of blue-green algae at Chaffey Dam.

Alternative strategies for maintaining oxic conditions in the hypolimnion should be considered. For example, direct injection of pure oxygen into the hypolimnion could be just as effective at reducing the internal nutrient load while at the same time preserving the thermal stratification. This has the advantage of keeping the nutrients lost from the surface layer through particle sedimentation in the hypolimnion and ultimately the sediments. This strategy

should produce lower algal biomass in summer and autumn than would destratification which resuspends some of the nutrients in the water column.

Increased emphasis on tracing catchment FRP as opposed to TP sources is required for informed catchment management decision making. A large proportion of TP (30%), is delivered by the Peel River as FRP. Geochemical sediment tracing techniques cannot identify the source of FRP within the catchment. Unequivocal identification of the catchment FRP source(s) will require the deployment of streamflow guages and stage-dependent samplers on the tributaries to the Peel upstream of Taroona in order to compute nutrient loads. An earlier attempt by DLWC to identify these sources using 'rising stage' samplers did not provide data of sufficient quality to estimate loads.

There is insufficient Fe available to scavenge all the FRP in the water column when the destratifier is operating. Operation of the destratifier converts reduced iron (Fe^{II}) with a low affinity to bind phosphorus to iron oxyhydroxide ($Fe^{III}OOH$) which has a high phosphorus binding affinity. The imbalance between Fe and FRP increases the importance of controlling FRP delivery from the catchment. Manganese is often present in higher concentrations than Fe in the anoxic hypolimnion but it does not play a significant role in P reduction.

Dessication of dam sediments decreased the capacity of sediments to both take up P, and to release P under anoxic conditions. The duration of this effect is unknown but is believed to depend on the time required for the anaerobic bacteria to recolonize the sediment following reinundation. It may be possible to reduce the internal P load by operating the dam to cause low water levels of sufficient duration to dessicate a significant portion of the sediments.

Extensive sulphate reduction occurs during summer stratification and this contributes a significant portion of the internal phosphorus load. Maintenance of aerobic conditions within the hypolimnion may prevent sulphate reduction and the attendant release of phosphorus.

Elbow-grab water samples gave higher biomass estimates than 5 m-integrated samples, especially during periods of blue-green algal dominance. We recommend the pooling of 5 m-integrated samples from 5 locations in the reservoir into a single sample for algal abundance estimates. This will provide a more representative estimate of reservoir conditions. However, if contact with algal scums is an issue, then surface samples need to be collected as well.

2 Glossary of terms

Abiotic - A process that does not require the action of living organisms, Non-biological e.g. a chemical reaction.

Absorption cross section – The area of the pigment molecules within an algal cell used to intercept light.

Adsorption - 'sticking' of chemical compounds to surfaces. Adsorption can either be by *physical adsorption,* when the chemical is held to the surface by some physical force (e.g. ionic attraction), or *chemical adsorption* where the adsorbed substance forms one or more chemical bonds with the surface.

Algal Blooms - excessive number of algae in a water body. Often, but not necessarily always, associated with nutrient pollution. As a rule-of-thumb, a **chlorophyll** concentration of greater than 20 µg per litre (0.00002 g per litre) is considered an algal bloom.

Ammonia - a gas with the chemical formulae NH_3

Anoxic - the absence of oxygen. Often used interchangeably with *anaerobic* which means in the absence of air.

Artificial destratification – The process of reducing the temperature difference between the bottom and top of the water column by increasing the vertical circulation of water. This is typically done by injecting compressed air in the deepest part of a reservoir (bubble-plume destratification, often called reservoir aeration), but can also be accomplished by the use of impellers (sometimes called surface pumps).

Assimilated - taken into an organism and used to produce **biomass.**

Base - a base is a substance which reacts with the hydrogen ion H^+. The opposite to base is acid. An *acid* is a substance which can release a hydrogen ion. See also proton.

Bioavailable - A description of how easily a compound can be assimilated by an organism.

Biodiversity - or species diversity. A measure of the number of plants and animal species present in an ecosystem. **Eutrophic** systems tend to have a large **biomass** but low biodiversity

Biofilm - thin layers of mixed groups of micro-organisms that coat submerged surfaces. The structure of biofilms can be quite complex and can contain both **oxic** and **anoxic** zones even though the water surrounding the biofilm is well oxygenated

Biomass - The weight of all the organisms in an ecosystem, trophic level etc.

Biota - a term used to describe all the organisms in an ecosystem. e.g. freshwater biota.

Chlorophyll - a green pigment found in most plants and algae. It is used to capture light in **photosynthesis.**

Colloids - small particles usually less than about 0.0001 mm across which are suspended in solution. They may be made of minerals, clays or **organic** compounds. They are important in **adsorption** in many freshwater systems.

Coupled nitrification-denitrification - process for the biological conversion of ammonia to nitrogen gas. Occurs where **oxic** and **anoxic** zones are close together.

Cyanobacteria – Also called blue-green algae. These photosynthetic bacteria are the main nuisance species present in Chaffey Reservoir due to their occassional release of toxins to the water.

Decomposition - decay of biomass usually into more simple compounds by micro-organisms. The process consumes oxygen and often has ammonia as a by-product - see also **mineralisation.**

Dinoflagellate – A type of phytoplankton that possess flagellae which allows it to swim within the water column under calm conditions.

Denitrification - process where **nitrate** is converted to nitrogen gas. Occurs under anoxic conditions. The process is mediated by bacteria.

Dissimilatory Nitrate Reduction to Ammonia - process where nitrate is converted to ammonia. This process occurs in the anoxic zone of sediments

Downwelling – Moving vertically downwards from the sky to the water.

Electron acceptor - The *oxidant* used in the oxidation of organic matter during respiration. For example under oxic conditions, an organism takes up oxygen.. The oxygen is used to **oxidise** carbon. Because the oxygen accepts electrons from the carbon molecules the oxygen molecules are said to be reduced (see **reduction).** Oxygen therefore is an electron acceptor. Where oxygen is unavailable (e.g. in **anoxic** zones), bacteria use other electron acceptors - e.g. ferric iron in **iron reduction** and sulfate in **sulfate reduction.**

Eutrophic - containing abundant nutrients - see **eutrophication.**

Eutrophication - process where excessive amounts of nutrients, usually N and P, are added to water bodies. Usually results in increased plant and algal **biomass** but decreased **biodiversity.**

External nutrient load – The supply of nutrients to the water column that is delivered to the reservoir from sources outside the high water level of the reservoir. Usually dominated by sediment and dissolved nutrients from sources within the catchment upstream.

Ferric iron - Oxidised form of iron. Stable in air. Has 3 positive charges - Fe^{3+}. Often in the form of solid iron oxides such as haematite.

Ferrous iron - Reduced form of iron. Iron compounds having a 2 positive charge - Fe^{2+}. Ferrous compounds are unstable in the presence of oxygen and are quickly oxidised to ferric compounds.

Filterable reactive phosphorus (FRP) – The amount of inorganic and organic phosphorus compounds dissolved in a water sample. The inorganic component is typically regarded as being immediately available to fuel algal growth.

Fluorescence – The portion of the energy absorbed by a substance exposed to an excitation light source which is reemited as light at a longer wavelength. The energy of a photon decreases as the wavelength increases so the shift to a longer wavelength reflects losses of the absorbed light energy (e.g. As heat or conversion to chemical energy) prior to reemission as fluorescence.

Food Chain - Chain of organisms through which energy, in the form of carbon, progresses. A simple food-chain consists of producers (plants), which convert the energy in sunlight into chemical compounds (biomass). Plants are inturn eaten by smaller animals (1st order consumers or herbivores) which are then eaten by higher order consumers (carnivores).

Hypolimnion – The lowest part of the water column. It extends from the sediments to the bottom of the thermocline.

Internal nutrient load – The supply of nutrients to the water column that originates from within the reservoir. Usually, the reservoir sediments are the dominant source.

Ion - an electrically charged atom or molecule. Compounds with a positive charge are called *cations,* compounds with a negative charge are called *anions.*

Iron-Reducing Bacteria - group of bacteria which reduce ferric iron to ferrous iron in **anaerobic respiration.**

Isotopes of oxygen, nitrogen, and carbon – Used to infer the source and age of nutrients assimilated by algal cells.

Longwave radiation – Infrared radiation emitted mainly from water vapour in the atmosphere.

Microstructure – Changes in the thermal or chemical structure of a reservoir that occur over very small distances of the order of a centimetre or less.dissolved inorganic nitrogen – The amount of inorganic nitrogen compounds dissolved in a water sample and available to fuel algal growth. Typically assumed to be ammonia plus nitrite plus nitrate.

Mineralisation - conversion of nitrogen in biomass to ammonia -see **Decomposition.**

Nitrate - oxidised form of nitrogen with the formulae NO_3^-. Can be assimilated by plants including algae.

Nitrification - process where ammonia is converted to nitrate. Usually goes through two steps. NH_3 is first converted to nitrite (NO_2^-) which is then converted to nitrate. Nitrification requires oxygen.

Nitrite - NO_2^- ion.

Nitrogenase - the enzyme responsible for **nitrogen fixation.**

Nitrogen Fixation - the process where atmospheric nitrogen (N_2) is converted to ammonia. Nitrogen fixation is an important pathway for N to enter both terrestrial and aquatic ecosystems.

Nucleic acids - large molecules containing N and P occurring in all living organisms. Nucleic acids are used to store and transfer the genetic make-up of the organism. DNA and RNA.

Organic Phosphorus - Chemical compounds which contain both phosphorus and carbon atoms. They usually contain a C-O-P bond (phosphate *esters)* but compounds containing a direct C-P bond (phosphonates) are also known to occur naturally. To become bioavailable to algae organic P compounds need to be broken down.

Ortho-phosphate - $H_xPO_4^{(3-x)-}$. The only form of phosphate that can cross bacterial or algal cell membranes, therefore, the most bioavailable form of P.

Oxic - Contains oxygen. The opposite of anoxic.

Oxidation - Chemical process where a molecule loses an *electron* and therefore loses some negative electrical charge or gains some positive charge e.g.
S^{2-} -> $S + 2e^-$ or
Fe^{2+} -> $Fe^{3+} + e^-$
It is almost always coupled with **reduction** reaction.

Photophysiology – The processes within an algal cell responsible for the conversion of light energy into chemical energy. This includes everything from the pigments such as chlorophyll-a used to capture light energy (photons) to the many chemical compounds used to process the captured energy.

Photosynthesis - process where energy from sunlight is used to make chemical compounds. These compounds are a form of energy which can be used in food chains.

pKa - the *pH* at which half of a compound is in it's **protonated** form and half in its basic form.

Prokaryotic - organisms whose DNA is not separated from the rest of the cell by a membrane. Includes both bacteria and blue-green algae (cyanobacteria).

Proteins - large molecules which contain nitrogen. Proteins are essential for living organisms. *Enzymes* are a type of protein.

Proton - The hydrogen ion H^+. The concentration of protons determines the pH of a solution

Protonated - gaining a proton.

Polymer - Large molecules which consist of one or more molecules joined to each other in a repetitive sequence.

Polyphosphate -polymer of orthophosphate ions such as **tripolyphosphate.**

Quantum yield – A measure of the efficiency with which captured photons are converted to chemical energy within an algal cell.

Reduction - chemical process where a molecule gains an electron - the converse of oxidation.

Respiration - The process where an organism gains energy from the oxidation of carbon compounds (such as sugars).

Secchi depth – The maximum depth under the water at which a white & black disk can be seen by an observer immediately above the water surface.

Sediment - The complex mixture of minerals, clays, organic material and biota found at the bottom of waterbodies. Varies in consistency from corse sands and gravels to very fine mud. Fine sediments often have an anoxic zone.

Sediment trap – A device that collects particles that move through the water column. Upwards facing traps collect sinking particles whereas downwards facing traps collect rising particles.

Shortwave radiation – Visible light from the sun.

Stratification – The presence of a changing temperature distribution within the water of a reservoir. Typically refers to the presence of warm water at the surface and colder water at the bottom of the water column.

Sulfate- oxidised form of sulfur - SO_4^{2-}

Sulfate-reducing bacteria - group of bacteria which reduce sulfate to sulfide in anaerobic respiration.

Sulfide - reduced form of sulfur S_2^- ion. When **protonated** it forms H_2S - rotten egg gas.

Surface mixed layer (SML)– The uppermost region of the water column that is well-mixed. Temperature, algal and chemical concentrations are uniform within the SML. Its depth varies continuously throughout the day.

Thermocline – The vertical portion of the water column with the greatest temperature change across it. At Chaffey Reservoir it typically extends from 4 or 5 m below the surface to approximately 12 m below the surface.

Total nitrogen (TN) – The total amount of nitrogen present in a water sample from all sources, i.e. Dissolved plus particulate.

Total phosphorus (TP) – The total amount of phosphorus present in a water sample from all sources, i.e. Dissolved plus particulate.

Tripolyphosphate - a polymer of phosphate groups used in detergents to decrease the hardness of water.

Turbulent velocity scale – The characteristic speed of parcels of water as they move about a turbulent region of the water column. The technology to directly measure the turbulent velocity scale is relatively new. It's value is more typically inferred from measurements of other more easily measured parameters, typically heat flux and wind speed.

Upwelling – Moving vertically upwards, e.g. from the water to the sky.

3 Introduction

Degraded water quality in reservoirs is a significant problem in Australia. The most common complaints relate to low dissolved oxygen and the presence of nuisance blooms of phytoplankton, especially toxic strains of cyanobacteria such as *Anabaena* and *Microcystis*. Low dissolved oxygen concentrations often are accompanied by high hydrogen sulfide, dissolved iron and manganese concentrations leading to pipe blockage, colour, taste and odour problems which increase treatment costs. Toxic algal blooms lead to the closure of recreational reservoirs and require expensive toxin removal treatment for drinking water supplies.

The development of density stratification is an important precursor to the onset of both of these problems. Density stratification suppresses the vertical transport of oxygen from the diurnally-mixed surface layer of a reservoir to the hypolimnion and the sediments below. Biological oxygen demand in the hypolimnion eventually leads to anoxic conditions which are accompanied by increased concentrations of reduced ferrous iron and manganese as well as enhanced release of phosphorus and ammonia from the sediments, nutrients essential to fuel algal growth.

The control of algal growth may be attempted in two ways: by reducing the supply of nutrients from the sediments (the internal load) and/or the catchment (the external load); and by reducing the supply of light through promoting deeper mixing of the surface layer. In the first case, the goal is to starve the algae of nutrients. In the latter case the goal is to deprive the algae of light by ensuring that the depth of the surface mixing layer, z_{SL}, is sufficiently greater than the euphotic depth, z_{eu}. Reduction of the external nutrient load must be approached at the whole-catchment scale and may require, for example, changed land use practices, alternative sewage disposal techniques, and construction of artificial wetlands. The efficacy of these measures will depend on the relative contributions of immediately bioavailable nutrients and forms that require reworking in the sediments and water column of the reservoir prior to becoming available for algal growth. Reduction of the internal nutrient load can be achieved by maintaining oxidising conditions at the water-sediment interface either through direct injection of oxygen (hypolimnetic oxygenation) or by increased downward transport of oxygen via artificial destratification. Artificial destratification can also produce a deeper surface layer thereby changing the light environment experienced by the phytoplankton. Artificial destratification's two-pronged approach to improving water quality (reduced internal nutrient load and surface layer deepening) has made it a popular reservoir management strategy throughout the world.

Since 1966, artificial destratification has been employed in more than 60 Australian storages in attempts to improve water quality. The results have been disappointing with 2/3 of artificially destratified reservoirs failing to show reduced algal biomass, 1/2 continuing to suffer from the presence of noxious algal species, and 1/3 with persisting high iron and manganese levels (McAuliffe and Rosich 1989).

This report presents the results of a 3-year study by the Cooperative Research Centre for Freshwater Ecology into the coupling between the physical, chemical and biological processes within Chaffey Reservoir that exert the greatest influence on the water column chemistry and the phytoplankton community. The ultimate objective of the study was to identify the intrinsic limitations of artificial destratification and to be able to provide sound advice to the NSW Dept. of Land and Water Conservation (DLWC), the Chaffey Dam Advisory Committee (CDAC), the National Eutrophication Management Program (NEMP), and the Australian water industry on the most effective management strategies for the control of cyanobacteria and the transport of oxygen to the hypolimnion.

From conception there has been a whole-ecosystem approach to the experimental design of the project. To do this it was necessary to study the physiological responses of the phytoplankton to changes in nutrient status and the light environment to identify the factors that controlled the growth of both individuals as well as the community as a whole. It was also necessary to study the sinks for the algae such as zooplankton grazing and sedimentation out of the euphotic zone. Detailed hydrodynamic and meteorological data were required to identify the major processes influencing the light and chemical conditions that confer competitive advantages to different phytoplankton species. Without nutrients there could be no algae so the major sources and sinks of nutrients had to be identified and the transformations between different chemical species considered. This meant that nutrient sources both external, i.e. the Peel River, and internal, especially the sediments, had to be quantified.

A complementary motivation was the desire to collect the most comprehensive data set yet available to rigorously test complex reservoir water quality models which for decades have encapsulated contemporary understanding of nutrient pathways and trophic dynamics - the conceptual models of reservoir ecology haven't changed significantly in 20 years - but have never been thoroughly validated. The vast number of processes and parameters in these models require extensive calibration and may produce plausible results for the wrong reasons; e.g. the presence of compensating errors is likely but often escapes detection because the relevant field data aren't available. Constraining these models by measuring the important rate coefficients, forcing parameters, etc. makes it possible to identify shortcomings in the models and to evaluate the significance of modelled processes for which field data are not easily obtained.

3.1 Why Chaffey Reservoir?

Chaffey Reservoir, near Tamworth in NSW, is an example of a storage where destratification has failed to live up to expectations. Despite the reduction in density stratification and the increased dissolved oxygen levels at depth produced by artificial destratification, the reservoir still suffered from massive blooms of the toxic cyanobacteria, *Anabaena* and *Microcystis*, which could occur at virtually any time of year.

Chaffey Reservoir was selected because it offered the best combination of attributes for such a large study. It's long history of algal bloom problems had led to a number of studies being carried out in the reservoir and the catchment upstream. There was a long and continuous historical data record that included algal abundance and vertical profiles of water column chemistry at weekly to

fortnightly intervals. An automated water quality sampler was available a few kilometres upstream of the dam so that the external nutrient load could be quantified. A compressed-air destratification system was available on-site which DLWC was willing to operate solely to comply with the research objectives of this project. There was also strong support for the project from the local community.

The outstanding data set compiled by this project owes much of its existence to the tireless support of the DLWC staff at Chaffey Dam. They maintained instruments for us, collected samples whenever asked, and made us feel very welcome every time we dropped in for a field experiment.

4 Site description

4.1 Location

Chaffey Reservoir is located in a historical gold-mining region of northeastern New South Wales approximately 32 km southeast of Tamworth (latitude 31° 21' S, longitude 151° 8' E) at an elevation of 518 m (Figure 4.1). Fed by the Peel River, the upstream catchment has an area of roughly 41,340 hectares and is characterised on the southern and eastern edges by steep slopes rising to 1300 m and covered mainly with native grasses and trees although some areas have been cleared for grazing and the harvesting of timber. The remainder of the catchment is undulating and has been cleared extensively for grazing on both improved and unimproved pasture (Young, 1993). Geologically, the upper catchment is comprised of Tertiary basalt whereas the lower catchment consists mainly of Carbonifierous to Devonian age sedimentary rocks (Caitcheon et al., 1994).

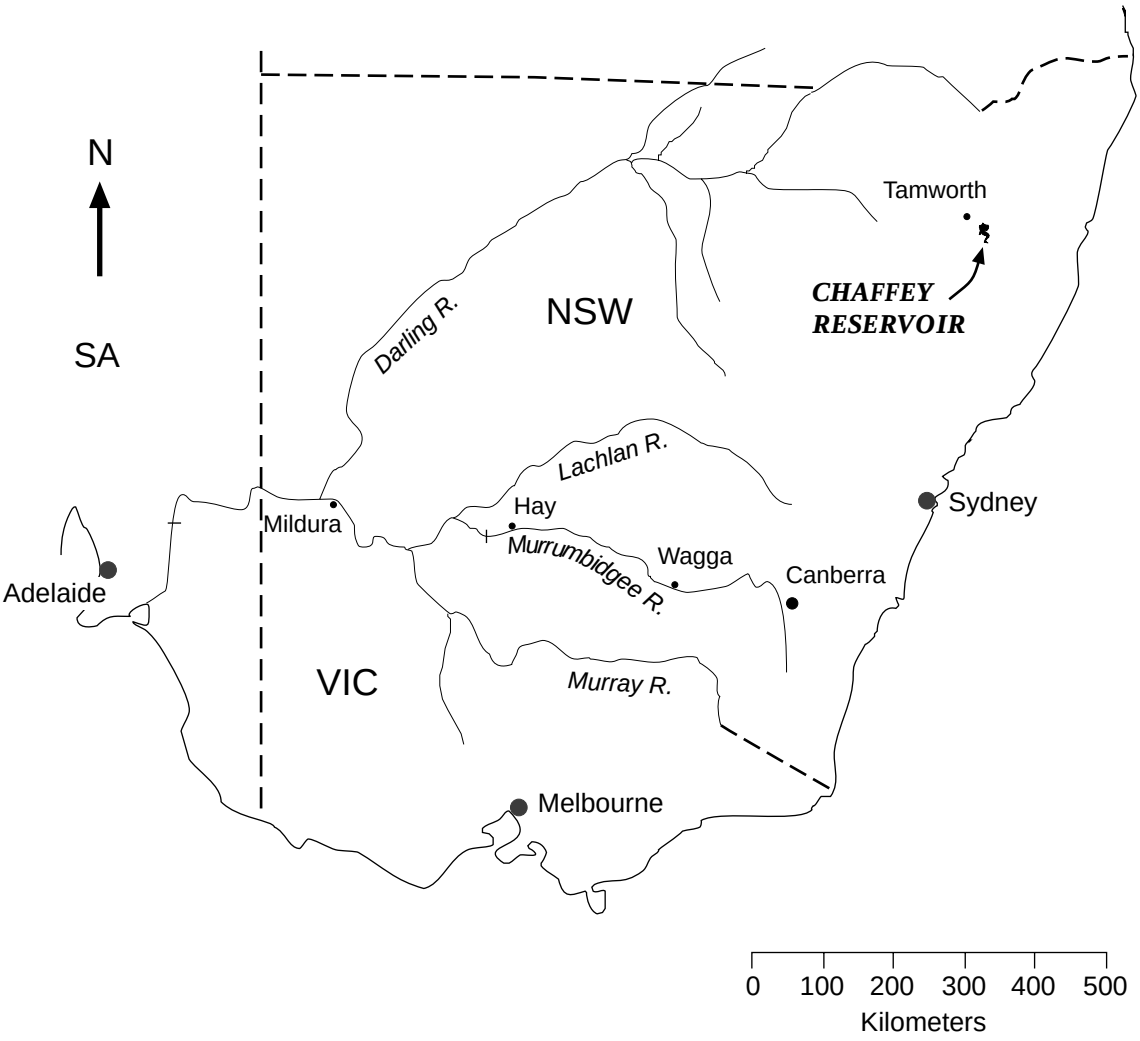

Figure 4.1 Map of New South Wales showing approximate location of Chaffey reservoir.

The reservoir, when full, holds 61,830 ML with a surface area of 542 hectares, a maximum depth of 28 m and a mean depth of 11.4 m. The elevation of the spillway crest is 518.6 m and the dam crest is at 533.5 m. Water from the reservoir

is used both for irrigation and to supplement the drinking water supply for the city of Tamworth, one of the largest cities in rural New South Wales.

The reservoir has a history of chronic algal blooms and is notable because toxic blooms of both *Microcystis* sp. and *Anabaena* sp. can occur at virtually any time of year with dense blooms often occurring during the winter months (see Chapter 7). This has motivated an unusually intensive routine data acquisition program by the dam's operator, DLWC. A number of field studies have also taken place over the years since the reservoir was first inundated in 1979 and cover a range of topics from catchment geology and phosphorus sources (Caitcheon et al. 1994, Beecham, 1995) to the biota of the Peel River and Chaffey Reservoir (May and Powell, 1986; Muschal, 1995). The issue of phosphorus sources has been particularly contentious with some arguing that the basaltic geology of the upper catchment is primarily responsible for the external phosphorus load (Donnelly, 1993; Caitcheon et al., 1994) while others assert that runoff from fertilised pastures are the dominant source of P (Beecham, 1995). As will be shown in Chapter 5, neither argument can be dismissed.

4.2 Facilities

4.2.1 Historical data archive

The NSW DLWC provided files containing virtually all of the historical data they had compiled from previous studies and routine monitoring at Chaffey Dam. The large number of fragmented and occasionally overlapping files were consolidated, checked for obvious errors, converted into a standard database file format (dBASE, .dbf) and made available to all project partners via ftp from the fileserver at CSIRO Land & Water. Historical data included Peel River inflow volumes, reservoir level and discharge values, compressor operating times, algal count data, and water chemistry data.

4.2.2 Destratification system

Since its inception, Chaffey Reservoir has had a compressed-air, bubble-plume destratification system. The initial system consisted of 3 diffusers anchored in concrete blocks about 100 m from the dam wall (Young, 1993). The compressor had a maximum free airflow rate of 100 L s^{-1}. In 1988, one of the airlines failed and the system was mothballed until the current project commenced because it was felt that the system hadn't performed satisfactorily.

The destratification system was redesigned for the current experiment following the design criteria described by Schladow (1993) and Lemckert et al. (1993). These criteria are based on research into the dynamics of bubble plumes (McDougall, 1978; Asaeda and Imberger, 1993) and identify the optimal configuration of a bubble plume to maximise the efficiency of a destratification system where efficiency is defined as the increase in potential energy[1] of the water column divided by the energy consumed by the compressor.

[1] The potential energy of a water column is defined as its mass times gravitational acceleration times the difference in height between the centre of masses of the stratified water column and a well-mixed water column of the same mass. A well-mixed water column has a higher centre of mass

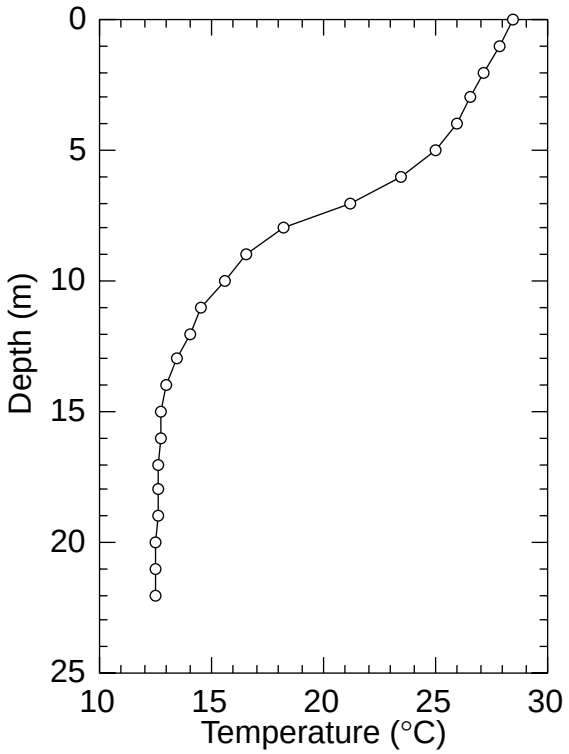

Figure 4.2 Temperature profile at Chaffey Reservoir on 2 Feb 1993.

The design objective for the new bubble plume system was that it should be able to destratify the maximum stratification observed in the reservoir under the typical summer meterological conditions, i.e. strong insolation, high air temperature and light winds. To facilitate testing of the intermediate disturbance hypothesis – one of the project's initial goals – complete destratification should occur within one week so that rapid, profound changes in the underwater light climate (i.e. z_{SL}:z_{eu}) on phytoplankton physiology could be assessed. This 7 day time scale for destratification is much more stringent than the 21 days considered acceptable for normal reservoir operation (Schladow, 1993).

The design temperature profile is shown in Figure 4.2. This profile is typical of summer conditions in the reservoir. When the reservoir level decreases, the hypolimnion becomes shallower whereas the surface layer and thermocline regions generally maintain the same dimensions. The temperature profile in deeper water columns was approximated by extrapolating the hypolimnetic profile downwards to the relevant depth.

For water depths between 22 and 28 m – the expected range of reservoir level for the project – the potential energy of the stratification in Figure 4.2 is equivalent to a linear temperature gradient of 0.62-0.59 °C m^{-1} which gives a buoyancy frequency range of 0.033-0.026 s^{-1}. The results of the design calculations are shown in Table 4.1. Also shown in the table are the results for the minimum water column depth during the project. For details regarding the derivation of the parameters in the table the reader is referred to the original articles by Schladow (1993) and Lemckert et al. (1993). The most energy efficient design for a bubble

---

and therefore a higher potential energy than a stratified water column because the density of a stratified water column is greater at the bottom than at the top.

plume system is usually achieved by using an air flow rate, Q_0, between the values for the 1st and 2nd efficiency peaks (Schladow, 1993).

Table 4.1 Destratification system design calculations.

Parameter	28 m		26 m		24 m		22 m		17 m	
	1st peak	2nd peak	1st peak	2nd peak	1st peak	2nd peak	1st peak	2nd peak	1st peak	2nd peak
dT/dz	0.591		0.605		0.614		0.618		1.15	
N	0.0265		0.0283		0.0304		0.0329		0.0411	
ΔPE	2128.1		1914.0		1699.9		1485.8		953.3	
M	0.50	0.069	0.44	0.054	0.33	0.042	0.29	0.034	0.31	0.038
C	745	5910	891	9760	1230	16200	1490	27100	1350	
η	9.4	7.0	9.1	6.7	8.7	6.3	8.3	6.0	8.2	5.8
Q_0	20	2.8	16	2.0	11	1.4	8.3	1.0	7.7	0.92
QT_{21}	500	670	480	650	470	650	450	620	340	485
QT_{02}	5200	7000	5100	6900	4900	6800	4800	6600	3600	5090

dT/dz	Linear gradient equivalent to potential energy of stratification (°C m^{-1})
N	Buoyancy frequency corresponding to dT/dz (rad s^{-1})
ΔPE	Change in potential energy to fully mix water column (J)
M	Source strength parameter (dimensionless, see Schladow, 1993)
C	Stratification parameter (dimensionless, see Schladow, 1993)
η	Mechanical efficiency of destratification (%)
Q_0	Design air flow rate per plume (L s^{-1}, at atmospheric pressure)
QT_{21}	Air flow rate to destratify reservoir in 21 days (L s^{-1}, at atmospheric pressure)
QT_{02}	Air flow rate to destratify reservoir in 2 days (L s^{-1}, at atmospheric pressure)

After considering several possible water depths with the maximum stratification observed in the historical record and using the existing compressor, an airflow rate of 10 L s^{-1} per plume was decided on as a reasonable compromise between the capital cost of the diffuser system and maximising the energy efficiency of the system. Constrained by the existing compressor's maximum free-airflow rate of 100 L s^{-1}, the new design consisted of 10 plumes located at 30-m intervals. The distance between plumes was chosen to minimise the amount of plume-plume interaction which reduces the efficiency of the system (Lemckert et al., 1993).

A significant limitation on the experimental design was the inadequate compressor capacity. The design calculations suggested total airflow rates of approximately 500 L s^{-1} to destratify the reservoir in 21 days and 5000 L s^{-1} to do the job in 2 days. Even at the low water level (max. depth 17 m) experienced early in the project, the minimum required airflow rate decreases only to 340 L s^{-1} (Table 4.1). The system was vastly undersized to accomplish one of the initial project objectives - to test the intermediate disturbance hypothesis.

Following Lemckert et al.'s (1993) calculations for the reservoir at 25% of capacity, the new system is expected to pass the entire reservoir volume through the bubble plumes once every 7 days. Based on the predicted mechanical efficiency of

the system (Schladow, 1993), it would be expected to take 2 months to destratify the reservoir completely during the summer under such a low volume condition.

Figure 4.3 shows some of the results of numerical simulations of the destratification system performed by Bruce Hindmarsh (NSW DLWC) using version 6.75.2 of the 1-D numerical model DYRESM 6 (Schladow 1992). Notice the small, but important, temperature change in the upper 5 m of the water column. The numerical simulations confirmed the design calculations and suggested that an airflow rate of 1800 L s^{-1} (data not shown) could remove most of the stratification within 7 days, *but it did not consistently eliminate the presence of a shallow surface layer*.

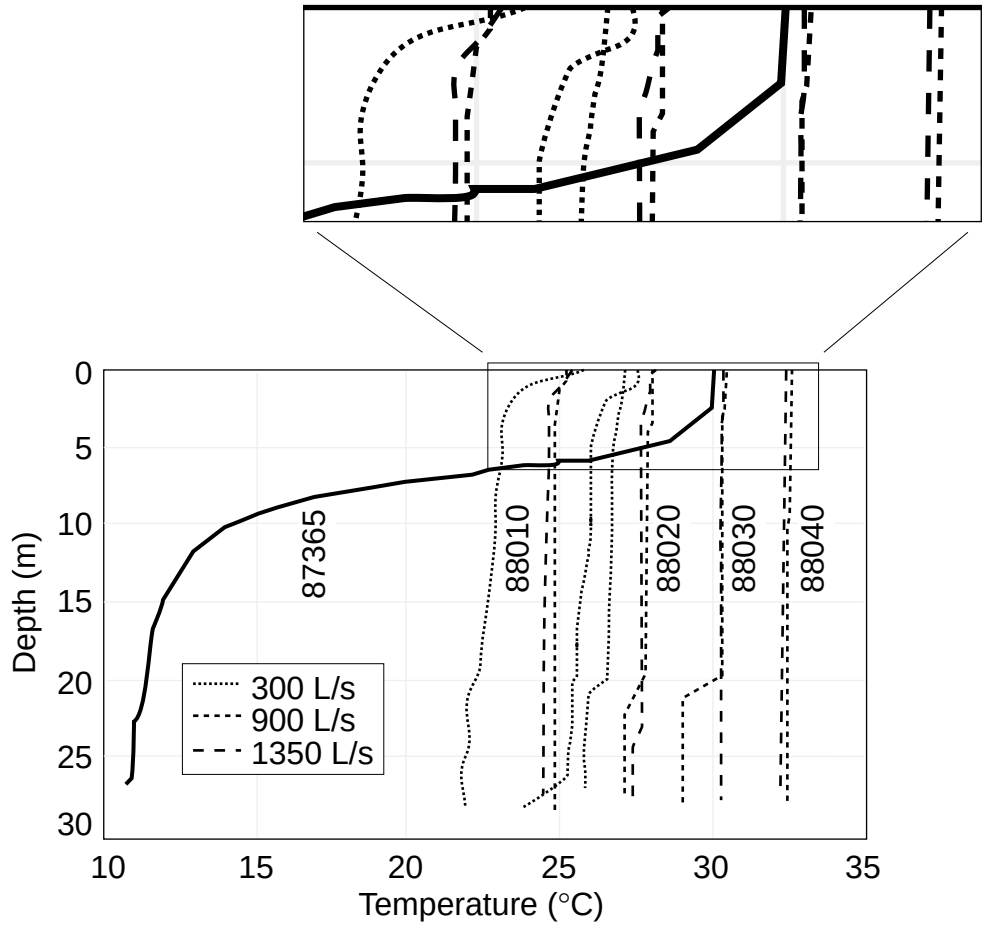

Figure 4.3 DYRESM simulated temperature profiles for compressor airflow rates of 300, 900 and 1350 L s^{-1}. Date format is yyddd. Compressor operation commences 88001 (1 Jan 1988).

4.2.3 Multilevel outlet structure

The dam is equipped with a morning glory spillway and a multi-level outlet structure which allows some control over the quality of water released from the dam. It takes 1 man-day to change the level of the outlet and so changes are not made frequently. Water is most often released from a depth of approximately 9 m (Figure 4.4).

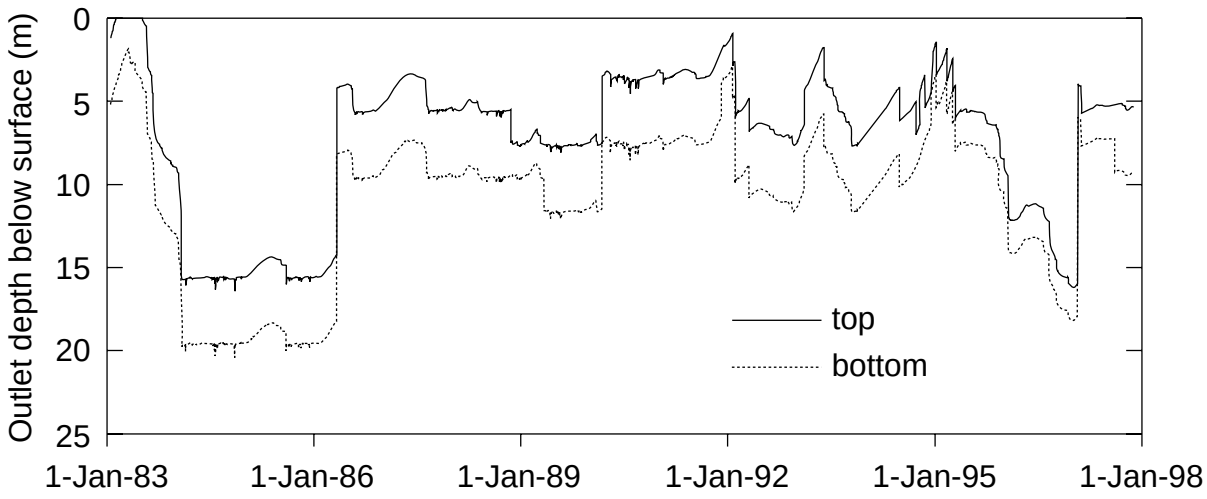

Figure 4.4 Location of top and bottom of outlet for water released from Chaffey Dam.

5 Methods

5.1 Routine monitoring program

The routine monitoring program consisted of: meteorological and thermistor chain data gathered every 10 minutes (CRCFE); weekly conductivity-temperature-depth-dissolved oxygen (CTDO) profiles at 5 - 6 sites (depending on water level) (DLWC); weekly to fortnightly water column sampling for chemical analyses (DLWC); weekly 5 m-integrated samples at five sites analyzed for chl-a and algal abundance (CRCFE); weekly 10 m-integrated samples for zooplankton abundance (CRCFE); weekly surface grabs for algal abundance (DLWC); fortnightly to monthly depth profiles of chemistry (CRCFE); stage-dependent sampling of the Peel River 6.7 km upstream of the reservoir at Taroona (DLWC-CRCFE); and river flow, height, temperature, turbidity, and conductivity every 15 min (DLWC). In addition, there was a Hobo-brand temperature logger continuously recording the Peel River temperature immediately upstream of the reservoir (when full). Table 5.1 shows details of the routine sampling program including instrumentation, measurement accuracy and frequency. The full sampling program commenced in September 1995 and continued uninterrupted through June 1997 except for a few periods when the meteorological station and thermistor chains were being serviced.

The locations of the sampling sites and the bathymetry of the reservoir are shown in Figure 5.1. The 518 m contour is the water level at 95% of capacity. During the course of the project the water level rose from a minimum of 506.6 m (20% cap.) during spring 1995 to 510.3 m (38% cap.) by 9 Jan 1996 with the reservoir ultimately spilling on 16 Feb 1997 when the water level reached 518.72 m.

5.2 Intensive sampling program

In addition to the routine monitoring, there were 10 field trips each of 7- 10 days duration during which intensive sampling of the reservoir's thermal, chemical and biological structure was undertaken. Temperature, depth, fluorescence, dissolved oxygen (TDFO) profiles were taken at 20-50 locations throughout the reservoir, often twice a day. The locations of the profiles was determined in the field and based on the properties of the water column at the time; the distance between profiles decreased when strong gradients or unusual features were detected. On two occasions, an acoustic doppler velocimeter (ADV) was used at sites TC1 and 12 to measure the water velocity profile when the destratifier was operated.

Depth profiles of detailed water chemistry (especially particle size fractions, phosphorus speciation and redox properties), were taken primarily at Stn 1 (Figure 5.1). Sediment traps were deployed here as well. Depth profiles of algal photophysiologal properties were taken mainly at TC1. Bottle experiments on raw water samples were deployed at A3 and TC1. Over 60 sediment samples were collected throughout the reservoir (within the 510 m contour) for xray fluorescence (XRF) analysis of their elemental composition, sediment particle size and organic carbon. Benthic chambers and peepers were deployed at several locations to quantify the sediment oxygen demand and the fluxes of nutrients from the sediments to the water column.

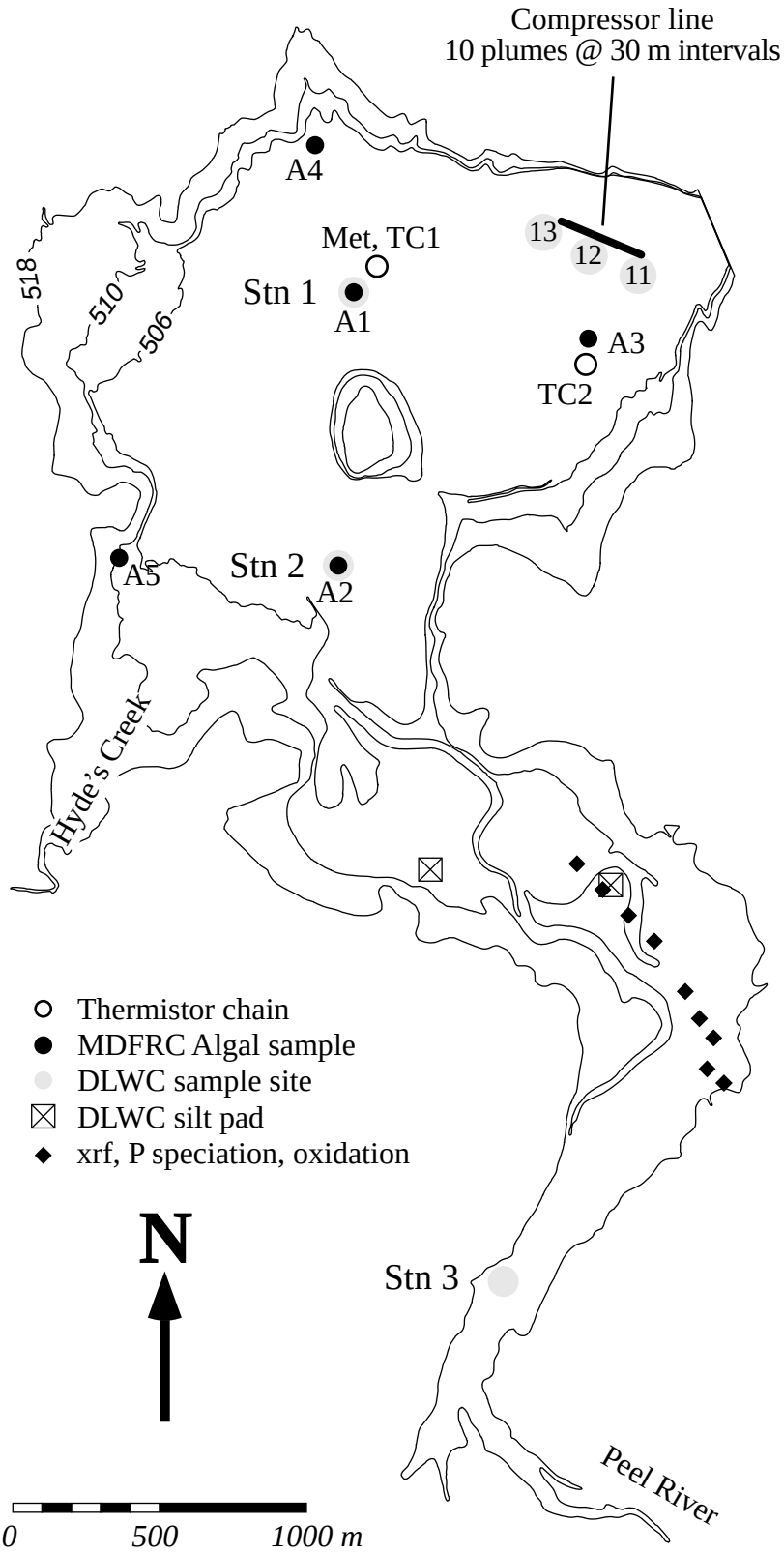

Figure 5.1 Location of algal sampling sites (A1-A5), meterological station (Met), thermistor chains (TC1, TC2), CTDO casts (Stn 1 – Stn3, 11-13) and sediment samples for speciation and oxidation experiments. The 518 m contour is the water level when the reservoir is nearly full (95% of capacity). The 506 m contour was the minimum water level during the project. See Table 5.1 for details.

Table 5.1 Chaffey project measurement program

Parameter	Manufacturer	Location	Frequency	Accuracy	Resolution
Meteorological and thermistor chain					
water temperature	Thermometrics P60	TC1, TC2	10 min	+/- 0.015 °C	0.007 °C
air temperature	Vaisala HMD30UYB	Met	10 min	+/- 0.2 °C	0.01 °C
relative humidity	Vaisala	Met	10 min	+/- 3% RH	0.15 %RH
shortwave radiation	Kipp & Zonen CM14	Met	10 min	+/- 3 Wm^{-2}	< 0.1 Wm^{-2}
longwave radiation (5-25 µm)	Kipp & Zonen CG2	Met	10 min	+/- 10%	0.1 Wm^{-2}
wind speed	Vaisala WAA-15	Met	1 min	+/- 0.1 ms^{-1}	0.002 ms^{-1}
wind direction	Vaisala WAV-15	Met	1 min	2.8 °	5.63 °
Water column chemistry (CRCFE)					
chlorophyll-a (TEL)	5 m-integrated	A1-A5	weekly		
cell abundance	5 m-integrated	A1-A5	weekly		
zooplankton abundance	10 m-integrated	A1-A5	weekly		
FRP,TN,TP,TKN,NO3, NH4, SO4, Si	4 – 12 depths	Stn 1	Weekly to fortnightly (DLWC) & field trips		
TDFO profiler		all	field trips		
in situ fluorescence	SeaTech		43 Hz		
temperature	Thermometrics fp07		43 Hz	+/- 0.1 °C	0.005 °C
pressure (depth)	Keller PAA-10		43 Hz	+/- 0.2 m	0.005 m
dissolved oxygen	YSI 5730		43 Hz	+/- 5 %	0.01 %
Water velocity					
x,y,z components	Sontek ADV	Stn 1, 12			
DLWC CTDO profiles		Stn 1 - 3, 11-13	weekly		
conductivity	Seabird SBE-19				
temperature	Seabird SBE-19				
dissolved oxygen	Seabird SBE-19				
depth	Seabird SBE-19				
Peel River at Taroona					
Flow	Stage recorder	Taroona	15 min	+/- 10%	
Temperature	Hobo	Peel R. Bridge	24 min	+/ 0.2 °C	
Temperature	Hydrolab H2O	Taroona	15 min		
Conductivity	Hydrolab H2O	Taroona	15 min		
Turbidity	Hydrolab H2O	Taroona	15 min		
Chemistry (FRP, TP, TN, NOx, NH4, TKN, SO4, pH, conductivity, turbidity, suspended sediment)	TEL	Taroona	event dependent		

6 Climate

6.1 Meteorology

The climate from spring through autumn at the Chaffey reservoir is characterised by strong insolation, high temperatures and light winds (Figure 6.1). In summer the average daily[2] air temperature was 21 °C (maximum value 26 °C), the mean daily shortwave radiation 275 W m^{-2}, and the average wind speed 2 m above the water surface just 2.5 m s^{-1}. The maximum shortwave radiation under clear-sky conditions was 378 W m^{-2}, a 30% increase on the average due to the absence of clouds. Downwelling longwave radiation averaged 360 W m^{-2}. Afternoon thunderstorm activity was not uncommon during the summer because of the relief of the Great Dividing Range which rises 600 m above the reservoir and is located just a few kilometres to the east.

In winter the average daily air temperature was 8 °C with a minimum value of 4 °C. Mean daily shortwave and longwave radiation decreased to 105 W m^{-2} and 305 W m^{-2}, respectively. Winter is also calmer than summer with a mean daily wind speed of 2 m s^{-1}. Snow often falls on the mountains.

[2] The terms average daily and mean daily refer to the average value of a parameter over a 24 hour period commencing at midnight.

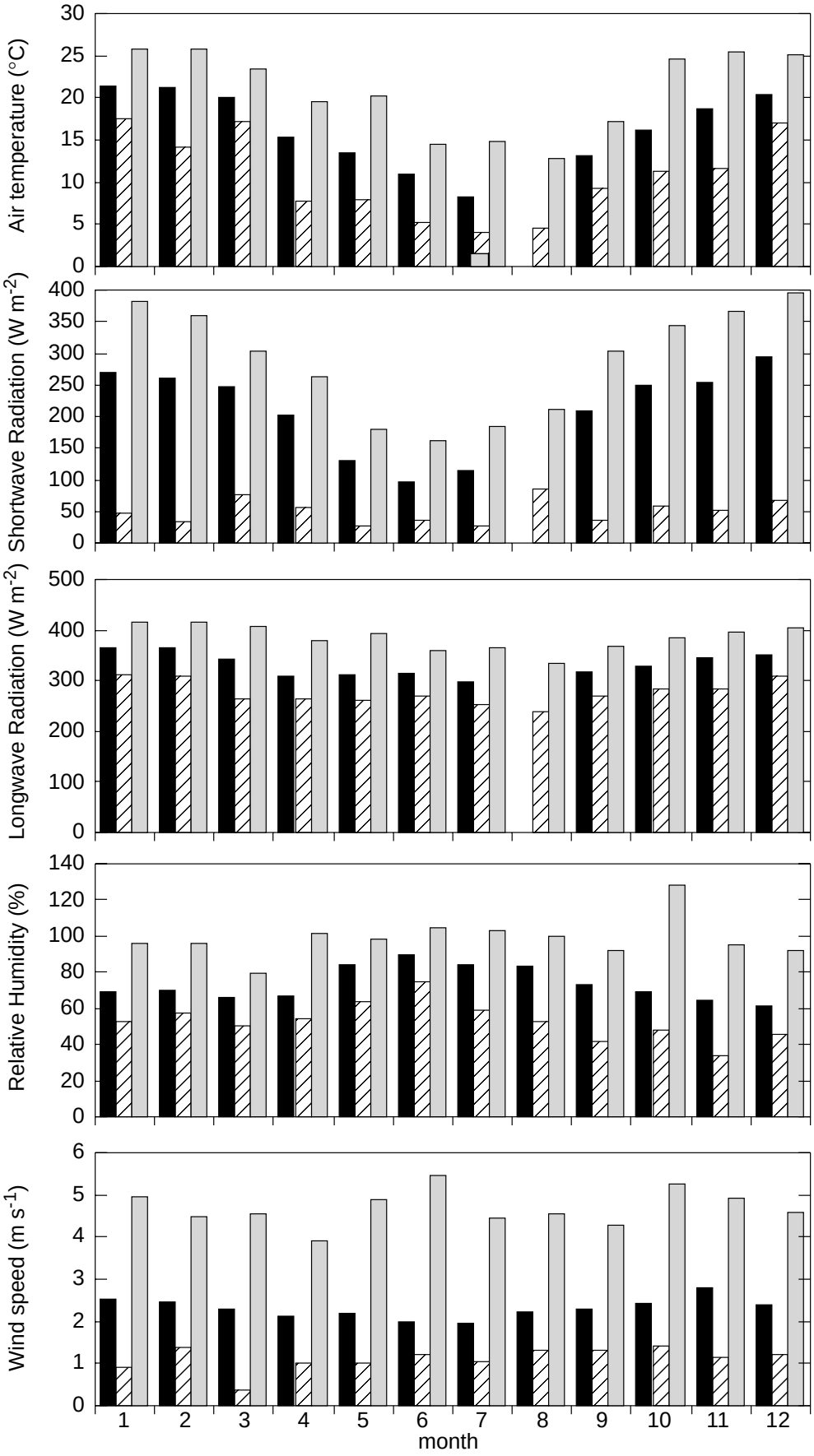

Figure 6.1 Minimum (hatched), maximum (gray), and mean (black) values of air temperature, shortwave radiation, downwelling longwave radiation, relative humidity, and wind speed at Chaffey Reservoir.

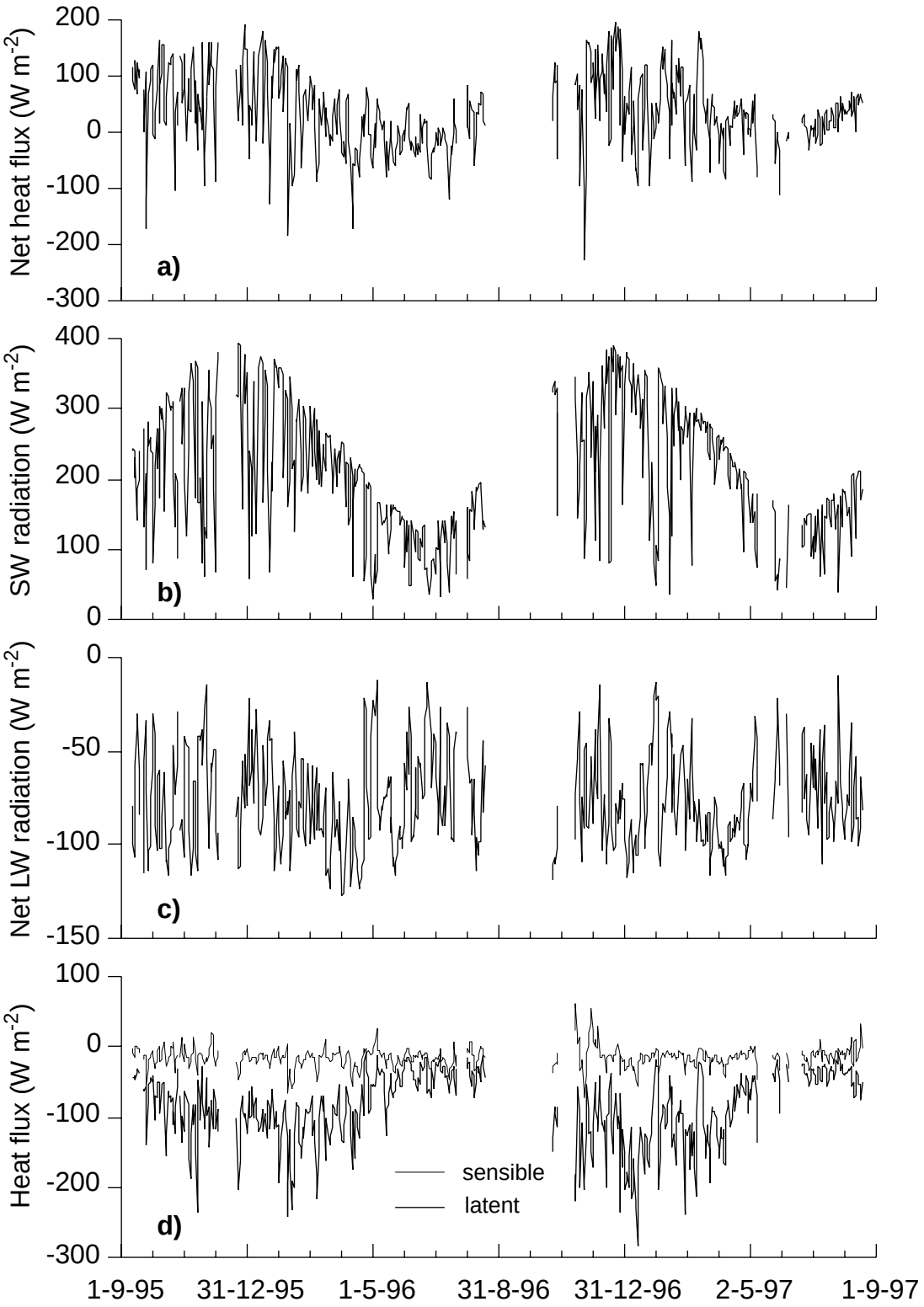

Figure 6.2 Daily values during the study period of net heat flux (a), shortwave radiation (b), net longwave radiation (c), and sensible and latent heat flux (d).

Atmosphere-water heat transfers are shown in Figure 6.2. The net atmosphere-water heat flux from 1 Sep 1995 to 1 Sep 1997 averaged 40 W m^{-2} into the water. The fact that the temperature of the reservoir at the onset of heating in early August was nearly the same in both years reflects the arrival of cold inflows during winter months, surface heat losses and the release of water from the dam. The increase in the mass of water in the storage combined with the inflow and

outflow dynamics allowed year-to-year increases in the heat content of the reservoir consistent with both the positive net surface heat flux and similar reservoir temperatures in both winters.

Despite the fact that short-duration (~ 1 day) significant cooling events occurred throughout the year (e.g. early Feb 1996), only in the months of May and June was there a consistent net loss of heat from the water to the air. Evaporation caused the largest heat loss during September to April whereas net longwave emission dominated from May through August. Over the entire period of record the mean daily latent heat flux was -85 W m^{-2} and the net longwave emission was –75 W m^{-2}. Significant cooling events during the spring - autumn period were usually caused by either high evaporation, unusually low insolation, or a combination of the two.

Comparing the heat fluxes during the Dec-May periods of both stratification seasons reveals significant differences in meteorological forcing between the summers. January 1996 had a significantly higher net heat flux, Q_{net}, into the water column than did January 1997. This situation was subsequently reversed with Q_{net} for each month of February-April 1996 lower than that for the corresponding period in 1997.

6.2 Inflows and outflows

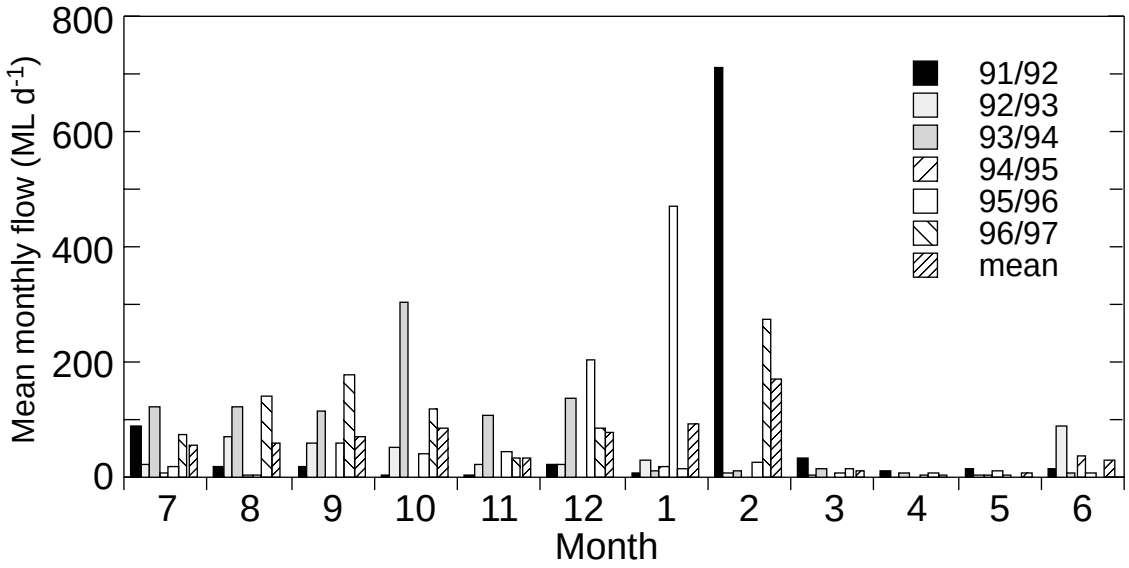

Figure 6.3 Monthly Peel River flows into Chaffey Reservoir.

Inflow to the reservoir is episodic with maximum flows occurring in January and February in response to heavy rains from summer tropical storms that occassionally venture down from the north. Flow in the Peel River occurs mainly from July through February with the autmn months March - May being very dry (Figure 6.3). There is not a strong seasonality to the inflow during the wet months apart from the tendency for major floods to occur in summer.

The study period commenced at the end of a major drought which resulted in a reduction in the amount of water stored to just 20% of capacity by mid-1995. Major inflows in December 1995 and January 1996 filled the reservoir to 53% of capacity. Inflows during Sep 1996, Oct 1996, Dec 1996, and Feb 1997 filled the

reservoir (518.6 m). The reservoir is normally operated to keep it as full as possible. Figure 6.4a shows the water level and discharge from the dam during the course of this project. Figure 5.1 shows the extent of the water surface at 20% (506 m), 53% (510 m) and 95% (518 m) of capacity.

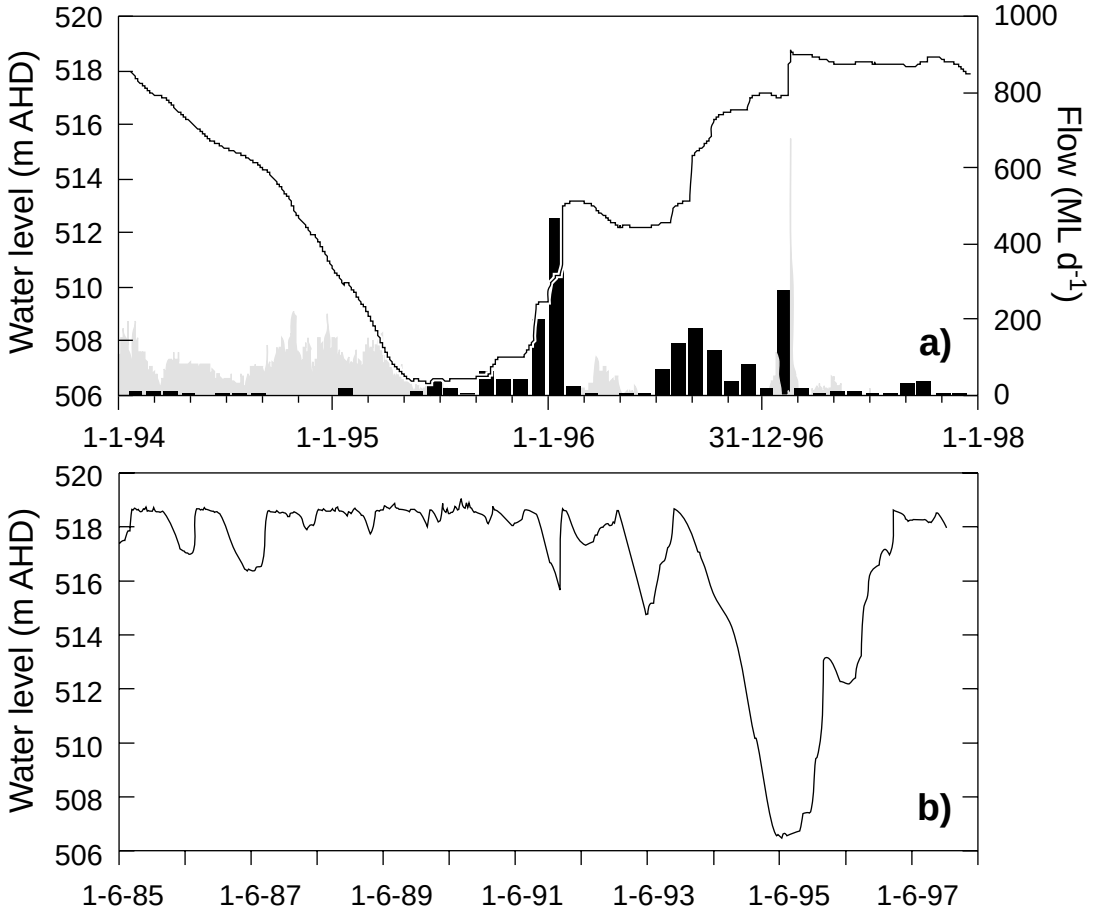

Figure 6.4 a) Reservoir level (solid line), daily releases from Chaffey Reservoir (grey shaded region), and mean monthly Peel River inflow (black bars) during the project. b) Historical reservoir level 1985 - 1998.

6.3 Reservoir heat and water budgets

Heat and water budgets provide a useful means of checking the internal consistency of the field data. The observed change in volume of the reservoir should balance the net inflow / outflow plus rainfall and evaporation. The change in heat content must be consistent with the heat contributed by all flows, rainfall and surface heat fluxes. Errors in these budgets help identify measurement uncertainties.

6.3.1 Water budget

The change in reservoir volume over an interval from time t_0 to t_1 was computed as,

$$dV = \int_{t_0}^{t_1} \Big(Q_{in}(t) - Q_{out}(t) + R(t)A(t) - E(t)A(t) \Big) dt$$

where dV is the volume change, Q_{in} and Q_{out} are the inflow and outflow discharges ($m^3\ d^{-1}$), R is the rainfall rate ($m\ d^{-1}$), E is the evaporation rate ($m\ d^{-1}$), and A is the surface area of the reservoir (m^2). Replacing Q_{in} - Q_{out} with dQ and combining the rainfall and evaporation volumes gives $dV = dQ$ + rain - evaporation. Any departure from this equality, which is denoted *ΔVerror*, indicates errors in one or more of the contributing terms.

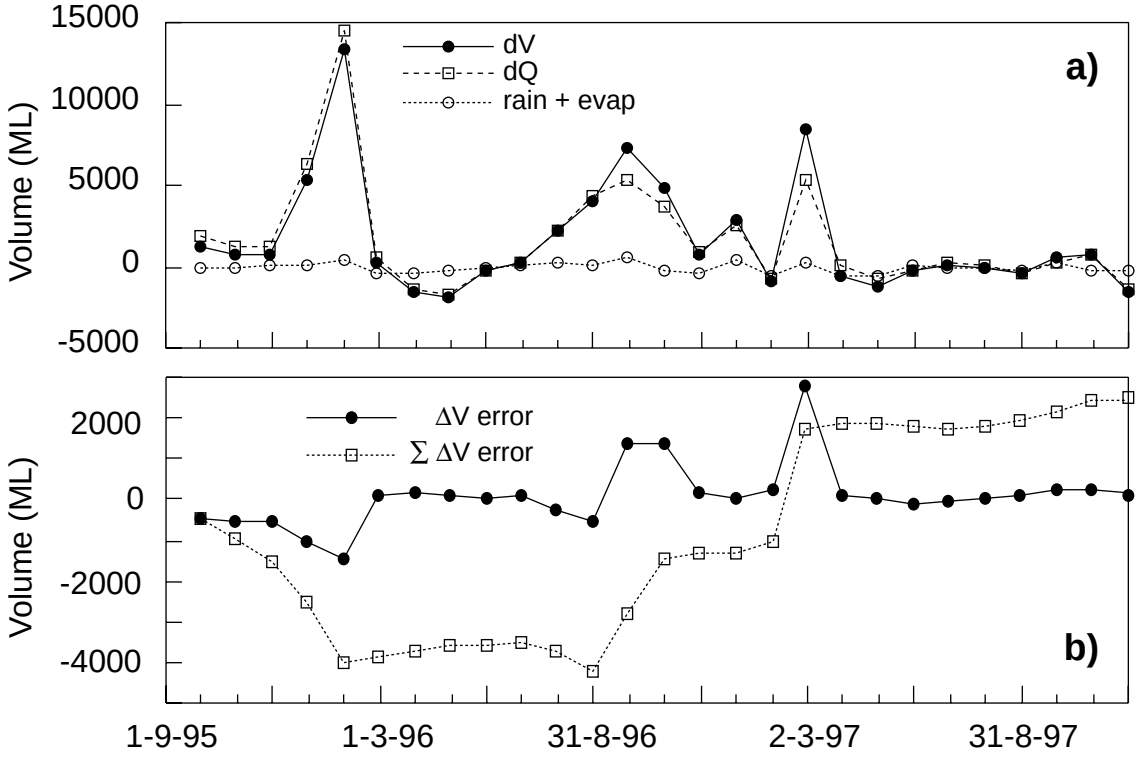

Figure 6.5 a) Components of the water budget at Chaffey Reservoir. Observed change in reservoir volume, dV, net inflow, dQ, and net rainfall + evaporation. b) Monthly (ΔV error) and cumulative (∑ ΔV error) errors in the water budget.

The components of the monthly water budget are shown in Figure 6.5a. Clearly, rainfall and evaporation are of secondary importance to the overall balance although they are of similar magnitude to *dQ* during Jun-Jul 1996 and Apr-Oct 1997. The large inflow events of January 1996 and Feb 1997 and the wet spring (Aug-Oct) of 1996 are the dominant contributors to the change in reservoir volume.

Figure 6.5b shows the monthly and cumulative values of *ΔVerror*. Significant errors (> 500 ML) only occur during months with large inflows. The small *ΔVerror* during months with little *dQ* suggest that the rainfall and evaporation estimates are sound.

The most likely source of error in the water balance appears to arise from inflows when the river stage exceeded the maximum gaged flow. There is a high uncertainty associated with the extrapolated values of the rating used to compute these flows from the river stage. During the period 1 Sep 95 - 30 Nov 97 the total

inflow was gaged at 58732 ML. Of this, 36290 ML occurred at discharges greater than the highest measurement used in the rating table, i.e. the flow exceeded 267 ML d^{-1}. The error in these flows can easily exceed 10% which could account for most of the cumulative error of 2500 ML. Errors in evaporation and rainfall could not account for the large errors in dV that coincided with large inflows because rainfall and evaporation were very small compared to inflow.

6.3.2 Heat budget

The heat content of the reservoir at any given time is,

$$HC = \rho C_p \int_0^{wsl} A(z)T(z)\,dz$$

where ρC_p is assumed constant (= 4.173×10^6 J m^{-3} $°K^{-1}$), $A(z)$ is the area of the reservoir at height z above the bottom (m^2), and $T(z)$ is the corresponding temperature of the water column (°K). The observed change in heat content during Δt is simply $\Delta HC_{obs} = HC(t+\Delta t) - HC(t)$.

The heat contributed during Δt by inflows, H_{in}, and outflows, H_{out}, is,

$$H_{in} = \rho C_p \int_0^{\Delta t} Q_{in}(t)T_{in}(t)\,dt$$

$$H_{out} = \rho C_p \int_0^{\Delta t} Q_{out}(t)T_{out}(t)\,dt$$

where Q is the discharge (m^3 s^{-1}), T is the temperature (°K), t is the time (s) and subscripting denotes inflow or outflow.

Rainfall and surface heat transfers act over the surface of the reservoir. The rain was assumed to have the same temperature as the inflow on the same day giving a heat contribution of,

$$H_{rain} = \rho C_p R(t)T_{in}(t)A(t)$$

where R is the rainfall (m) and A is the surface area of the reservoir (m^2) at time t.

The surface heat flux was computed as the sum of sensible, Q_{sens}, latent, Q_{lat}, net shortwave, Q_{sw_net} and net longwave radiation Q_{lw_net},

$$H_{surf} = \int_0^{\Delta t} \left(Q_{sens}(t) + Q_{lat}(t) + Q_{sw\_net}(t) + Q_{lw\_net}(t) \right) A(t)dt$$

If all data are internally consistent, the predicted change in heat content,

$$\Delta HC_{predicted} = H_{in} - H_{out} + H_{rain} + H_{surf}$$

should exactly match ΔHC_{obs}. Note that H_{surf} can be negative when a net loss of heat to the atmosphere occurs.

The observed and predicted daily reservoir heat contents are shown in Figure 6.6a. The observed change in heat content, ΔHC_{obs}, and the components that make

up $\Delta HC_{predicted}$ are shown, computed on a monthly basis, in Figure 6.6b where surface heat transfers and rainfall have been combined because they both act upon the same surface area. There is clearly a large discrepancy between observed and predicted heat contents.

The potentially major sources of error are: inflow volumes; reservoir volume; and surface heat fluxes including rain. The quantities ΔHC_{error}, ΔHQ_{error}, and $\Delta HC_{residual}$ shown in Figure 6.6c represent respectively the difference between observed and predicted changes in heat contents, the heat contribution associated with the error in the water balance, and the residual error in the heat budget after adjusting for the water balance error. After correcting $\Delta HC_{predicted}$ for the heat contained in the water balance error, the residual error in the heat budget is consistently negative and varies between 1 and 3% of the total reservoir heat content with a mean value of 2%.

The most likely explanation for the residual heat budget error is that the storage table (area vs depth) for the reservoir is biased and underestimates areas by 2% from their actual values. The corresponding heat content would then be underestimated by a similar percentage. This is not an unreasonable error given that storage tables are derived from contour maps using planimetry. An error in measuring the mean reservoir temperature of nearly -4.5°C, which is not possible, would be required to produce a comparable heat content error.

6.3.3 Conclusion

Heat and water budget calculations have highlighted the errors associated with streamflow and reservoir volume measurements. Water balance calculations showed that 62% of the total inflow to the reservoir occurred at river stages exceeding the highest measured flow. Uncertainty in the rating of the Taroona streamflow gage at high flows is the most likely explanation for the observed imbalance in the water budget.

The total heat contributed by inflow during the project was comparable to the heat content of the reservoir when full and approximately 6 times greater than the total heat supplied from surface heat fluxes. Heat budget calculations, after correction for the heat content of the water budget volume error, consistently underestimated reservoir heat content by 2%. This suggests that the storage table is biased and that areas should be increased by a corresponding amount. Other possible sources of error associated with calculated surface heat fluxes, rainfall, horizontal variability in temperature make only a minor contribution to the error in the heat budget calculations.

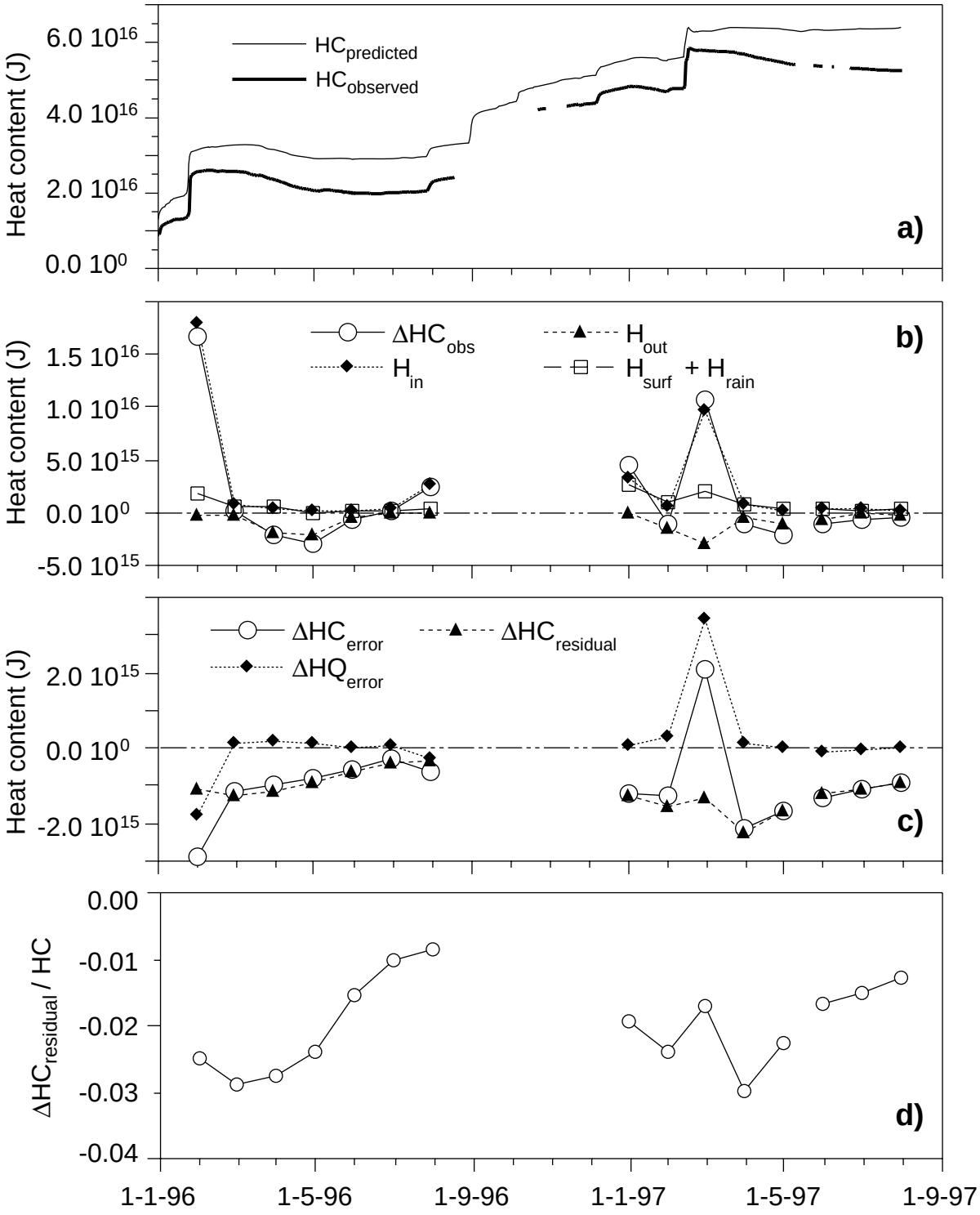

Figure 6.6 a) Predicted and observed daily reservoir heat contents. b) Monthly observed change in heat content (ΔHC_{obs}), predicted change due to inflow (H_{in}), outflow (H_{out}), and surface heat trnasfers + rainfall ($H_{surf} + H_{rain}$) c) Difference between observed and predicted heat content change (ΔHC_{error}); heat content associated with the water balance error (ΔHQ_{error}); and residual error ($\Delta HC_{residual}$) after correction for the water balance error. d) Residual error as a proportion of the reservoir heat content.

7 Transport processes

The physical transport processes in the reservoir establish the conditions under which the phytoplankton must grow. Of particular concern are changes in the depth of the surface layer, which governs the light climate, and the supply of nutrients to the water column, and especially to the euphotic zone. Atmospheric conditions and thermal stratification in the water column are the most significant factors controlling the depth of the surface mixed layer. Inflow events introduce sediments and nutrients from the catchment and transport them horizontally into the water column. Turbulent diffusion, surface layer deepening, and large-scale circulation caused by artificial destratification and differential cooling transport nutrients upwards from the sediments to the euphotic zone. Boundary mixing caused by both surface and internal waves breaking along the shoreline can liberate nutrients from the sediments and transport them laterally.

In this chapter we examine the most important transport processes in the reservoir. This information will then provide the physical context of the biology and chemistry in the chapters that follow.

7.1 Inflow events

When the sediment-laden inflows typical of the Peel River enter the reservoir they first mix with the ambient water at the upstream (south) end of the dam and then they plunge to a level where the density of the inflowing water matches that of the undisturbed water column. This is called the ‘level of neutral buoyancy’ and depends mainly on the temperatures of the inflow and the water at the upstream end of the storage. Our measurements showed significant changes in the temperature of the inflow over the 6.7 km between Taroona, where temperature has been measured historically, and immediately upstream of the reservoir; this has significant implications for accurately predicting the level at which the intrusion will form.

The inflow intrudes into the rest of the basin at the level of neutral buoyancy carrying with it nutrients and suspended sediment. As the intrusion proceeds towards the dam wall it spreads out laterally and decelerates. This allows the larger sediment particles to sink out of the intrusion. The shallowness and gentle slope at the south end of the reservoir (Figure 5.1) ensure that significant mixing of the inflowing water with reservoir water can occur for up to 2 km (depending on reservoir level) after the river enters the reservoir, after which inflows may plunge and intrude into the deeper main basin.

The two largest inflow events during the study occurred in January 1996 and February 1997 (Figure 6.3). In both cases the inflow intrusion propagated into the water column below the surface mixed layer. The January 1996 inflow was very turbid and intruded below a depth of 11 m while the destratifier was operating. Approximately 2 days after the flood peak was recorded at the Taroona gauging station, water within the bubble plumes became muddy while the surrounding water remained relatively clear, implying that the intrusion had finally arrived at the dam wall.

The 13-16 February 1997 inflow produced an intrusion with high nutrient concentrations and a very strong conductivity signature (Figure 7.1). The conductivity profile on 11-02 shows the conditions in the dam prior to the inflow. One week after the inflow, the conductivity profile on 21-02 shows a prominent intrusion of lower conductivity water between 4 and 11 m depth. The intrusion contained very high phosphorus concentrations and increased the TP concentration at a depth of 10 m by over 100 µg L^{-1} from pre-inflow value (Figure 7.1, bottom); most of the increase in TP was in the form of FRP. The intrusion remained relatively undisturbed between 4-12 m through 4 Mar 97. During the following weeks autumnal cooling caused the surface layer to deepen (heavy line, Figure 7.1, top) which lowered the top of the intrusion's conductivity signature as water from the top of the intrusion was entrained into the surface layer. Surface layer FRP and TP concentrations increased as a result of the entrainment and a spurt of algal growth followed immediately (Section 9.2.4.1). The magnitude of the conductivity peak diminished as well due to a combination of diffusive transport and, presumably, in-situ chemical reactions affecting CO_2 concentrations. This illustrates vividly how vital both the surface layer dynamics and the inflow temperature are in determining the response of the reservoir to external contaminant loads.

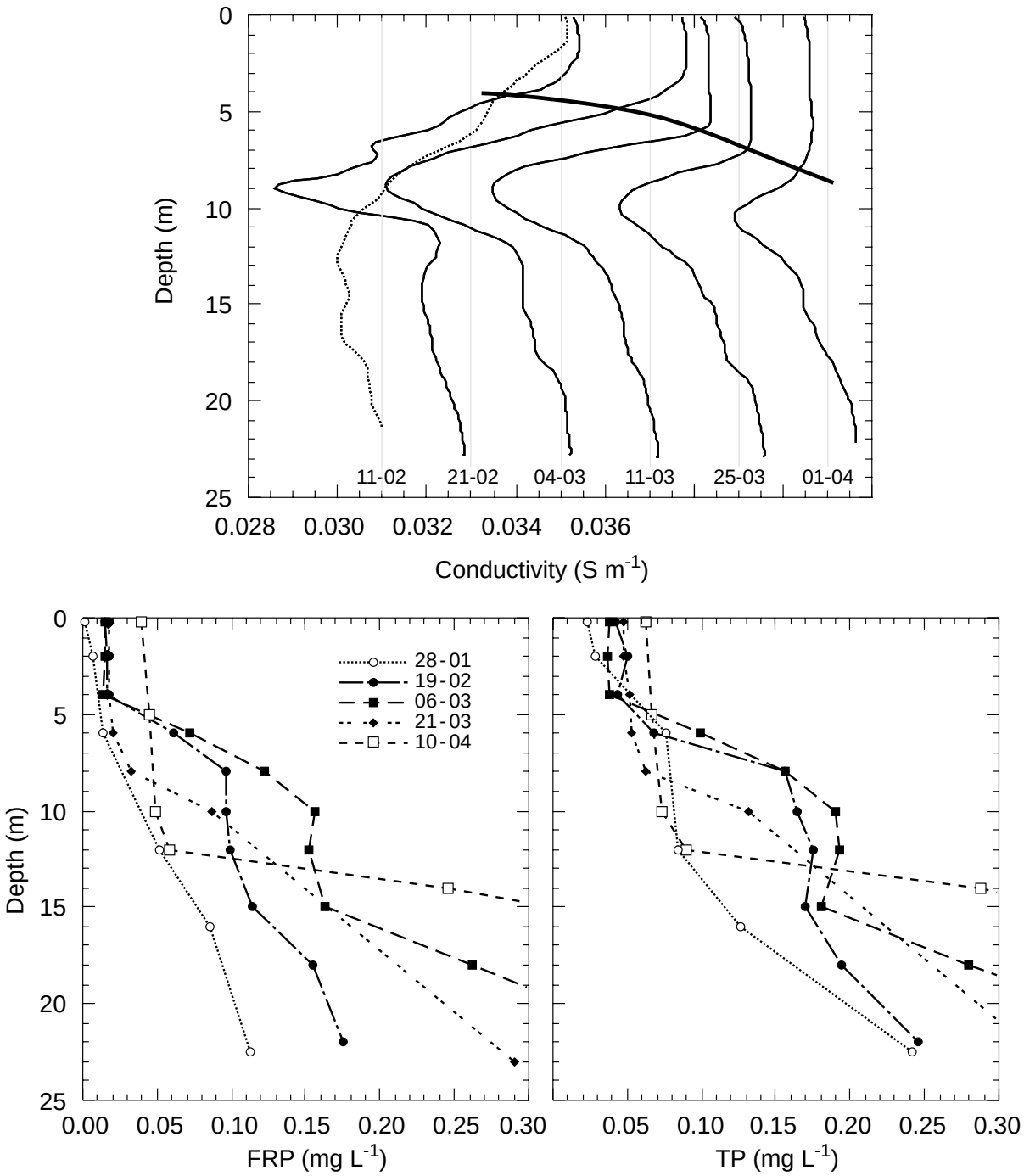

Figure 7.1 Conductivity (top) and FRP and TP (bottom) profiles measured at Chaffey Reservoir before and after the Feb 97 inflow. Conductivity profiles are offset by 0.002 S m^{-1}; gray vertical lines are located at 0.031 S m^{-1} for each profile. The trajectory of the maximum surface layer depth between profile is shown by the heavy line in the upper figure.

7.2 Surface layer dynamics

The dynamics of the surface mixed layer (SML) control the amount of light experienced by the phytoplankton and is an important determinant of algal growth rates. The intimate coupling between surface layer depth, turbulence, phytoplankton photophysiology and growth are detailed in Chapter 8. In this chapter the focus is on the essential physical attributes of the SML; its depth, h, and the characteristic turbulent velocity of the water in it, q^*.

The depth of the surface layer is particularly important for regulating phytoplankton growth. As h increases, the light dose experienced by the phytoplankton decreases until eventually there is insufficient light to allow a population to grow. Buoyant or motile phytoplankton such as *Anabaena* sp., *Botryococcus*, and *Ceratium* are particularly well-adapted to grow in systems with strong stratification and where $h/z_{eu} \sim 1$, where z_{eu} is the euphotic depth (1% light penetration). The harmful cyanobacterium *Anabaena circinalis* is particularly sensitive to the daily photon dose and usually is not present in significant quantities when $h/z_{eu} > 3$ (Sherman et al. 1998). Artificial destratification is often employed in hope of deepening the SML in order to light-limit the growth of phytoplankton.

There are many operational definitions of h. These are usually based on some sort of temperature criterion, with the exact choice depending on how detailed the knowledge of the thermal stratification of the water column is. Recently, Visser et al. (1997) have drawn on theory originally presented by Monismith (1986) and computed a surface layer depth from local wind speed and intermittent (daily to weekly) temperature profile data. In their scheme, the surface layer depth is defined as that depth which produces a surface layer Wedderburn number of 1; this is the condition for upwelling at the upwind end of a water body subjected to a wind stress (Monismith 1986). One weakness of the Wedderburn number-based definition is that it assumes the wind blows from a constant direction for a sufficiently long time to allow the thermocline to upwell. Recknagel (1983) defined h as the depth where $dT/dz \geq 1.0$ °C m^{-1}. Both of these definitions can allow the presence of chemical gradients within the SML.

We prefer a more stringent definition of the SML as the region adjacent to the water surface without any thermal or chemical gradients, i.e. a region that is truly well-mixed. Our interest is in the chemical and biological characteristics of the reservoir and this is the zone that is occupied by the nuisance algal species of most concern. Microstructure TDFO profiles have revealed that temperature changes as small as 0.05 °C are sufficient to prevent downward transport of buoyant algae in Chaffey Dam (Figure 7.2, Sherman et al. 1999).

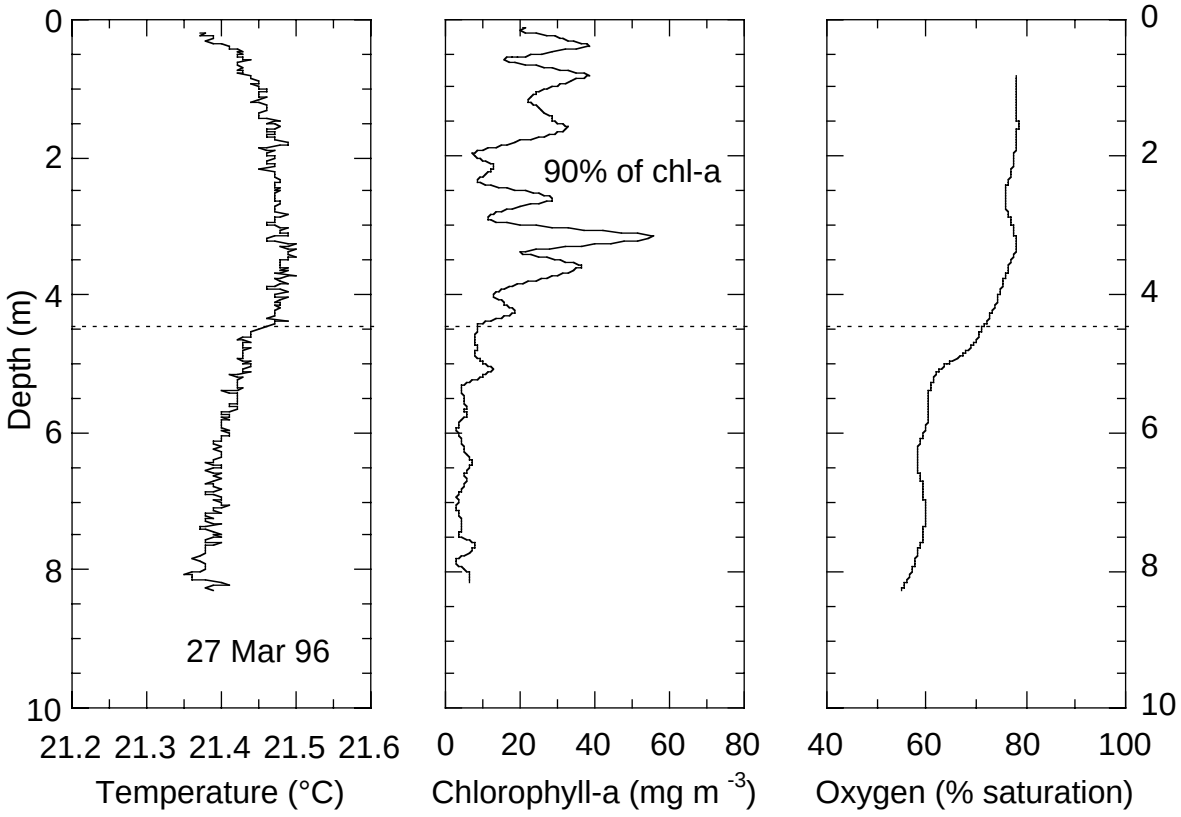

Figure 7.2 TDFO profile taken 27 Mar 96. 90% of chl-a was located above the 0.04 °C temperature change at 4.5 m (dashed line). The dissolved oxygen profile shows that the homogenous region is between the surface and 3.5 m, the depth at the bottom of the unstable temperature distribution and corresponding to the top of the chl-a gradient. Figure from Sherman et al. (1999).

Because TDFO data are seldom available, the surface layer depth, *h*, was determined from the thermistor chain data as follows. If an unstable temperature profile existed (colder water overlying warmer water) , e.g. due to nightime cooling at the water surface, the surface layer was assumed to have mixed downwards to the next successive thermistor and the mean temperature of this 'deepened' surface layer was computed. This process was repeated until the mean temperature of the surface layer was at least 0.05 °C warmer than the temperature at either of the next 2 thermistors down the chain. The temperature profile between the next two thermistors below this layer was extrapolated until it intersected the temperature of the surface mixed layer. The point of intersection was considered to be the depth to which thermal convection would mix the surface layer and is defined as the surface layer depth, *h*. This definition of *h* generally was in good agreement with the instantaneous depth of the isothermal surface layer determined from the TDFO profiles but can underestimate *h* by up to 0.5 m from the microstructure value (Whittington et al. submitted).

Figure 7.3 shows the average and maximum daily surface layer depths, *h*, during 1995-1997. The maximum *h* represents the depth to which algae in the SML are homogeneously mixed at the start of each day and is generally less than 5 m during the summer, but often deeper than 10 m during the winter. However, there can be *sustained periods of shallow maximum SML depth during the winter*, for example mid-June to mid-July 1996, in which case buoyant and motile algae would not have to travel far to occupy the euphotic zone. Another striking

feature is that the average daily *h* is usually significantly less than 5 m at all times of year. Notice also that the SML was deeper during winter 1997 than in winter 1996. The difference may be due in part to the deeper water column in 1997, which reduced the horizontal temperature gradients produced by differential cooling (section 7.5) and thereby reduced the vertical temperature gradients as well (i.e. decreased temperature differential across a deeper water column).

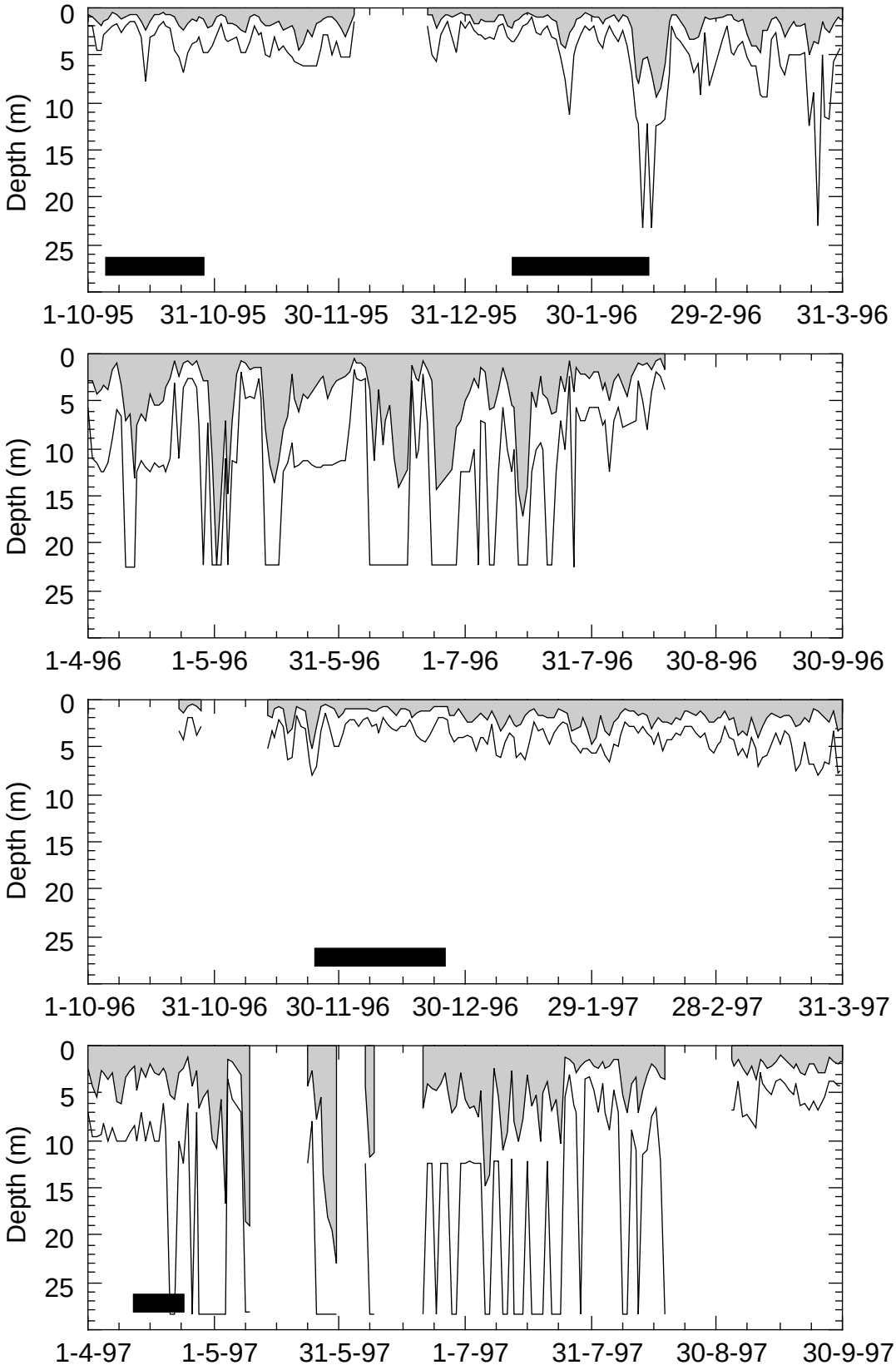

Figure 7.3 Average (shaded area) and maximum (solid line) daily surface layer depth, h, computed from thermistor chain data during summer and winter periods from 1995 to 1997. Gaps indicate periods of missing record. Solid black bars denote operation of the destratifier.

Figure 7.4 shows the time course of *h* for an 'average' day at Chaffey reservoir. The water column, on average, is stratified all the way to the surface from 09:00 to

16:00, i.e. h = 0, and never deeper than about 4 m, which is roughly the euphotic depth, i.e. $h / z_{eu} \sim 1$. Perhaps more surprising is that the surface layer was never deeper than 7-8 m from 10:30 – 13:30. These data include the winters of 1996 and 1997! If just the data from June and July are considered, h is nearly identical apart from being 5 m deep at 06:00. Even in winter, the diurnal stratification creates a suitable physical environment for buoyant (e.g.*Anabaena*.) or motile (e.g. *Ceratium*) phytoplankton that can maintain themselves in the surface layer where light conditions are favourable.

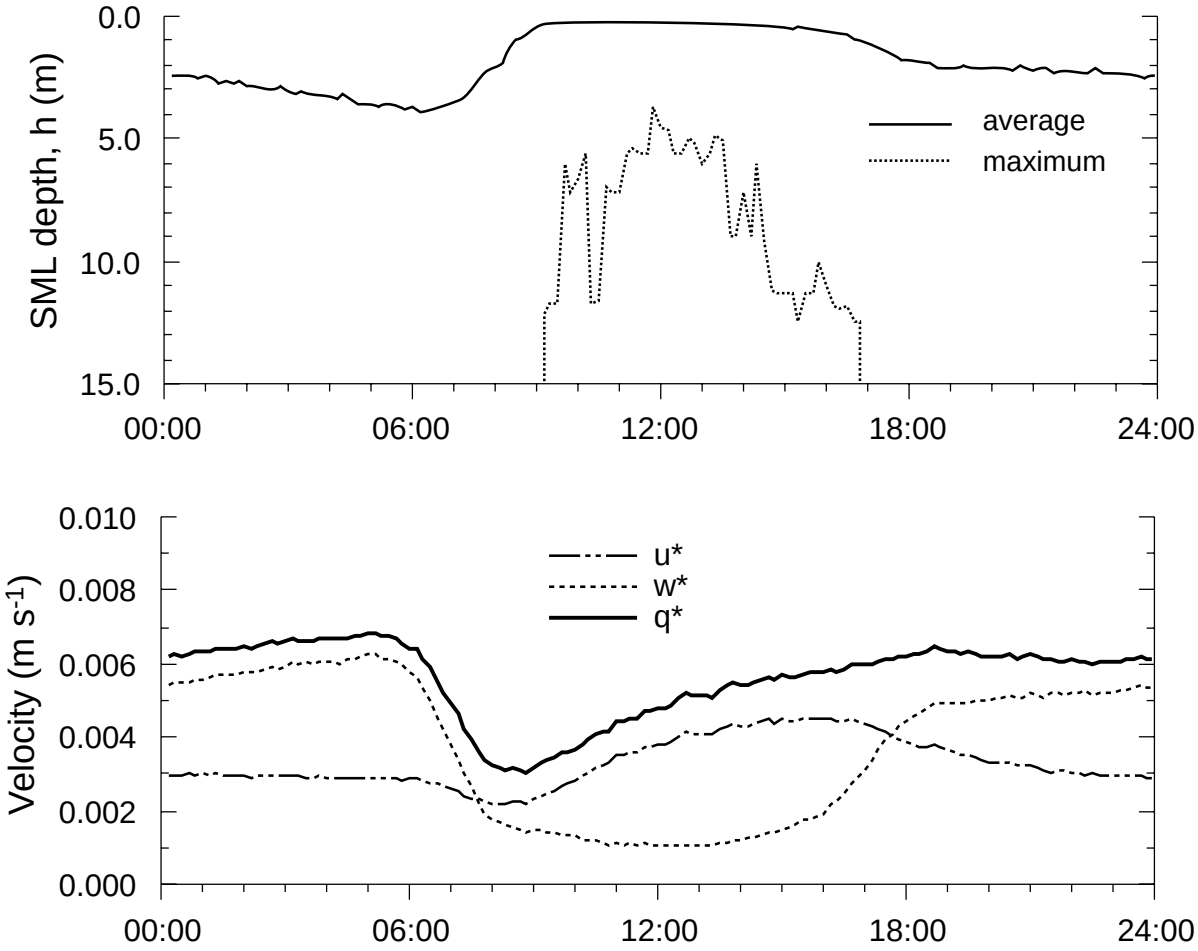

Figure 7.4 Average and maximum surface mixed layer depth, h, (top) and average u*, w*, q* (bottom). Data shown are for a composite day averaged from 644 days of 10-minute data.

The turbulent velocity scale, q^*, is important because it determines whether or not buoyant or motile species can effectively position themselves in the water column (Humphries and Imberger 1982). It also influences the time required for sedimenting particles to fall out of the surface layer. The relationship between q* and swimming (or floating) speed of phytoplankton in Chaffey Reservoir is described in chapter 8.

Wind stirring and convective cooling both contribute to q^* according to Fischer *et al.* (1979) as,

$$q^* = (w^{*3} + \eta^3 u^{*3})^{1/3} \qquad (7.1)$$

where η is a constant (= 1.23) and w^* and u^* are the turbulent velocity scales in the water column due to cooling and wind stirring, respectively, and are derived from the turbulent heat and momentum fluxes across the air-water interface. The diurnal time courses of u^*, w^*, and q^* for an 'average' day are shown in Figure 7.4. Between 09:00 and 15:00 the average q^* is 0.0047 m s^{-1}; during the winter months it is about 20% less.

7.3 Impact of destratification

We focus here on the effects of the destratifier (described in Section 4.2.2) on the thermal stratification and circulation within the reservoir. When operating, each cone-shaped rising plume of bubbles entrained ambient fluid from throughout the water column and carried it up to the water surface. At the surface, the plume spread out radially over a short distance (~5-7 m), then plunged to a depth where its density matched that of the reservoir (the level of neutral buoyancy), and finally intruded into the body of the reservoir at this depth (Figure 7.5). The maximum speed at which the intrusion propagated away from the plumes was about 0.08 m s^{-1} close to the plumes in January 1996 but varied depending on the thickness of the intrusion and distance from the plumes. In April 1997 the intrusion was thicker and drogues deployed in the intrusion travelled more slowly at 0.01-0.04 m s^{-1} or about 2 km, approximately the width of the reservoir, in one day.

Flow away from the plume in the intrusion was balanced by a return circulation consisting of two gyres; one above the level of the intrusion and one below it. The return flow below the intrusion is entrained into the bubble plume and must be supplied by a net downwards movement of the water column below the intrusion. Computer simulations (McCord, pers. comm.) of the entrainment during January 1996 showed a downward velocity of roughly 1.1 x 10^{-5} m s^{-1}, or about 0.95 m d^{-1}.

Because the temperature of the water entrained from the SML varies diurnally, the level of the intrusion also varies with the time of day; it is closer to the surface in the afternoon and deepest at dawn.

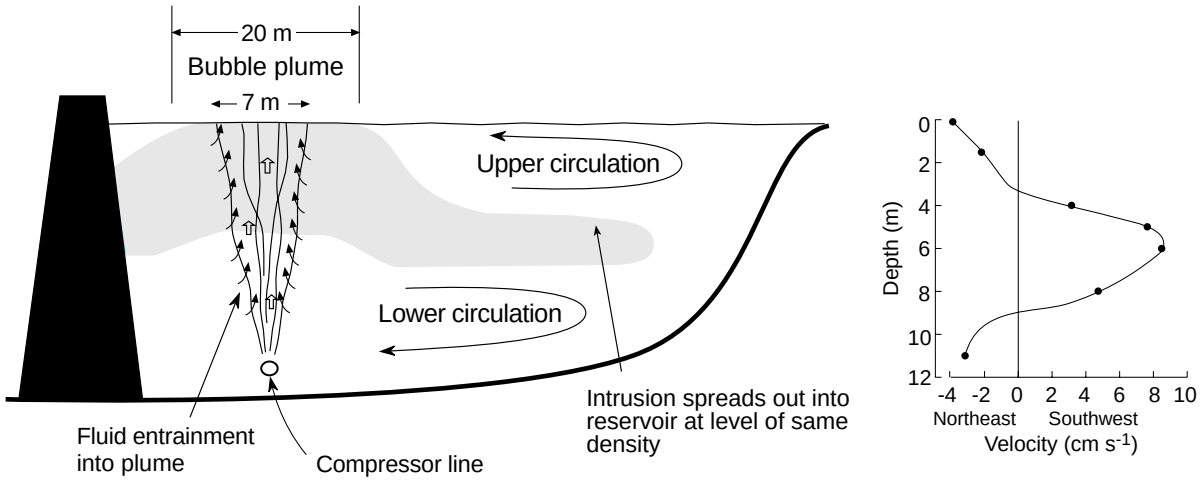

Figure 7.5 Schematic diagram of the circulation patterns established by artificial destratification at Chaffey Reservoir. Also shown is the velocity profile measured

on 13 Jan 1996 at a location 70 m south of the center of the line of bubble plumes. Positive velocities move towards the southwest, away from the plumes.

As soon as the destratifier was turned on a steady increase in the temperature at the bottom of the water column was observed and the shape of the profile changed from approximately exponential to roughly linear (Figure 7.6). This quasi-equilibrium linear temperature gradient typically was approached within a fortnight of turning on the compressor. As the operation of the compressor continued, the temperature difference between the surface and the bottom remained approximately constant during the spring, when the reservoir was heating up, whereas it decreased slowly in summer and autumn. The quasi-equilibrium profile represents a balance between heat transfers across the air-water interface, absorption of solar radiation and the artificially enhanced downward advection of heat.

The apparent overturn of the water column on 12 Feb 1996, indicated by isothermal conditions, was caused by a period of unusually cold and windy weather on 9-10 February. Operation of the destratifier helped facilitate the mixing by weakening the stratification, but it was the unusually extreme meteorological conditions that did the mixing. At this point the destratifier was turned off and the SML shoaled back to 2-3 m soon afterwards (Figure 7.3). Other periods of destratifier operation had no impact on SML depth despite changing the temperature profiles and highlight how significantly undersized the destratification system is.

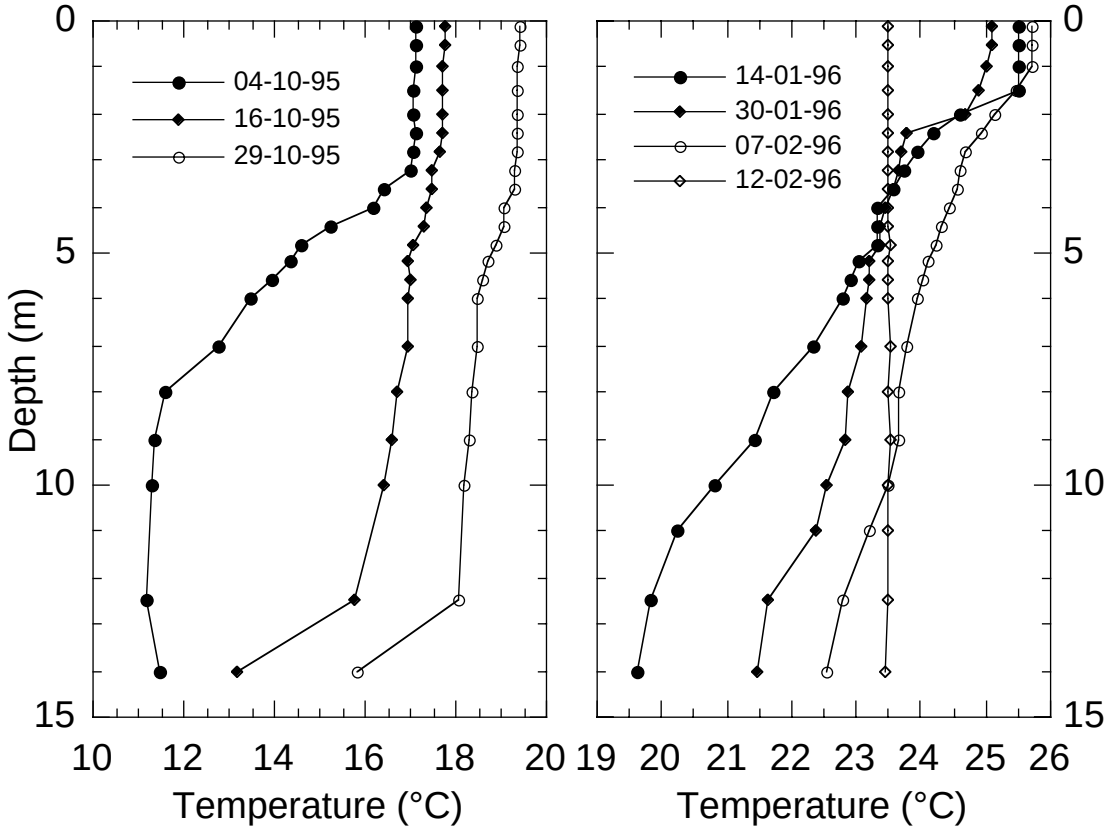

Figure 7.6 Temperature profiles at Chaffey Dam during the operation of the destratifier from 4 - 28 Oct 1995 and 11 Jan - 13 Feb 1996. A 3 - 4 m deep surface layer persisted during the October 1995 operation and in January 1996 the layer

was just 2 m thick. Unusually cold, windy weather on 9 - 10 Feb eliminated the stratification by 10 Feb 1996.

The vertical distribution of dissolved oxygen (data not shown) also assumed a linear quasi-equilibrium gradient, but required longer - at least 3 weeks - to do so. Typically the DO at the bottom of the water column was maintained at 50-60% of saturation and at the surface it was 70-80% of saturation. In the case of dissolved oxygen, equilibrium represents a balance between air-water exchange, in-situ photosynthetic production (near the surface), in-situ demand for oxygen and the vertical transport of oxygen resulting from the increased circulation.

The actual volume of water mixed by the bubble plumes themselves on any given day is quite small and it is important to remember that large-scale mixing of the reservoir only occurs as a result of the introduction of mixing energy from the atmosphere through a combination of wind stirring and heat loss. The function of destratification is to reduce the resistance of the water column to mixing, not to provide all the mixing energy itself.

7.4 Turbulent diffusion (hypolimnion to epilimnion)

Turbulent diffusion from the hypolimnion to the SML is an important vertical transport process in the absence of inflows or the operation of the destratifier. Increases in turbulent diffusive transport beyond the molecular levels reflect the contributions of internal wave activity including processes such as mixing at the boundaries and internally breaking waves.

The magnitude of turbulent diffusion was estimated by the flux-gradient method. The diffusivity, κ, is computed from,

$$\Delta H = \Delta T \rho c_p V = \kappa \rho\, c_p A \frac{dT}{dz} \Delta t$$

$$\kappa = \frac{\Delta T / \Delta t}{dT / dz} \frac{V}{A}$$

where ΔH is the change in heat content of the hypolimnion during the time interval Δt, dT/dz is the temperature gradient in the thermocline above the hypolimnion and ρ and c_p are the density and heat capacity of water, V is the volume of the hypolimnion, and A is the area at the top of the hypolimnion. The term V/A is approximated as the height of the hypolimnion. This method is most reliable for intervals with minimal inflows and outflows and no operation of the destratifier.

Table 7.1 Turbulent diffusivity calculations for Chaffey Reservoir.

year	Tend (°C)	Tbegin (°C)	Δt (s)	$\Delta T/\Delta t$ (°C s^{-1})	$\Delta T/\Delta z$ (°C m^{-1})	κ_{turb} (m^2 s^{-1})
Sep 95	10.25	10.86	1.0368e+06	5.65e-07	0.545	8.0e-06
Mar 97	17.68	17.77	3.2832e+06	3.24e-08	0.392	8.2e-07
1998	13.0	11.4	1.4435e+07	1.08e-07	0.68	2.1e-06
1999	12.9	11.0	1.8744e+07	1.00e-07	0.74	1.8e-06
2000	12.8	11.5	2.0876e+07	5.99e-08	0.72	1.1e-06

Two periods were chosen for the calculation: 11-23 Sep 1995 and 6 Mar-13 Apr 1997. These periods had little or no inflow and a positive net heat flux into the water column. During spring 1995, the calculated κ was 80 times greater than the molecular value whereas in autumn 1997 it was 8 time greater. The results are shown in Table 7.1 which also gives seasonal estimates of turbulent diffusivity computed from fortnightly CTDO profiler data collected by DLWC during 1997-2000. The lower values are more typical of conditions in the reservoir during summer and autumn. In comparison, the downward advective transport of heat caused by operation of the destratifier would be equivalent to a turbulent diffusivity 1000 times greater than the molecular rate.

The flux-gradient method is commonly used to estimate turbulent diffusivity in lakes and oceans and provides a basin-wide average of vertical transport (Imberger 1998; Wüest and Gloor 1998). A reasonably universal finding is that this average transport is typically 10-100 times faster than molecular rates. Most of the time Chaffey Reservoir falls at the low end of this range, presumably a result of the mild climate and light winds. Another common finding is that transport occurs at near molecular rates in pelagic regions implying that the overwhelming majority of transport and mixing occurring in the benthic boundary layer. This latter result is consistent with the higher turbulent diffusivity computed for Chaffey reservoir in Sep 1995 when the storage was just 20% full and would have had a much higher ratio of benthic boundary layer volume to total reservoir volume as compared to Mar 1997.

7.5 Differential cooling

When heat is lost from the water surface, the SML temperature decreases at a uniform rate across the reservoir surface until the SML deepens to the sediment. This occurs first at the edge of the reservoir where the water is shallow. Since all of the heat loss comes from the SML, once it deepens to the bottom in the shallower regions, these areas become colder more quickly than the rest of the reservoir where the SML is still deepening. As the cooling continues, a horizontal temperature gradient is established where water in the shallow areas is colder than water at the same depth in the deeper areas. The horizontal temperature gradient produces a density current in which denser (colder) water from the shallows flows along the bottom of the reservoir until it reaches its level of neutral buoyancy at which point it intrudes into the main basin of the reservoir. Figure 7.7 shows the circulation for the case where the intrusion occurs along the bottom. This process is called differential cooling. Given its ubiquitous nature it is surprising that relatively few field studies have examined it in detail (e.g., Wells and Sherman, accepted; Sturman et al., 1999; Finnigan and Ivey, 1999; Monismith et al., 1990).

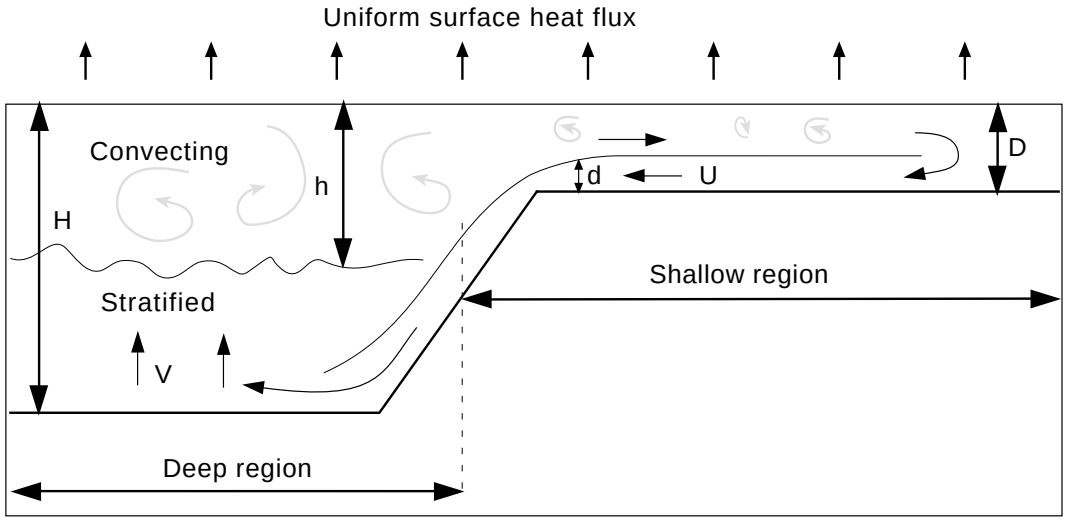

Figure 7.7 Schematic diagram of circulation induced by differential cooling. Reproduced from Wells and Sherman (submitted).

During the winters of 1995 and 1996, a cold intrusion that covered the bottom 4.5–5 m of the reservoir appeared in each of the weekly CTDO casts at Stn1 (Figure 7.8). Each week, the temperature profile became colder everywhere while at the same time stratification persisted. In a purely rectangular basin one would expect the initial stratification to be mixed out followed by progressive cooling of a persistently well-mixed water column. The particularly prominent intrusion on 20-6-95 reflects the presence of an inflow that occurred during the previous week. During winter 1996 there were no significant inflows and the volume of the intrusion (see below) comprised less than 5% inflow from the catchment.

The persistent presence of the intrusion suggests that the lower region was being refilled continuously with differentially-chilled water. Wells and Sherman (submitted) extended the experimental results and theoretical analysis of Wells et al. (1999) to the Chaffey data and computed a time scale of 7.6 days for the renewal of the intrusion during 1995. This in turn implies a circulation time of roughly 5 weeks for the entire reservoir during winter 1995 because the intrusion accounted for approximately 20% of the volume of the reservoir. The fact that the surface layer temperature in each of the 1996 profiles (Figure 7.8, bottom) is colder than anywhere in the preceding profile confirms that the entire intrusion must have been renewed at least weekly, otherwise we would expect the SML to deepen further by entraining the top edge of the intrusion.

Interestingly, the 1995 data are consistent with sediment trap measurements taken at the time and which required the nutrient content of the surface layer to be replenished roughly every 30 days to maintain the observed downward particulate N & P fluxes.

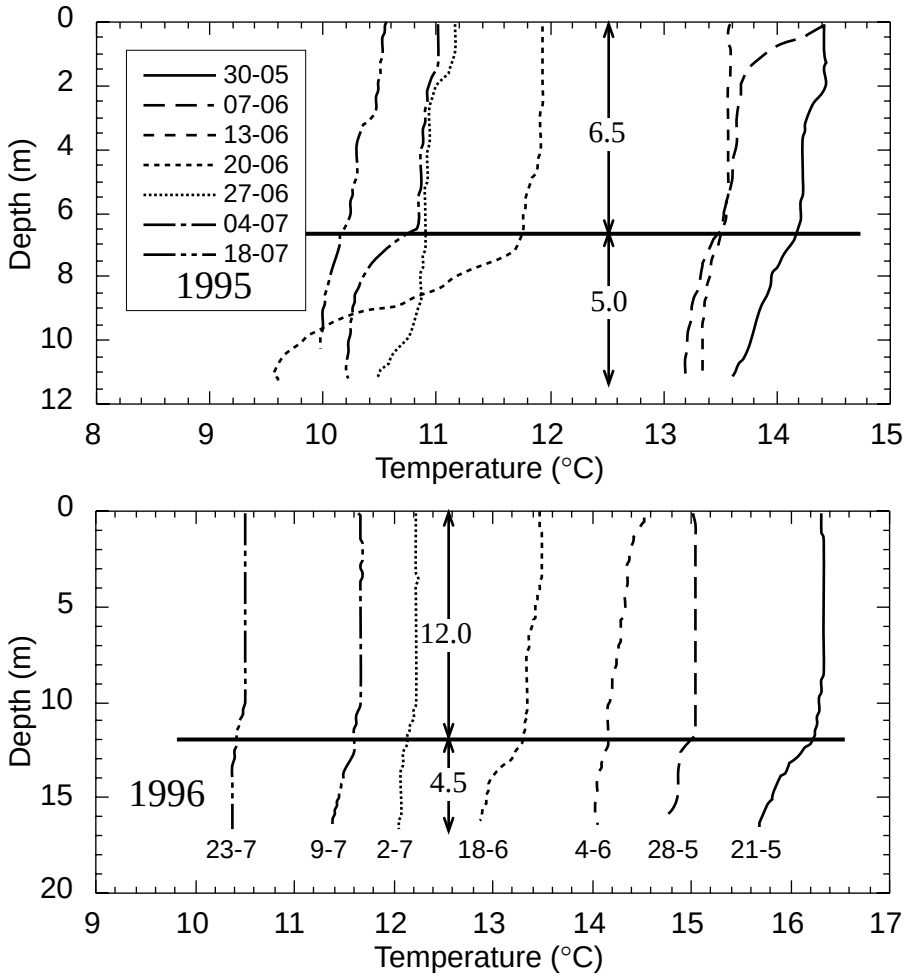

Figure 7.8 CTDO temperature profiles during the winters of 1995 and 1996 reveal a persistent cold intrusion along the bottommost 4.5-5 m of the reservoir.

Comparison of the surface layer temperatures in the CTDO profiles at Stn1 and Stn2 (data not shown, see Figure 5.1 for locations) revealed that the SML was on average 0.47 °C (median = 0.35 °C) colder at Stn2 each morning. Similar behaviour was observed in winter 1996 with Stn2 0.28 °C colder than Stn1 and Stn3 colder than Stn2. The horizontal temperature difference was less in 1996 because the reservoir was deeper than in 1995 and a deeper water column realises a smaller drop in temperature for a given surface heat flux. Notice that the horizontal temperature differences between Stn1 and Stn2 are similar to the changes in temperature between the intrusion and the SML in Figure 7.8.

The mean upward vertical velocity between the top of the cold intrusion and the bottom of the surface layer can be computed by dividing the volume flux of the intrusion, Q_i, by the surface area at the top of the intrusion, A_i, such that $v_i = Q_i / A_i$. During winter 1995 the average reservoir surface level was 506.6 m. Assuming the top of the intrusion was located 6.5 m below (Figure 7.8) gives an intrusion volume of 2.75×10^6 m^3 and surface area $A_i = 1.02 \times 10^6$ m^2. Using the flushing time scale of 7.6 days (Wells and Sherman, submitted) gives $v_i = 4.1 \times 10^{-6}$ m s^{-1} (0.36 m d^{-1}) or about 37% of the vertical velocity associated with the operation of the destratifier (but directed upwards rather than downwards)!

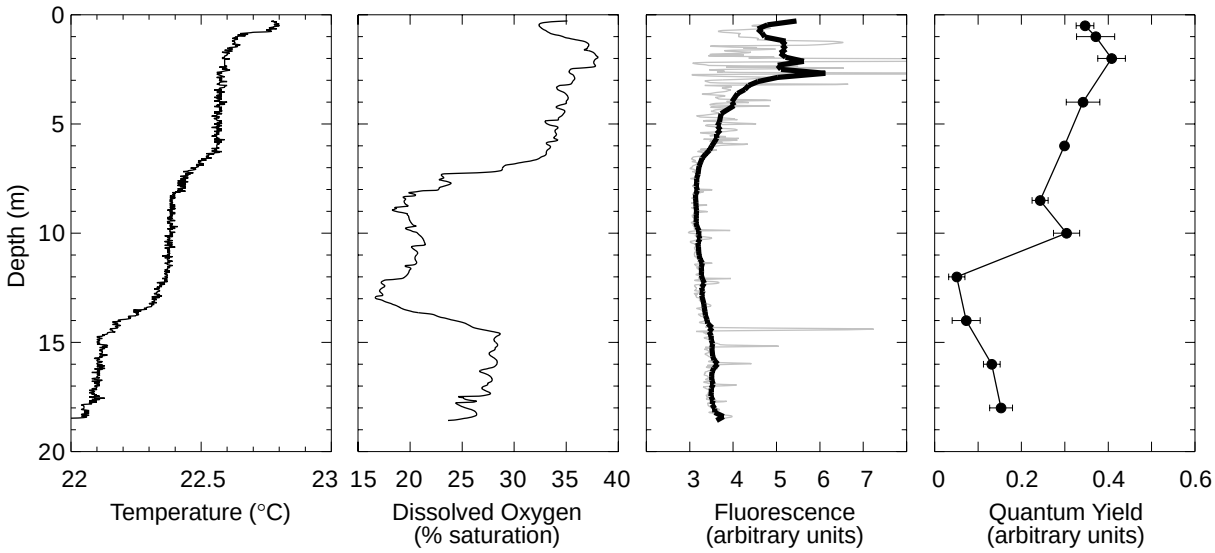

Figure 7.9 TDFO and quantum yield profiles in Chaffey Reservoir on 16 Feb 96. The bold line in the fluorescence plot is a moving average of the raw fluorescence data (gray line).

TDFO profiles taken in February 1996 showed that differential cooling also occurred in the summer on days when there was a net heat loss from the water column. Increases in dissolved oxygen, chl-a fluorescence and quantum yield of PSII (Figure 7.9) all confirmed the existence of water at the bottom of the water column (depth ≥ 15 m) that had to have been present in the SML within the previous 2 days. Note also the local increases in quantum yield and dissolved oxygen at 10 m depth which indicates the presence of a second intrusion in addition to the underflow. However, significant cooling events (net heat loss > 75 W m^{-2}) during October through March were rare and occurred on just 12 days during 1995-1996 and on 6 days in 1996-1997.

Differential cooling may explain the presence of winter blooms of buoyant cyanobacteria and the dinoflagellate *Ceratium hirundinella* as well as the relative lack of diatoms from the water column. The upwards circulation transports nutrients from the sediments into the surface layer, but the velocity is not fast enough to maintain diatoms in suspension. This circulation also produces a persistent SML that provides habitat for buoyant and motile phytoplankton species. Differential cooling appears to be a major factor influencing vertical transport within the water column at Chaffey Reservoir.

7.6 Summary

There are 3 main vertical transport processes that operate throughout the thermocline and hypolimnion in Chaffey Reservoir. Ranked in terms of an equivalent thermal diffusivity, destratification is the biggest at approximately 1000 times greater than molecular diffusion. This is followed by differential cooling during the winter months (375 x), and turbulent diffusion (8 – 80 x).

8 The nutrient story

8.1 Introduction

For algal blooms to develop, it is essential that there be sufficient nutrients available in the water column to allow the production of essential cellular constituents. The year-round shallow surface layer depths (section 7.2) ensure that there is an ample supply of light for photosynthesis to those organisms that can maintain a population within the surface layer, so the supply and composition of bioavailable nutrients is likely to be of paramount importance in establishing the maximum achievable biomass as well as the dominant phytoplankton species. Past experience in the Murrumbidgee River (Webster et al. 1996, Sherman et al. 1998) suggests that the availability of phosphorus is likely to limit the maximum achievable biomass whereas nitrogen availability may play a vital role in determining the species composition. Effective management of algal blooms in the reservoir requires an understanding of the quantities, composition and sources of nutrients that enter the water column.

Most of the nutrients within the reservoir originate from two principal sources: the catchment upstream and the reservoir's sediments. Of course, the reservoir's sediments originally were supplied from the catchment, but here they are treated as a separate nutrient source because they are now part of the reservoir environment and may be managed in a different way from the catchment. The contributions from airborne sources such as smoke and birds are expected to be small by comparison and little can be done to manage them in any event.

Nutrients that enter the water column are either available or unavailable for immediate consumption by algae. Unavailable nutrients are typically bound to sediment particles or in a form that requires intermediate processing, usually by bacteria, to make them available for algal growth. Available nutrients such as orthophosphate can be immediately consumed. Delivery of sediment from the catchment is therefore akin to adding a log to a fire whereas adding available nutrients, either released from anoxic sediments or directly from inflows, is like pouring kerosine on the fire.

The oxygen concentration in the water column acts as a throttle controlling the rate at which unavailable nutrients are converted to an available form. The rates of both sediment nutrient release and the adsorption and desorption of orthophosphate onto iron-based compounds depend on the amount of oxygen available. Some control can be exercised over these processes by controlling the amount of oxygen in the water column, for example by artificial destratification. Nothing can be done about catchment delivery of bioavailable nutrients other than to identify and manage the source up in the catchment.

This chapter describes the chemistry of the water column and sediments. It also addresses the rate at which sediment has been accumulating in the dam. Special emphasis has been placed on understanding the forms that phosphorus takes and the way in which it is converted between these forms as it is most likely the nutrient that limits the maximum achievable algal biomass. As well, the relative supply of nutrients from both internal (sediments) and external (catchment) sources is determined by computing mass balances for the major nutrients. The

physiological effects of nutrients on phytoplankton growth are described later in Chapter 9.

8.2 Sediment chemistry

Previous research by Caitcheon *et al.* (1994) and Donnelly (1993) had found that the sediments in Chaffey Reservoir are derived from the soils of the catchment upstream. These are comprised of tertiary basalts from the relatively undisturbed steep upper eastern catchment and sedimentary Devonian soils from the more gently rolling western catchment most of which is used as pasture for livestock production. The vast majority of these sediments enter the reservoir via flood events in the Peel River (section 8.5.1). The rate at which sediments are supplied has been determined by measuring the accumulation of sediments at the bottom of the dam since construction and on shorter time scales by measuring the downwards particulate flux in the water column.

In this section we examine the elemental composition and mineralogy of the sediments and the speciation of phosphorus within them. Knowing the elemental composition of the sediments allows us to identify their sources within the catchment. The phosphorus speciation data gives an indication of how spatially variable the phosphorus containing compounds within the sediments are and how difficult it is to liberate the phosphorus contained in these compounds.

8.2.1 Methods

Sediments were sampled from both Chaffey and Dungowan Reservoirs using either an Eckman grab (submerged sediments) or hand auger (exposed sediments), stored in polyethylene bags and returned to the laboratory. Dungowan Reservoir is located in an undistrubed catchment just north and adjacent to the Peel River catchment. Sampling sites were located by GPS. Altogether, 59 sediment samples were taken from Chaffey Dam - 8 from sites near the inlet of Hyde's Creek, 31 from the main basin of the dam, 16 from exposed sediments at the southern end of the dam adjacent to the Peel River, and 4 from the wash zone on the periphery of the dam (Figure 8.1). Twenty-three samples were taken from Dungowan Dam - 21 from the western reach of the dam and 2 from the eastern reach. Access to the eastern reach was constrained by low water levels and poor GPS performance. The particle size distribution was determined by wet sieving.

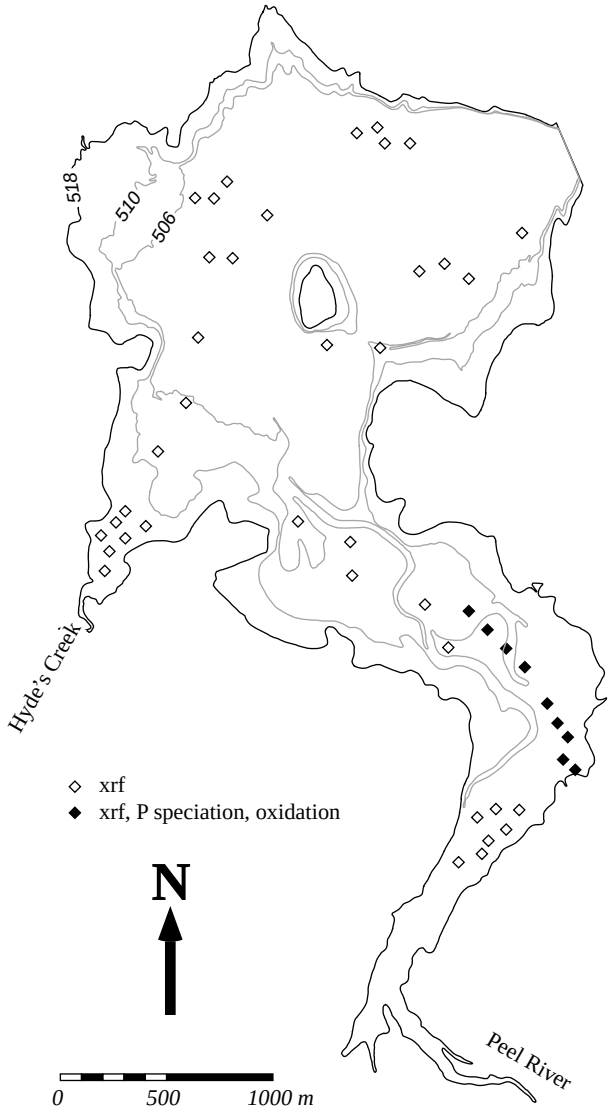

Figure 8.1 Locations of sediment samples collected from Chaffey Reservoir. Some sites not shown.

In the laboratory, the sediments were air dried, ground to a fine powder and then oven-dried to constant weight at 105 °C. Major elemental composition (Al, Ca, F, Fe, K, Mg, Mn, Na, P, S, Si, and Ti) for each sediment sample was determined at the Advanced Analytical Centre, James Cook University, Townsville, Australia by X-ray fluorescence (XRF) spectroscopy. The organic composition of the sediments was characterised using classical gravimetric methods and mass-spectroscopy to determine the amounts of organic carbon and nitrogen. Total nitrogent (TN) and total phosphorus (TP) were determined using standard wet chemical methods. A further 40 samples were collected for x-ray diffraction analysis (XRD) for sediment mineralogy.

The phosphorus speciation was determined for several of the Chaffey Dam sediment samples (Figure 5.1) using two methods: selective extraction using a modified Sedex procedure (Ruttenberg 1992; Baldwin 1996a); and ^{31}P nmr (nuclear magnetic resonance). Sequential extraction uses a series of chemical reagents of increasing severity to remove different classes of adsorbed / chemically-combined P in sediments. The measurement of ^{31}P nmr spectra on sediment extracts offers a potentially more precise determination of P speciation compared to the selective

extraction method. In the nmr method, approximately 20 g of sediment was extracted into 10 mL of 0.5 M NaOH. Following extraction approximately 1 g of Chelex resin was added to the extractant, which was then allowed to sit overnight prior to filtering. ^{31}P nmr spectra of the extractants were obtained by Dr Max Kinery, ANU.

8.2.2 Reservoir siltation

The low storage level in February 1995 allowed us to visit two of the silt pads located in the southern basins (Figure 5.1) that were installed when the dam was constructed. The silt pads are 6 m x 6 m concrete blocks poured so that their surface was level with the surrounding ground prior to the initial inundation of the reservoir. They serve as a reference level for measuring the siltation rate of the dam. The pad in the central basin had an average of 11 cm of dry sediment on it, indicating an average siltation rate of 8 mm per annum. This is a value local to the silt pad and does not necessarily reflect a basin-wide average. However, measurement at another silt pad on the opposite side of the river channel confirmed this value. Further confirmation is provided by the sediment core data presented in section 8.2.4.

8.2.3 Elemental and mineralogical composition of the sediments

Baldwin et al. (1998) used a variety of non-parametric statistical techniques (Multi-Dimensional Scaling (MDS), Analysis of Similarity (ANOSIM) and Similarity Percentages (SIMPER)) to analyse the XRF elemental composition data and define the spatial variability of sediment composition within the reservoir and between Dungowan and Chaffey reservoirs. The analysis showed three groups of sediments were present: the Peel R. floodplain sediments, Hyde Ck. floodplain sediments, and the sediments in the main basin. The results were consistent with the findings of Caitcheon et al. (1994) and Donnelly (1993) that the majority of the sediment is derived from the Tertiary basalts in the eastern catchment.

The geographical grouping of sediments is not surprising as the sediments carried by the Peel R. and Hyde Ck. have significantly different origins (Tertiary basalt vs Devonian sediment) and the coarser particles sediment out preferentially in the flood plains close to where the streams enter the reservoir. The main basin sediments contain a relatively higher content of fine particles due to sediment focusing. Sediment focusing refers to the resuspension of fine particles (clay, containing more aluminium) from the periphery of a reservoir which are subsequently deposited in the deeper portions of the dam. The sands, which contain more silica, are left behind.

Semi-quantitative XRD analysis detected four minerals in the sediments: smectite, quartz, plagioclase, and kaolinite. Smectite was dominant, with the three remaining minerals being present in accessory (5-20%) or trace components (<5%). The variation of concentration of phosphorus in the sediment was strongly correlated ($r^2 = 0.98$) with iron, manganese, and magnesium in the sediment. There was no correlation between the sedimentary phosphorus concentration and particle size, nor with total organic carbon.

8.2.4 Organic carbon in the sediments

Organic matter in the sediment is supplied from the Peel River (and to a lesser extent Hyde's Ck) and from algae that grow within the reservoir itself. This organic matter provides essential nutrition to a wide variety of protists and bacteria in the sediments which may, in turn, enhance the rate at which dissolved iron, manganese and nutrients (especially orthophosphate) are released from the sediments to the overlying water. Organic matter imported from the catchment is often harder for the microorganisms in the sediment to break down than that produced by the algae within the reservoir.

To understand the processes controlling the release of nutrients from the sediment we must characterise both the composition of the sediments and the supply of sedimenting material from the water column. Carbon, nitrogen, phosphorus and sulphur concentrations in sediment cores provide a record of significant events during the history of the dam. In the water column they tell us about the rate at which material is being recycled before it reaches the sediment. The ratio of the naturally abundant isotopes of carbon and nitrogen indicates the sources of organic matter found in the sediments. Organic matter derived from terrestrial sources and from algae have quite different 'signatures'.

On a dry weight basis the surficial sediments contained about 3% C and about 0.1 to 0.2% N. There is, however, a significant interseasonal variation in the carbon and nitrogen contents (Table 8.1). The January 1997 carbon content maximum follows a large phytoplankton bloom which collapsed in January (see Figure 9.3). The November 1997 high value could be associated with the following season's bloom, but no biomass data were not available at the time of writing. The sediment trap data (Table 8.2) shows higher mass fluxes of material with a high carbon content in the summer (albeit in 1998) relative to the winter flux rates and the carbon content of the sedimenting material. The sediment traps in the surface layer also contain freshly deposited algae, indicating a downward flux of new organic material.

Table 8.1 Seasonal variation of the chemical composition of the sediment at Chaffey Reservoir.

Month	TOC (%)	TN (mg/kg)	TP (mg/kg)	Fe (mg/kg)	Mn (mg/kg)	Mg (mg/kg)
Jan. '97	4.50	2832	244	866.1	11.07	67.67
Mar. '97	2.45	2665	243	822.8	12.28	68.48
Apr. '97	2.11	3630	351	556.4	9.41	93.45
Sept. '97	0.25	814	106	808.7	8.83	76.80
Nov. '97	5.72	1654	157	806.8	4.57	72.04

The profiles of carbon and nitrogen had a similar shape down the core although they differed in magnitude (Figure 8.2). Both showed a reversal in gradient at about 10 cm which is close to the original reservoir floor level. The decrease in carbon and nitrogen content at about 3 cm may be associated with the extended period the dam was dry in the 1993 drought. Roughly 30% of the total organic carbon was charcoal and not subject to further bacterial breakdown (Dr Jan Skjemstad, pers. comm.).

Isotopic ratios of carbon ($\delta^{13}C$), oxygen ($\delta^{18}O$), and nitrogen ($\delta^{15}N$) from a core collected in the western portion of the main basin also are shown in Figure 8.2. The predam soil surface was clearly recognisable at 14.2 cm depth within the profile. It was marked by a distinct change in texture and the presence of residual plant roots. This gives an independent estimate of the sedimentation rate of 1 cm per annum in good agreement with the silt pad estimates (section 8.2.4). The 3 isotope profiles all showed a discontinuity at approximately 12 cm from the surface consistent with a change from a terrestrial to an aquatic environment. The slight change in $\delta^{13}C$ at the transition from sediment to soil probably reflects the different sources of the 2 materials.

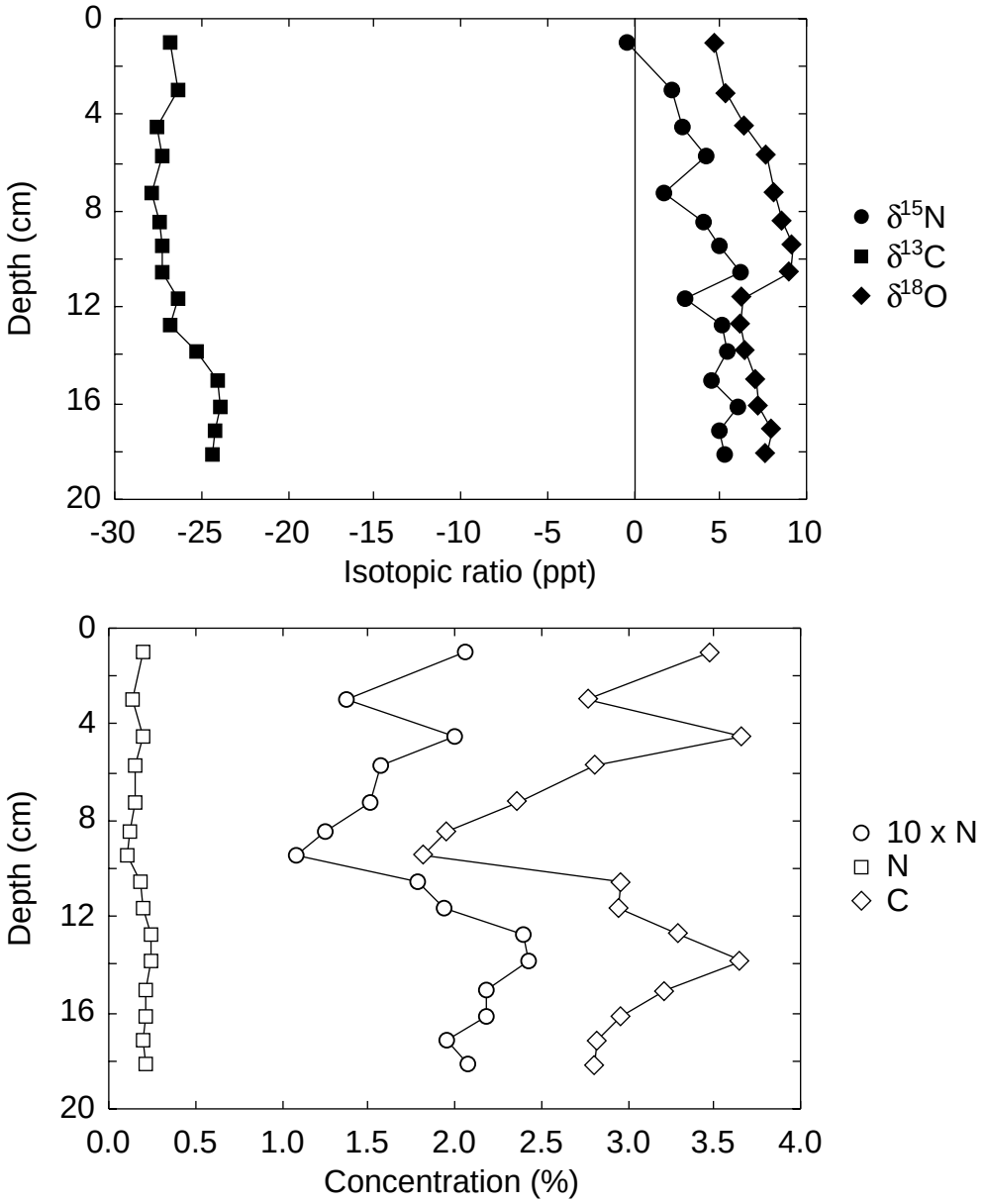

Figure 8.2 Profiles of $\delta^{13}C$, $\delta^{18}O$, and $\delta^{15}N$ (top) and % C, %N, and %N x10 (bottom) in a sediment core taken from the centre of the south basin of Chaffey Reservoir on 5 March 1997.

There was no systematic variation in the $\delta^{13}C$ value within the sediment portion of the core. The average value of -27.1 is consistent with phytoplankton being the principal source of organic carbon. The C:N ratio and natural isotopic abundances

of the sedimenting material (Table 8.2) indicates that the majority of the carbon and nitrogen was derived from algal and zooplankton sources. The reduced $\delta^{15}N$ values suggest that nitrogen derived from sedimented materials is undergoing microbial decomposition. The $\delta^{13}C$ values indicate that fermentative pathways producing methane do not play a significant role in the diagenetic process liberating nutrients from the sedimented organic matter. If they did, we would expect values of $\delta^{13}C$ much closer to zero as methane produced in freshwater environments usually has a $\delta^{13}C$ in the range -50 to -65 ppt (Whiticar et al 1986) leaving the residual organic matter with increasingly positive values. It is possible that the sulphate concentrations are sufficient to inhibit methane production. In a marine system methane production was reported to be negligible until the sediment concentration of sulphate had decreased to below 0.02 M (Alperin et al 1993). It is also consistent with the demonstration that sulphate reducing bacteria can outcompete methanogens for acetate and H_2 (Kristjansson et al, 1982; Schonheit et al 1982).

8.2.5 Sediment traps and the downward flux of organic carbon

Sediment traps were deployed on five occassions (March 1997 – May 1998) with upward- and downward-facing traps placed at 1 m intervals to capture upwelling and downwelling materials. The fluxes and chemical parameters of the sedimenting material are given in Table 8.2.

Table 8.2 Vertical flux rates, %C, %N, C:N ratio and isotopic ratios from sediment trap deployments and average (Nov 1997 – May 1998) chemical composition and isotopic composition of algae and shrimp.

Month	Nett Flux Rate ($gm^{-2}d^{-1}$)	% C (avg.)	% N (avg.)	C isotope	N isotope	C:N ratio
Sep 1997	-0.21	3.0	1.8	-29.6	6.8	1.6
Nov 1997	0.18	10.6	1.5	-24.8	8.5	7.3
Jan 1998	0.65	16.3	2.8	-29.1	4.8	5.9
May 1998	1.11	3.0	1.8	-22.9	1.8	1.7
Algae	-	tba	0.8		12.34	
Shrimp	-	2.5	5.3	-28.28	13.34	0.5

The traps in the surface layer contained freshly deposited algae whereas the midwater traps contained little material. This implies a rapid breakdown of the particulate organic material as it settled through the water column. Thus, a significant component of the nutrients removed by the phytoplankton are regenerated in the water column. The apparent downward flux of material, measured by the bottom-most sediment traps, appears to increase again. Microscopic examination, higher iron and manganese content and isotopic carbon content all point to this being bottom sediments which have been resuspended or transported laterally by differential cooling.

8.2.6 Sediment phosphorus speciation

8.2.6.1 Speciation by selective extraction

Figure 8.3 shows phosphorus speciation determined by selective extraction on sediment samples from 5 sites ranging from inundated (NW end of transect, Figure 8.1) to desicated (SE end of transect). The amount of phosphate contained

in the readily desorbable fractions ($MgCl_2$ frp, $NaHCO_3$ frp, CBD TP) increases marginally with the degree of inundation. There are minor differences between the amounts of phosphorus extracted by NaOH and by HCl. Given that sequential extraction methods are imprecise, we conclude that there are no substantial differences in the phosphorus speciation across the reservoir.

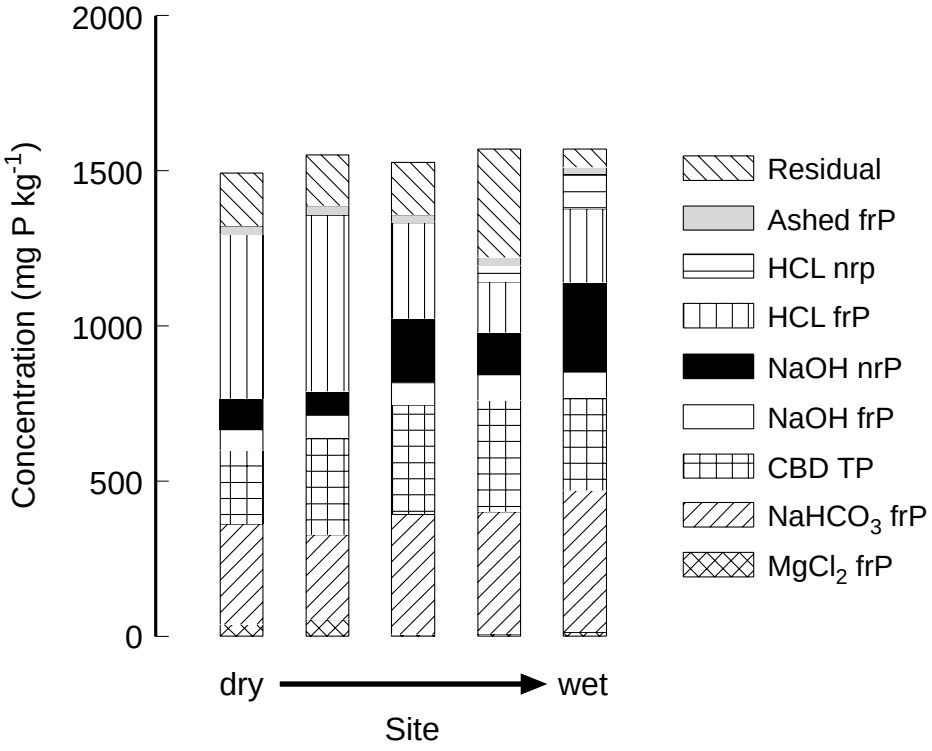

Figure 8.3 P-speciation of Chaffey Reservoir sediments using modified selective extraction. From Baldwin (1996b).

8.2.6.2 Sediment P speciation by ^{31}P nmr (nuclear magnetic resonance)

All of the nmr spectra were dominated by a single large spike in the region 3-4 ppm assigned to free orthophosphate. In addition, samples taken from both the Peel River and from Hyde's inlet showed the presence of phosmono and/or diesters (i.e. organic P compounds). Minor amounts of unidentified phosphorus containing species are indicated by peaks in the range –50 to –70 ppm. The method indicates, however, that orthophosphate is the principal phosphorus species in the sediment.

8.2.7 Desiccation and sediment phosphorus cycling

The sediments are both a large source and a large sink for nutrients in Chaffey Reservoir. By increasing the oxygen content of the hypolimnion, destratification offers one method to effectively reduce the release of phosphorus from the sediments (Section 8.5.3.1) even though it only affects the very top layer of the sediments. The very low water levels during this project offered the opportunity to study an alternate method of sediment oxidation - exposure.

The drought conditions that prevailed at the beginning of the project (Figure 6.4) exposed reservoir sediments to the atmosphere for the first time in many years. It was expected that the exposure and subsequent desiccation of sediments would

greatly affect both the abiotic (e.g. mineralogical) and biotic (particularly microbial) components of the sediment and, consequently, should have a profound effect on the nutrient dynamics in the sediments. Here we report on the effects of desiccation/oxidation on the sediment's capacity to adsorb P under oxic conditions (analogous to a flood event); and the effects of drying on the potential for sediments to release P under anaerobic conditions.

8.2.7.1 The effects of desiccation/oxidation on the sediment's capacity to adsorb P under oxic conditions

Most of the external nutrient load entering into the dam occurs during flood events (Section 8.5.1). Although much of these nutrients are associated with particles, a significant amount are dissolved in the (oxic) floodwaters and potentially may be adsorbed by reservoir sediments.

The capacity of sediments of varying oxic status to adsorb inflowing dissolved phosphorus was studied by taking 11 sediment samples along a transect (Figure 5.1) which covered heavily desiccated, wet-littoral and submerged sediments from both above and below the oxycline and measuring P adsorption isotherms (Baldwin 1996b). The isotherm experiments showed a clear transition in P affinity along the transect; sediments taken from the driest sites had the least adsorptive capacity, those from the wet littoral regions had an intermediate capacity to adsorb P while sediments taken from beneath the oxycline had the highest affinity for P. Also, the rate of P uptake was faster from sediments which were initially anoxic than from wet littoral or desiccated sediments. The differences in P affinity are believed to be a consequence of increasing crystallinity as a function of aging (Baldwin 1996b).

Figure 8.4 shows a conceptual model of Fe cycling under oxic/anoxic conditions - the so called 'ferrous' wheel. Fe(III) is reduced under anoxic conditions to give Fe(II). Fe(II) is subsequently oxidised under oxic conditions to give Fe(III) - usually forming amorphous iron oxyhydroxides [Fe(OOH)].

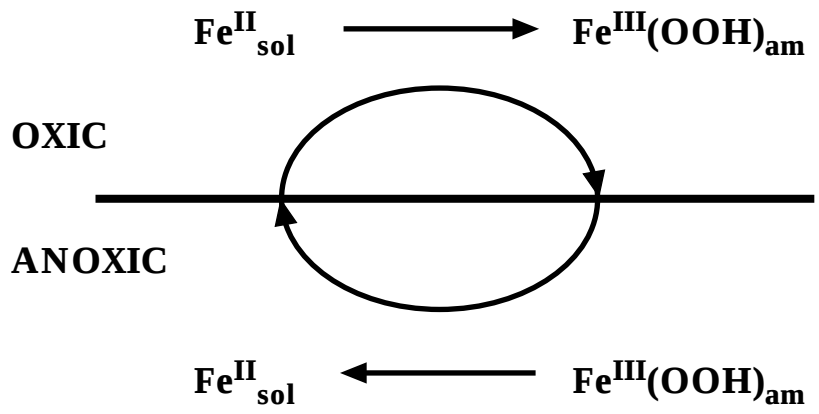

A) The 'Ferrous Wheel' Under Cyclic Oxic Conditions

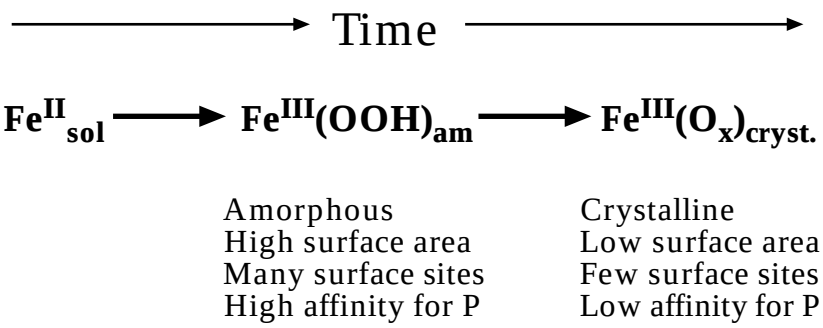

B) Under Continual Oxic Conditions

Figure 8.4 The 'Ferrous' Wheel

Amorphous Fe(OOH) has a large surface area and a high affinity for P. If the cycling does not occur (i.e. the Fe(OOH) is not reduced to Fe(II)) the Fe(OOH) becomes more crystalline, the surface area decreases as does the affinity for P (Figure 8.4, B). Sediments from beneath the oxycline would have high concentrations of both Fe(II), which when exposed to the oxic flood water would be oxidised to amorphous Fe(OOH), as well as a high proportion of fresh Fe(OOH) raining down from the oxic boundary. Therefore, these sediments will have a high affinity for P. The desiccated sediments on the other hand should be more crystalline, and hence have a lower affinity for P.

8.2.7.2 The effects of desiccation/oxidation on the potential for bacterially mediated P release from sediments.

Bacteria may indirectly mediate P release from sediments in a number of ways. If P is associated with Fe phases (see above), iron reducing bacteria can directly reduce Fe(III) to Fe(II) with a concomitant release of any P associated with the Fe(III) mineral (Roden, 1997). Sulfate reducing bacteria can reduce sulfate to

sulfide. Sulfide is a strong enough reducing agent that it can reduce Fe(III) to Fe(II) again liberating any bound P (Berner, 1984; Caraco, 1993). P may also be directly released from bacteria which contain poly-phosphate granules during anaerobic respiration (Davelaar 1993, Gächter and Meyers 1993). If anaerobic P release is bacterially mediated, then oxidation / desiccation of sediments should lead to a significant change in the sedimentary bacterial community structure and hence, sedimentary P cycling.

To examine this possibility, sediments were taken from 4 sites in the reservoir, two sites which had remained inundated and were covered by anoxic waters, one which had recently been inundated after a prolonged period of exposure and, one which had yet to be inundated. Sediment samples from the four sites were slurried under anaerobic conditions in the presence of a toxicant (formaldehyde), various carbon sources (glucose or acetate), an electron acceptor (sulfate), or with no additional augmentation (Mitchell and Baldwin 1997).

In the absence of any augmentation, the sediments from the two sites which were not desiccated released significant quantities of P under anaerobic conditions, while the sediments from the two sites which were desiccated showed no significant P release - clearly indicating that anaerobic P release can be substantially reduced as a consequence of desiccation / oxidation. No P release occurred from sediments from the two wet sites if the sediments were poisoned with formaldehyde - indicating that P release was indeed bacterially mediated. Further evidence for bacterial mediation was the enhancement of P release from the wet sites when carbon (in the form of acetate), an electron acceptor (sulfate) or both were added to the slurries. P was released from the desiccated sediments when additional carbon was added, suggesting that P release from desiccated sediments may be carbon limited, but no additional P release was observed when sulfate was added indicating that, unlike the wet sediments, sulfate reduction was not occurring.

Exposure of sediments to the atmosphere and subsequent desiccation has a profound effect on sedimentary nutrient cycling. Depending on how much time is required for bacteria to recolonize recently inundated sediments, sediment dessication may provide a useful tool for changing the sediment chemistry of reservoirs.

8.3 Water column chemistry

8.3.1 Methods

Routine measurement of water column chemistry (cations, anions, nitrogen, phosphorus and silica) at Chaffey Reservoir commenced in 1979. The sampling effort was most intense during 1988-1993 and 1995-1997 and the number of analytes determined varied from year to year. Prior to the commencement of this project in mid-1995 samples were typically collected by DLWC at Stn 1 (Figure 5.1) from the surface layer (typically ca. 25 cm depth) and from 1 m above the bottom. On some occasions an additional sample was collected at mid-depth. The frequency of sampling was typically fortnightly, although it varied from weekly to montly. As well, samples were collected occasionally at Stn 2 and Stn 3 and at several other sites including the Peel River and some of its tributaries during periods of more intensive monitoring. Full depth profiles (1-2 m intervals) were

also taken on occasion. These samples were analyzed at the DLWC Arncliffe labs following the procedures in Standard Methods (APHA, 1985).

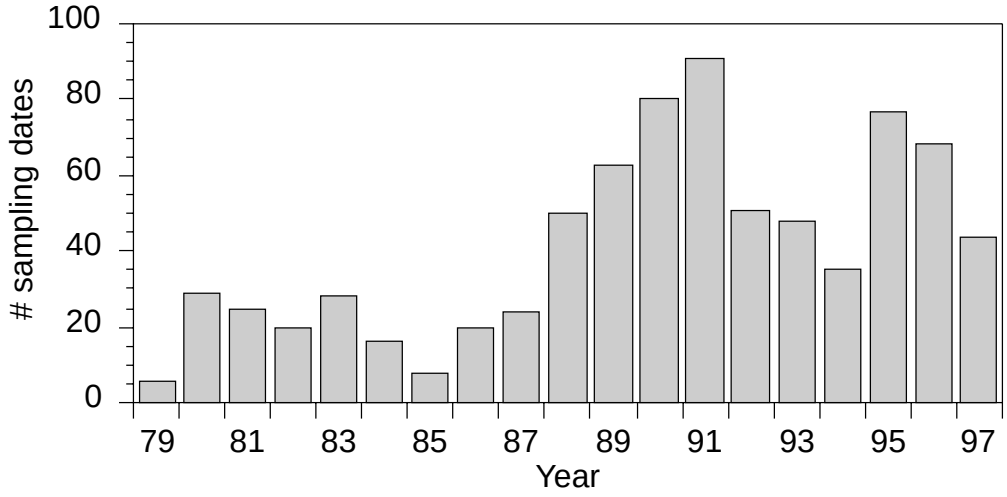

Figure 8.5 Annual number of visits to Station 1 to collect samples for chemical analysis.

From 1995-1997, DLWC's routine sampling was supplemented to include a greater number of depth profiles from the reservoir as well as stage-dependent sampling of the Peel River at Taroona, 6.7 km upstream of the reservoir. These samples were generally collected by DLWC staff, taken to the Tamworth Environmental Laboratory (TEL) within a few hours of collection and then analyzed using Standard Methods for TP, FRP, TN, NH_4, NO_x, Fe, and Mn. Many of the samples were analyzed also for SO_4, total organic carbon (TOC) and dissolved organic carbon (DOC). Phosphorus determinations by TEL prior to November 1995 used an inappropriate method and have not been included in the analyses that follow. As part of the technology transfer component of the project, TEL staff were subsequently trained by the manager of the MDFRC analytical lab in the procedures required to determine small concentrations with sufficient accuracy for scientific research purposes.

To gain an understanding of the reservoir's oxygen dynamics, CTDO (conductivity, temperature, depth, dissolved oxygen) profiles were taken weekly by DLWC at Stations 1, 2, and 3 (water depth permitting) from 1992-1997 using a Seabird SBE-19 profiler. Additional dissolved oxygen data were collected during project field trips using a Horiba water quality meter and CSIRO's TDFO profiler.

Particle chemistry was examined for water samples collected at discrete depths throughout the water column during several of the field trips. Most of the samples were collected at station A1 (Figure 5.1). Using tangential flow filtration (TFF), each sample was filtered into 3 size classes: dissolved (< 0.003 µm); fine colloidal (0.003 – 0.2 µm); and colloidal (0.2 – 1.0 µm). The filtrate in each class was preserved with 1 mL of concentrated HCl per 100 mL of sample and then analysed for total (TP) and reactive phosphorus (RP), Fe and Mn. TP determinations used a persulfate digestion and were then analysed using the ascorbic acid colorimetric method. Flow injection analysis (FIA) was used to determine RP and the standard methods were used for Fe^{2+} and Mn^{2+}, respectively. Xray diffraction (XRD) was used to determine the crystalline structure of the particles and organic surface

coatings were studied using sedimentation field-flow fractionation (SdFFF) coupled with inductively-coupled plasma mass spectroscopy (ICP-MS).

Reactive phosphorus that has passed a 0.003 µm filter is referred to in this report as $FRP_{0.003}$, to avoid confusion with the conventional use of the term FRP which implies passage through an 0.45 µm filter. We believe $FRP_{0.003}$ is a good surrogate for orthophosphate, but it is possible for other small chain phosphate molecules to pass the 0.003 µm filter.

Phosphorus and dissolved organic matter (DOM) speciation were also determined by weak anion exchange chromatography.

8.3.2 Historical trends in water chemistry

To understand the seasonal patterns in nutrient concentrations, it is useful to consider individually the three classic regions of the water column: the epi-, meta- and hypo-limnia. At Chaffey Dam we have used our knowledge of the surface layer dynamics (Figure 7.3) and oxygen profiles to define these 3 regions as occupying the water column from 0 - 5 m, 5 - 12 m, and below 12 m, respectively. The surface layer (epilimnion) is where virtually all algal growth occurs. The hypolimnion best reflects the sediment-water exchanges and the metalimnion is a relatively quiescent stratified region through which both particulate matter rains down from above and dissolved nutrients are transported upwards by turbulent diffusion and large scale circulation (Section 7.6).

It is important to bear in mind that the volume of the hypolimnion varies from year to year depending on how full the reservoir is. For a given nutrient flux from the sediment to the water column, the resultant hypolimnetic concentration will increase with decreasing water level. In other words, differences in the annual maximum hypolimnetic nutrient concentrations do not necessarily imply differences in the sediment nutrient release rates.

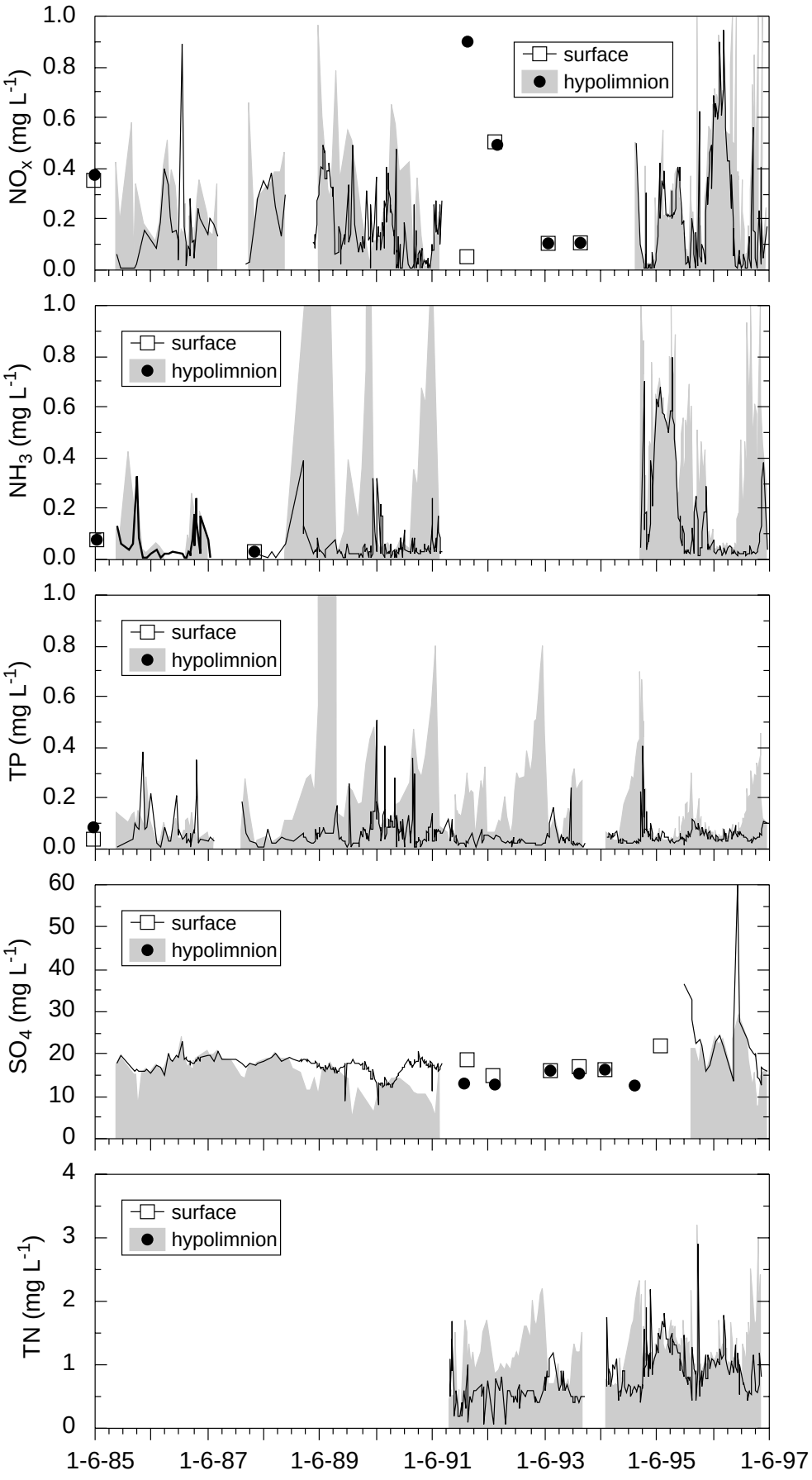

Figure 8.6 Seasonal changes in nutrient concentrations in the surface layer (0 – 5 m, solid line) and hypolimnion (> 12 m depth, shaded region) of Chaffey Reservoir from winter 1985 to winter 1997. From top to bottom, nitrate + nitrite

(NO_x), ammonia (NH_4), total phosphorus (TP), sulphate (SO_4), and total nitrogen (TN). The reservoir was destratfied continuously 1985-1988 and intermittently during 1995 – 1997.

The historical record for nutrient concentrations in the surface layer and hyplimnion of Chaffey reservoir is shown in Figure 8.6. The seasonal pattern of hypolimnetic nutrient concentrations in Chaffey reservoir is typical of strongly stratified reservoirs; nutrient cycling follows changes in the redox state of the water column. As soon as persistent stratification is established, the oxygen concentration below the surface mixed layer declines rapidly (section 8.3.7). Often by late October, hypolimnetic oxygen concentrations are so low that enhanced release of nutrients from the sediments commences. Phosphorus (mainly orthophosphate, section 8.3.4) and nitrogen, especially ammonia, accumulate in the hypolimnion while sulphate concentrations decrease, presumably due to transformation to hydrogen-, iron-, and manganese-sulphides (Section 8.3.5). This behaviour was especially apparent during the period after the destratifier was decommissioned (1989-1991).

Eventually, autumnal cooling causes the entire water column to mix; the first deep mixing event occurring typically in May or June. Deep mixing brings the accumulated nutrients from the hypolimnion into the surface layer where they become available to the phytoplankton. They may also be transformed due to exposure to increased oxygen concentrations, e.g. ammonia may be oxidised to nitrate and orthophosphate may be adsorbed onto iron oxyhydroxide particles. Nutrients accumulated in the hypolimnion are significant determinants of the following season's mean algal biomass (Section 9.2.4).

By elevating dissolved oxygen concentrations, artificial destratification had a pronounced effect on hypolimnetic nutrient concentrations. Operation of the destratifier from 1985-1988 (continuous) and 1995-1997 (intermittent) greatly reduced the amount of phosphorus that accumulated in the hypolimnion. Continuous operation also produced a significant decrease in the ammonia concentration; this effect was not observed when the destratifier was run intermittently. Destratification also prevented most of the seasonal cycling of sulphate in the hypolimnion.

When the water column was undisturbed by destratification or major inflow events, surface layer nutrient concentrations had an inverse seasonal variation compared to those below the surface layer. Uptake of nutrients by algae during spring and their subsequent sedimentation out of the surface layer reduced summertime nutrient concentrations in the euphotic zone at the same time as high nutrient concentrations were building up just a few metres below. The first autumnal deep mixing event redistributed nutrients from the hypolimnion to the surface layer and caused hypolimnetic concentrations to decrease while surface layer concentrations increased. This pattern could be interrupted in years when large inflows deposited high loads of bioavailable nutrients close to the surface layer.

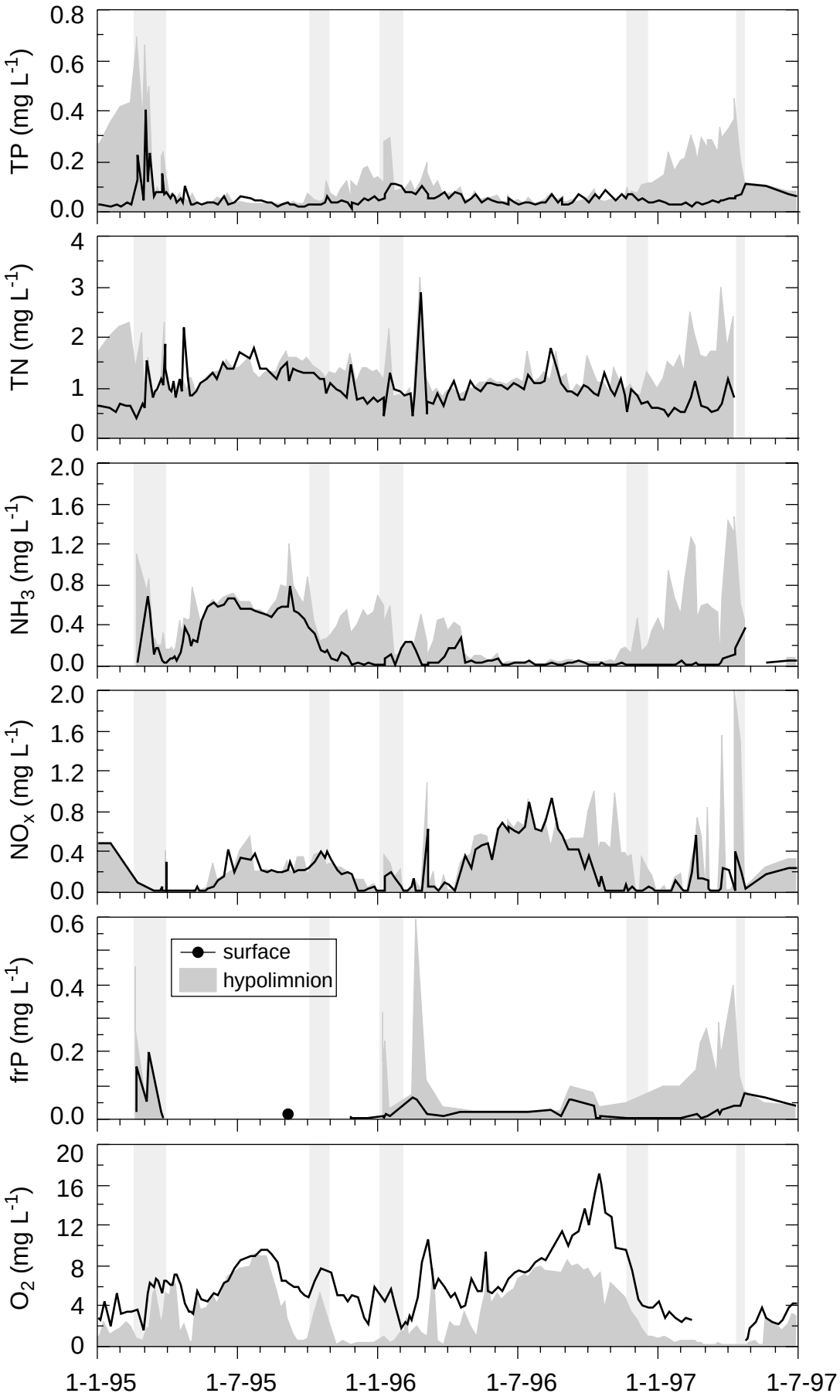

Figure 8.7 Hypolimnetic (> 12 m depth, shaded region) and surface layer (0 – 5 m, solid line) nutrient and dissolved oxygen concentrations during this project

(1995-1997). From top to bottom, total phophorus (TP), total nitrogen (TN), ammonia (NH_4), nitrate + nitrite (NO_x) filterable reactive phosphorus (FRP), and dissolved oxygen (O_2). Light shaded bars indicate operation of the destratifier.

Nutrient and dissolved oxygen concentrations during the period of our investigations are shown in Figure 8.7. These data show a clearer seasonal trend in NO_x with comparable concentrations of NO_x (almost exclusively nitrate) in both the epi- and hypo-limnia during the winter overturn. This gradually declined in spring as it was taken up by phytoplankton and presumably underwent denitrification as well. Ammonia, in contrast, was more abundant during the times of stratification, especially in the hypolimnion, although significant quantities were present throughout the water column during winter 1995.

FRP in the surface layer generally decreased during spring and summer due to consumption by algae and was at the limit of detection from Nov 96 to Feb 97 despite its significant accumulation in the hypolimnion. Surface layer TP increased in response to mixing events that carried FRP into the layer. Surface TP gradually declined with increasing duration of stratification as particle-bound phosphorus sedimented downwards into the hypolimnion.

Operation of the destratifier after stratification had been established decreased hypolimnetic concentrations of TP, NH_4, and FRP, and usually increased the corresponding concentrations in the surface layer. Short-lived increases in hypolimnetic NO_x were also observed. At the same time, dissolved oxygen concentrations in both layers could either increase or decrease depending on the *in situ* production of and demand for oxygen and the rate of gas exchange with the atmosphere (Section 8.3.7).

Ultimately, the nutrient concentrations in the water column reflect a balance between the supply of nutrients from the sediments and inflowing streams and the loss of nutrients through sinking of particles and withdrawal of water for downstream use. It is therefore necessary to examine the sources of nutrients in greater detail.

8.3.3 Major ion chemistry

The major cations present in Chaffey Reservoir are sodium, calcium and magnesium and they are present in proportions (Figure 8.8, top) which are very similar to the Australian average freshwater composition. Chaffey Reservoir differs somewhat from other storages in upland northeastern New South Wales (Banens, 1987), as well as from upstream reaches of the Murray system which have a higher proportion of divalent cations *vis-a-vis* monovalent sodium.

The anion chemistry (Figure 8.8, bottom) of the water column departs from the Australian norm – as well as the regional pattern – of bicarbonate/chloride dominance. It conforms more closely to the world average with about 20% of the anions in the sulphate component. Sulphate concentrations wax in spring and wane during summer and autumn (Section 8.3).

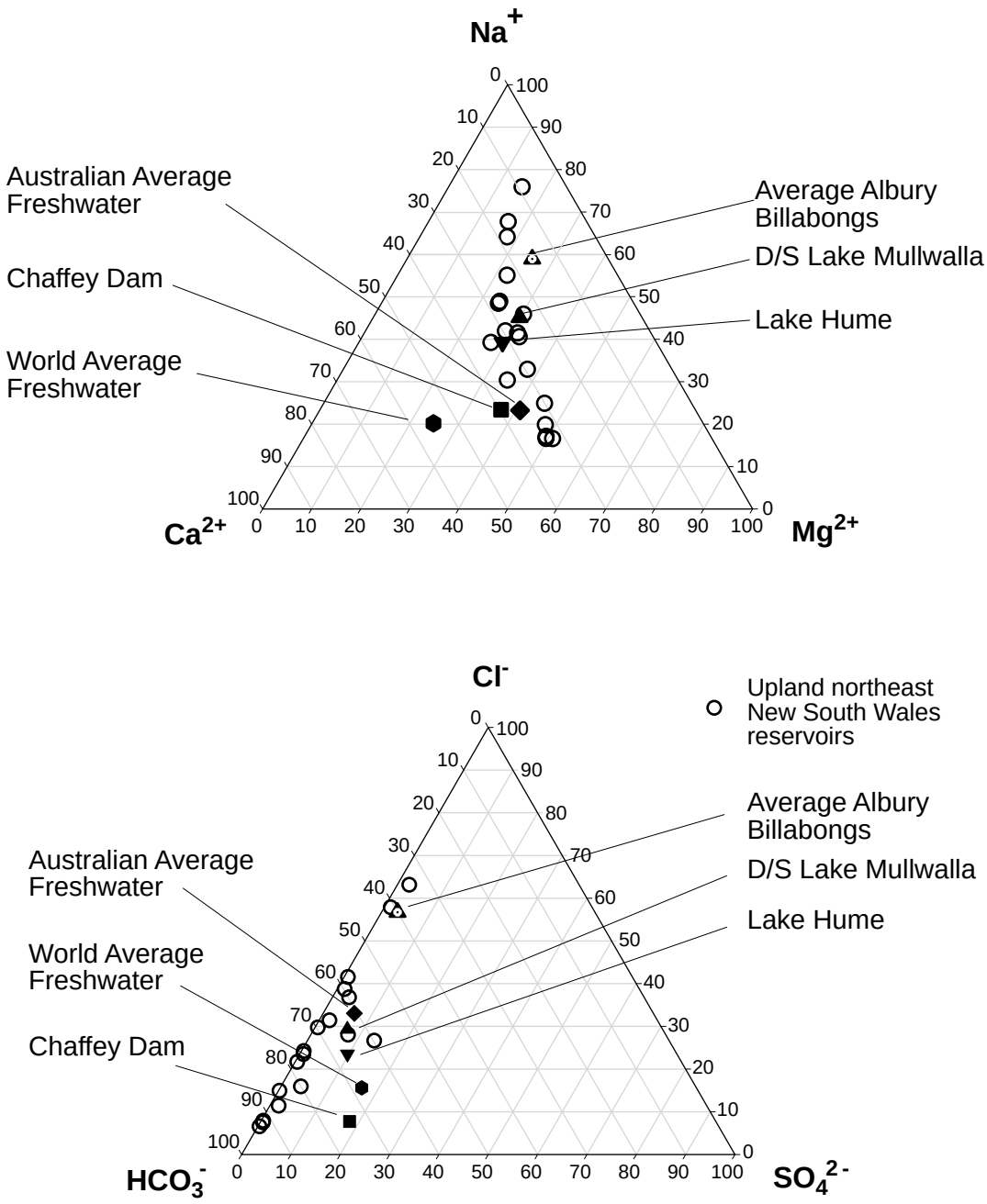

Figure 8.8 Major cations (top) and anions (bottom) in the water column at Chaffey reservoir.

8.3.4 Water column P speciation

8.3.4.1 Speciation by weak anion exchange chromatography

The P speciation results presented in Figure 8.9 show that the amount of P in the surface layer was quite variable. It was lowest in January 1996 and highest in June 1997. The samples in November 1996, June 1997 and September 1997 were all dominated by one large peak at an elution volume of ca. 600 ml. All the P associated with this peak was reactive (white region), and indeed co-elutes with the free ortho-P ion suggesting that free ortho-P was the dominant P species in solution on these sampling occasions. Very little dissolved P was in the sample taken on 14 January 1996; the P that was present eluted as a broad band, which although it contained reactive P, was too broad and eluted at the wrong position

to unequivocally be assigned as ortho-P. Likewise, in the sample taken on 3 March 1997 the P eluted in 3 overlapping peaks, all of which were reactive but only one of which could be free ortho-P. At this stage it is not possible to assign structures to the two other peaks. Likewise it is not possible to assign structures to the small amounts of 'organic' P species present in the 3 June 1997 sample. Consistent with the nmr results for the sediments (Section 8.2.6.2), the dominant dissolved phosphorus species in the water column is orthophosphate, but accompanied by lesser amounts of other reactive species.

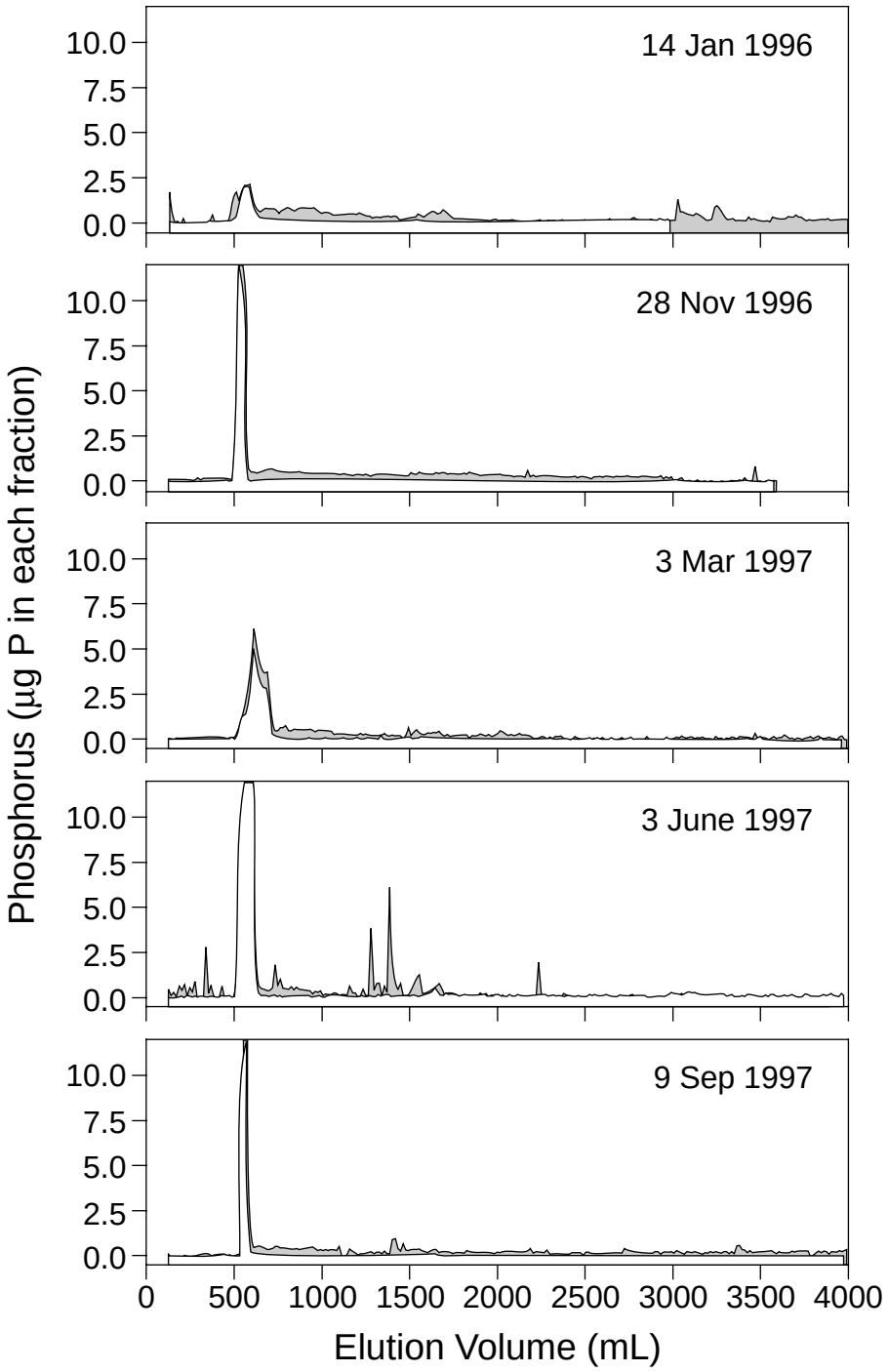

Figure 8.9 Total (gray) and reactive (white) phosphorus speciation in water column samples as determined by weak anion exchange chromatography.

8.3.4.2 Speciation of particle-bound P in water column

The phosphate size speciation data for February 1995 is given in Table 8.3. The oxic water at a depth of 2 m contained < 28 µg/L of reactive phosphorus in the 117 µg/L of P that was in the < 1.0 µm (TFP, total filterable phosphate[3]) fraction. Thus 76% of the TFP may have been associated with either colloidal particulate matter, indicating bacteria, or with complex phosphates (i.e. condensed or organophosphates). Further analysis revealed that of the 86 µg/L of P in the < 0.003 fraction, less than 10 µg/L was reactive, i.e. $FRP_{0.003}$ (assumed to be orthophosphate). This implies that most of this phosphate was complex phosphate.

Both TFP and FRP increased with increasing depth below the surface layer. The proportion of reactive P in the TFP increases with depth, being 46% at a depth of 8 m and 66% at 14 m.

At 14 m, the concentration of $FRP_{0.003}$ was quite high, accounting for 52% of the total filterable phosphate at this depth. Most of this would have originated from the sediments. The samples consisted of very fine FeS and MnS colloidal particles. A considerable proportion (82%) of the phosphorus in the 0.2-1.0 µm fraction was reactive, however this represented only 9% of the total filterable phosphate measured at this depth.

The results suggest that a large percentage of the total filterable phosphate in the bottom anoxic waters was orthophosphate, whereas in the surface waters, most of the phosphate was in a complex phosphate form.

Table 8.3 Size speciation as determined by filtration of complex phosphate and reactive phosphate measured in February 1995 at Station 1 (units µg/L). Reactive phosphate concentrations are shown in brackets.

Depth (m)	<0.003 µm	0.003-0.2 µm	0.2-1.0 µm	< 1.0 µm	TFP
2	86 (<10)	0 (14)	3 (4)	89 (28)	117
8	117 (24)	- (75)	37 (31)	154 (130)	284
14	155 (402)	94 (36)	16 (72)	265 (510)	775

The phosphate size speciation experiments were repeated in late March 1995 after four weeks of destratifier operation to examine the effect of destratification on the phosphate distribution within the water colum. The large pool of $FRP_{0.003}$ observed in February 1995 in the bottom anoxic water was carried upwards (section 7.3, Figure 7.5) and mixed with the surface waters where it doubled the $FRP_{0.003}$ concentration at a depth of 2 m (Table 8.4). A major blue-green algae bloom had also developed, presumably as a consequence of the transport of orthophosphate into the surface layer. TFP at the surface also increased significantly, mostly in the fine colloidal (0.003 – 0.2 µm) size fraction. The concentration of phosphate in the colloidal size range (0.2-1.0 µm) remained low.

[3] The total filterable phosphorus, TFP, is the sum of all complex and ortho-phosphorus passing through a 1.0 µm filter. All phosphate passing a 0.003 µm filter, $FRP_{0.003}$, is assumed to be orthophosphate although it may contain other short-chain phosphate molecules. Phosphate measured in the 0.003 – 0.2 µm fraction is associated with fine colloids and the 0.2 – 1.0 µm fraction represents colloidal-bound P.

Throughout the water column, approximately 10% of TFP was $FRP_{0.003}$ with the remainder present as condensed phosphates, organic phosphates, and/or adsorbed onto colloidal or particulate matter and not detected by the colorimetric procedure. Virtually all size fractions at all depths contained more complex phosphate than reactive phosphate (Table 8.4). At a depth of 14 m, 23% of the TFP (229 µg/L) was associated with the colloidal particles; the phosphate was most likely adsorbed onto the surfaces of the hydrous metal oxides which precipitated upon operation of the destratifier.

Table 8.4 Size speciation as determined by filtration of complex phosphate and reactive phosphate measured in March 1995 at Station 1 (units µg L^{-1}). Reactive phosphate concentrations in brackets.

Depth (m)	<0.003 µm	0.003-0.2 µm	0.2-1.0 µm	< 1.0 µm	TFP
2	59 (21)	99 (4)	2 (6)	160 (31)	191
8	145 (23)	59 (10)	7 (2)	211 (35)	246
14	100 (25)	41 (10)	49 (4)	190 (39)	229

By late November 1995, the volume of water in the reservoir had fallen due to the drought (Figure 6.4) and the water column had stratified. The surface waters contained relatively small amounts of $FRP_{0.003}$ (< 10 µg/L at 2 m, Table 8.5). This is consistent with chromatographic data that showed a low orthophosphate concentration in January 1996 (section 8.3.4.1, Figure 8.9). As the water column became more anoxic with increasing depth, the concentration of $FRP_{0.003}$ increased. At 14 m, 60 µg/L of the measured TFP (70 µg/L) was reactive. Operation of the destratifier in October 1995 delayed the onset of anoxia in the hypolimnion and phosphorus release until just a fortnight prior to the measurements. Inflows from the Peel R. between 26 Oct 1995 and 28 Nov 1995 supplied more than enough TFP to account for the observed accumulation below 2 m (see section 8.2.6.2). Most of the TFP measured in November 1995 was present as $FRP_{0.003}$.

Table 8.5 Size speciation as determined by filtration of complex phosphate and reactive phosphate measured in November 1995 at Station 1 (units µg L^{-1}). Reactive phosphate concentrations in brackets.

Depth (m)	<0.003 µm	0.003-0.2 µm	0.2-1.0 µm	< 1.0 µm	TFP
2	2 (<10)	2 (0)	0 (2)	4 (12)	16
8	8 (12)	4 (2)	5 (6)	17 (20)	37
14	9 (51)	0 (4)	1 (5)	10 (60)	70

8.3.5 Iron and manganese

To understand the processes responsible for transforming phosphorus between biologically available and unavailable forms in the water column required detailed knowledge of the elemental composition of particles in several size classes from dissolved to fine colloidal and colloidal. Particular attention was paid to the redox chemistry of iron and manganese as these elements can adsorb and

release phosphorus in large quantities depending on the oxygen content of the water which itself can be manipulated by the operation of the destratifier.

8.3.5.1 Fe^{2+} size speciation.

The concentration of soluble Fe^{2+} increased with depth when the dam was stratified in February and November 1995 and January 1996 (Table 8.6). Samples taken from the oxic layer of the dam showed relatively low concentrations of Fe^{2+} as expected. During the field trip in March 1995, the destratifier had been operated for 4 weeks and only very low concentrations of Fe^{2+} were observed at Stn 1.

The concentration of Fe^{2+} varied seasonally, increasing with increasing duration of the stratified period prior to measurement. Fe^{2+} concentrations in January 1996 were much lower than those observed in February 1995. The January 1996 values reflect the shorter duration of stratification due to operation of the destratifier in October 1995 and possibly the diluting effect of a number of inflow events during the months before the January 1996 field trip (Figure 6.3). The trends associated with particle size in February 1995 and November 1995 were similar.

Data from the Feb 1995, Nov 1995, and Jan 1996 field trips all show very low concentrations of Fe^{2+} in the fine colloidal (0.003-0.2 µm) and colloidal (0.2-1.0 µm) size fractions at the depth of 8 m. This is consistent with the colourless appearance of the samples when collected from the water column. Samples from a depth of 14 m had a black appearance and their colloidal size fractions contained considerably larger concentrations of Fe^{2+}. The black colour of theses samples are believed to have been caused by fine colloidal FeS and MnS. Approximately 40% of the Fe^{2+} measured at 14 m in February 1995 was determined to be colloidal (FeS), whilst the remaining 60% existed as dissolved Fe^{2+} (Table 8.6).

Table 8.6 Size speciation as determined by filtration of Fe^{2+} at station 1 during the field trips of February, November 1995 and January 1996.

Depth (m)	Field Trip	<0.003 µm	<0.003-0.2 µm	0.2-1.0 µm	Total
8	Feb 1995	216	28	51	295
	Nov 1995	298	32	124	454
	Jan 1996	109	60	74	243
14	Feb 1995	565	243	179	987
	Nov 1995	374	70	210	654
	Jan 1996	160	226	0	386

8.3.5.2 Mn^{2+} size speciation

Figure 8.10 shows depth profiles of Fe^{2+} and Mn^{2+} in the water column in April 1997. TDFO casts detected no dissolved oxygen below 12.5 m at this time. Note that the concentration of Mn^{2+} is approximately 5 times greater than the Fe^{2+} concentration. Similar to the Fe^{2+} size speciation results, the colourless 8 m sample had very low concentrations of Mn^{2+} in the fine colloidal (0.003-0.2 µm) and colloidal (0.2-1.0 µm) size ranges (Table 8.7). The black coloured sample from 18 m can be explained by the increased Mn^{2+} concentrations in the colloidal fractions (MnS) which comprised approximately 80% of the Mn^{2+} measured at this depth. In contrast, at 8 m, just 2% of the Mn^{2+} was colloidal, and the remaining 98% was in the dissolved and fine colloidal forms.

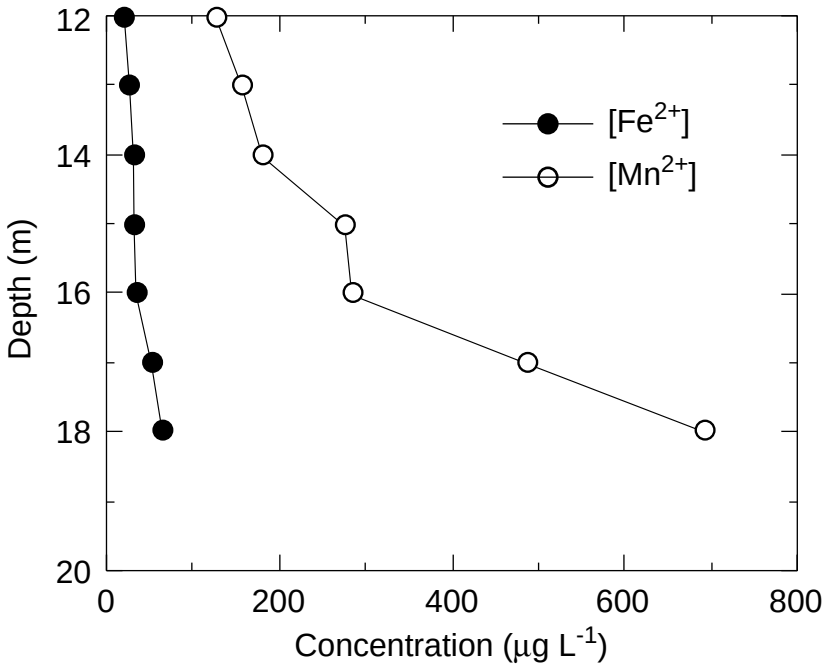

Figure 8.10 Filterable Fe^{2+} and Mn^{2+} Profile when stratified during April 1997 at Station 1.

Table 8.7 Size speciation as determined by filtration of Mn^{2+} during April 1997 at Station 1 (units µg L^{-1}).

Depth (m)	<0.003 µm	0.003-0.2 µm	0.2-1.0 µm	Total
8	30	16	1	47
18	104	152	256	512

In summary, the Fe^{2+} and Mn^{2+} size speciation data collected from the four field trips (February, November 1995, January 1996 and April 1997) when the dam was stratified, showed very little colloidal Fe^{2+} and Mn^{2+} at a depth of 8 m. At 14 m (or 18 m during April 1997), there was a much larger concentration of colloidal Fe^{2+} and Mn^{2+}. Only very low concentrations of reactive phosphate were observed in the colloidal size fractions. Most of the reactive phosphate was found to exist in the dissolved (<0.003 µm) fraction. Therefore, both the colloidal FeS and MnS found in the deeper anoxic waters were poor adsorbers of orthophosphate.

8.3.5.3 Kinetics of the reductive dissolution and oxidation of iron and manganese.

The kinetics of the oxidation of Fe^{2+} and Mn^{2+} were investigated both in the laboratory and *in situ* during the operation of the destratifier. The measured rate constants and half lives of the reduced species in oxic conditions agreed with the literature values with $t_{1/2}$ for Fe^{2+} approximately 10 minutes and that for Mn^{2+} about 20 hours. Simultaneous observation of FRP and these reduced species at different positions along the outward-moving plume during the initial stages of destratification showed that scavenging of phosphate upon oxidation of anoxic bottom waters was relatively rapid but incomplete. When all the Fe^{2+} had been removed only 63% of the initial FRP had been scavenged.

Laboratory experiments showed that manganese oxides were ineffective in scavenging P from the water column. These results suggest that the Fe^{2+}:P ratio in the hypolimnion is too small to provide enough FeOOH to scavenge all the FRP

on oxidation. The imbalance in this ratio may be exacerbated by the burial in the sediments of FeS colloids formed during anoxic conditions. Consequently, operation of the destratification system once anoxia had been established raised, rather than lowered, concentrations of FRP in the surface layer. This result has potential management implications.

8.3.5.4 Crystalline structure of colloids.

The anoxic water samples consisted of very fine black sulphide colloids. X-ray diffraction (XRD) analysis of these sulphide particles showed no crystalline structures (except silica), only a very broad peak (Figure 8.11). As the sample oxidized, large brown aggregates formed which were suspected to be amorphous hydrous Fe and Mn oxides. There were no detectable concentrations of aluminium from inductively coupled plasma-mass spectroscopy (ICP-MS) analysis, hence the particles were not aluminosilicates. XRD also showed that the particles which precipitated from the oxidation of the sulphide colloids maintained an amorphous structure (Figure 8.12). The concentrations of metal ions in solution suggested the anoxic colloid particles were mainly amorphous Fe and Mn sulphides.

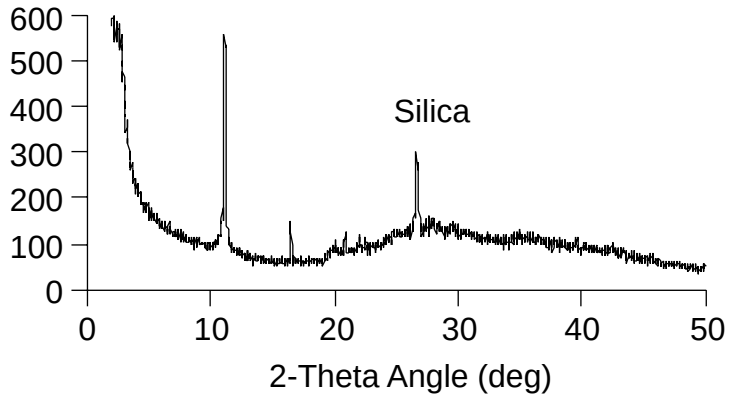

Figure 8.11 Figure 3 X-ray diffraction of Chaffey Reservoir anoxic particles.

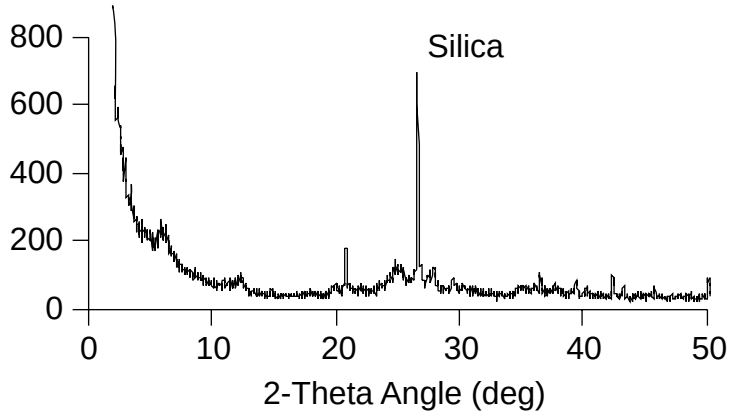

Figure 8.12 X-ray diffraction of Chaffey Reservoir oxidized particles.

However, XRD analysis has shown that the fine colloids entering Chaffey Reservoir via the Peel River consist of aluminosilicate. The particles observed were illite and kaolinite. Sedimentation field-flow fractionation (SdFFF) coupled with ICP-MS indicated these particles possessed both Fe oxide surface coatings and organic matter surface coatings. It would appear from analogous work (van

Berkel & Beckett 1997) that the Fe oxide surface coating increases phosphate adsorption whereas the organic matter surface coating decreases phosphate adsorption.

8.3.6 Examination of dissolved organic matter by weak-anion exchange chromatography.

Chromatograms of DOM speciation in the water column of Chaffey Reservoir on four different dates show that there is very little temporal variability in DOM (Figure 8.13). All the samples show a large broad band centred around ca. 1250 ml. A number of smaller sharper peaks are superimposed on this broad band; the most notable being the sharp peak at an elution volume of ca. 500 ml on all but the 3 March 1997 sample and, the large number of small sharp peaks associated with the sample taken on the 28 November 1996.

While it is impossible to unequivocally assign a chemical structure to the DOM it is certainly possible to speculate on the origin of the material. The broad DOM band centred at 1250 ml on all the chromatograms has been found in quite disparate Australian waters. The broad nature of these bands suggest that they represent polymers or mixtures of polymers. The wide temporal and spatial distribution of this compound would suggest that the (putative) polymer is formed by a ubiquitous chemical process. One such process is the oxidative polymerisation of polyphenols - i.e humification (HASLAM 1989). In oxidative polymerisation, polyphenolic compounds such as tannins and lignins combine to form large polymers. As part of the polymerising process smaller molecules, such as carbohydrates and proteins, are also incorporated into the polymer (SJOBLAD 1981).

The availability of this broad DOM fraction to support bacterial production is not known. However, the fact that this peak is always seen in these samples could be interpreted as suggesting that the compound is relatively recalcitrant. This is consistent with previous studies on the availability of humic substances to bacteria (THOMAS 1997). Conversely, the distribution of the smaller peaks (superimposed on the large broad peak) change over time. This suggests that these compounds are labile and probably being used by the microbial community.

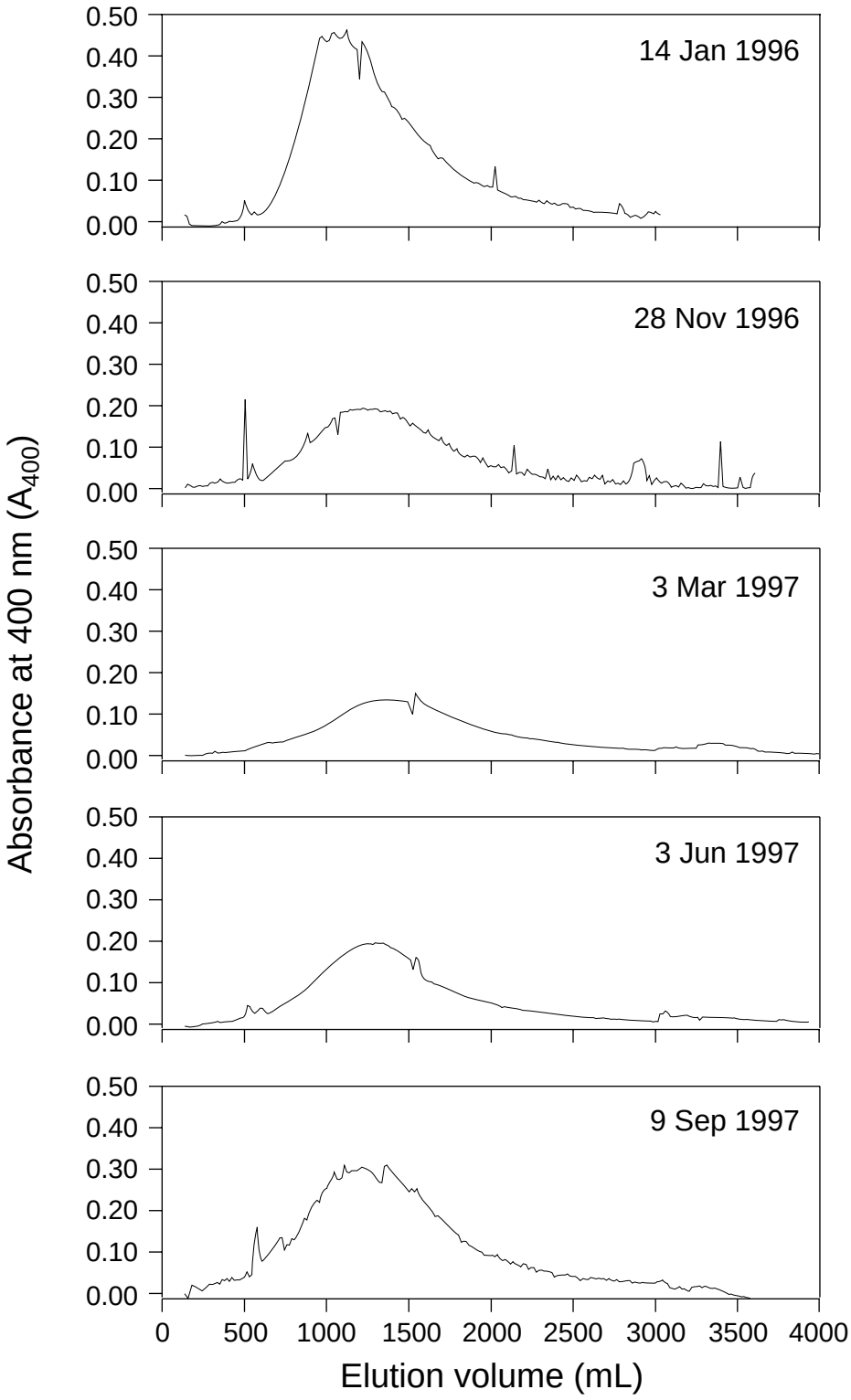

Figure 8.13 Chromatograms of dissolved organic matter (DOM) speciation in Chaffey Reservoir.

8.3.7 Oxygen dynamics

The oxygen concentration in the water column plays a fundamental role in controlling the rates of sediment nutrient release and the absorption and desorption of phosphorus onto iron-based compounds.

The dissolved oxygen concentration in Chaffey Reservoir varies inversely with the duration of thermal stratification and is greatest at the end of winter and least just prior to autumnal overturn. Figure 8.14 (bottom) shows the average surface layer (0 – 5 m) and hypolimnetic (> 12 m) dissolved oxygen concentrations from the weekly CTDO casts. These concentrations reflect a balance in the water column between photosynthetic production, respiratory and chemical oxygen demand and the transfer of oxygen across the air-water interface. Superimposed upon these processes is the vertical transport arising from the operation of the destratifier. This process facilitates the exchange of surface layer water containing relatively more oxygen and organic carbon with water from the hypolimnion.

The onset of persistent thermal stratification occurred each year within a week of 10 August and oxygen depletion in the hypolimnion commenced shortly afterwards. Dissolved oxygen concentrations during the summers from 1992-1994 (Figure 8.14) and SO_4, TP and NH_4 concentrations from 1988 - 1991 (Figure 8.6) show that anoxic ($[O_2] \leq 1$ mg L^{-1}) conditions prevailed in the hypolimnion for 6 - 8 months each year in the absence of artificial destratification. The very high surface layer O_2 during Oct-Nov 1996 was produced by a massive bloom of *Botryococcus* which was accompanied by extreme oxygen supersaturation (> 200% saturation and > 200 mg Chl-a m^{-3}). Conditions were so calm during the bloom that the escape of the supersaturated dissolved oxygen to the atmosphere was limited by diffusion through the water column resulting in effervescence at the surface, especially in the presence of a boat wake.

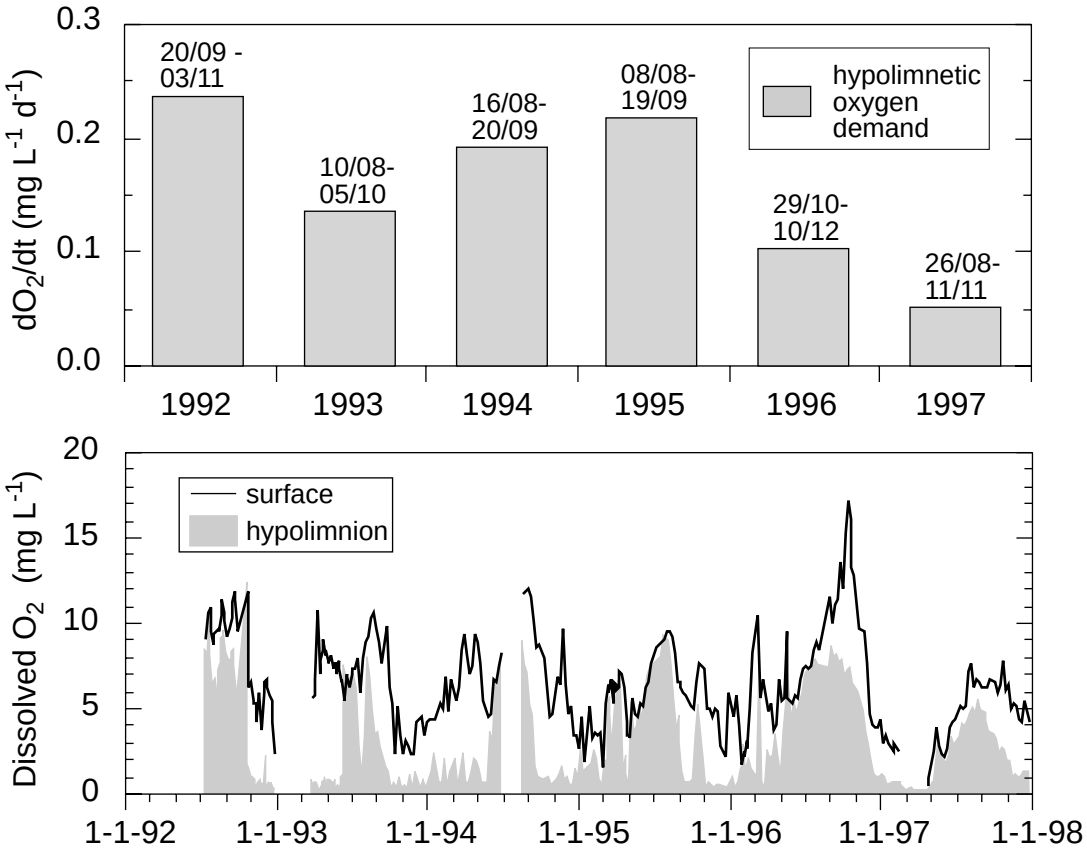

Figure 8.14 Top) Hypolimnetic oxygen demand following the onset of persistent stratification. Dates on top of bars indicate the period used for the calculation. Bottom) Mean surface (0 - 5 m, solid line) and hypolimnetic (> 12 m, shaded region) dissolved oxygen concentrations from the weekly CTDO casts.

Operation of the destratifier in Feb-Mar and Oct 1995 increased hypolimnetic O_2 substantially whereas its operation in Jan-Feb 1996 had little effect and in Nov-Dec 1996 and Apr 1997 actually decreased both surface and hypolimnetic O_2. The operation in late 1996 was an attempt to increase the rate of oxygen depletion both by transporting organic carbon from the *Botryococcus* bloom downwards and by raising the temperature of the hypolimnion. The April 1997 destratification actually purged the entire water column in the main basin of oxygen causing an accumulation of yabbies in a shallow band near the edge of the reservoir early in the morning followed by a migration of fish both in the pelagic and littoral zones to the south end of the reservoir where O_2 concentrations were higher. The destratifier was turned off after a dead fish was observed by one of the dam operators, possibly the result of severe oxygen depletion.

The hypolimnetic oxygen demand (HOD) was computed for each year by calculating the rate of decline in hypolimnetic O_2 during the period when O_2 consistently dropped from near saturation to approximately 1 mg L^{-1}. HOD varied from 0.24 – 0.14 mg L^{-1} d^{-1} during 1992-1995 (Figure 8.14, top) but was not correlated with reservoir volume which ranged from 20 to 100% of capacity. As the reservoir filled during 1996 and 1997, HOD progressively decreased to 0.10 and 0.05 mg L^{-1} d^{-1}, respectively. We do not know why this decrease occurred. One possibility is that the organic carbon load to the hypolimnion was less in 1993, 1996 and 1997. This would be consistent with the observation of a relatively larger proportion of buoyant and motile phytoplankton species during 1993, 1996, and a large bloom of benthic algae (*Cladophora* and *Spirogyra*) during spring of 1997 which removed the FRP from the surface layer before pelagic phytoplankton could get established. The benthic algal mat occupied the shallow perimeter of the reservoir where it had access to sufficient light for photosynthesis at all times. This region was always within the diurnal surface mixed layer, i.e. the depth to which the SML deepened each morning.

The temperature sensitivity of the *in situ* oxygen demand was tested during the *Botryococcus* bloom in Oct 1996. A sample of surface layer water was collected at a depth of 2 m and divided into 3 lots of 9 black 300 mL BOD bottles. Each lot of 9 bottles was suspended into one of three 150 L baths, thermostatically-controlled to maintain constant temperatures of 20, 24, and 28°C ± 0.2 °C. The warm ambient air temperature in the workshop prevented any lower temperatures being included in the experimental protocol. Each day for three days, 3 bottles were removed from each bath and Winkler titrations performed to determine the dissolved oxygen concentration. A very good correlation ($r^2 = 0.998$) was found between ln(k) and 1/T where k is the rate constant that describes the oxygen consumption and T is the temperature in °K. If the hypolimnetic oxygen demand is assumed to have the same temperature dependence as the surface layer sample used in this experiment, then a typical destratification-induced increase in the hypolimnetic temperature from 14 to 24 °C would increase the *in situ* oxygen demand by a factor of 2.7.

8.4 Inflow (Peel R.) chemistry

8.4.1 Methods

All major inflows after 1992 were sampled using an automated stage-dependant sampling device (GAMET) located at Taroona on the Peel River, 6.7 km upstream

of the reservoir. Based on the findings of earlier studies, the Peel R. was assumed to be the only significant source of inflow to the reservoir. Samples from the GAMET sampler were taken to TEL for analysis each morning following sample collection, i.e. typically within 24 hours of collection depending on the timing of the inflow. Samples were analysed using standard methods for NH_4, NO_3, NO_2, TKN, TN, TP, FRP, SO_4, total suspended solids (TSS), turbidity, conductivity, and pH. In addition, data from a HYDROLAB H2O conductivity, temperature and turbidity sensor installed at the Taroona site were also available although this device suffered frequent outages.

8.4.2 Relationships between nutrient inputs and suspended sediments in the Peel River inflows.

As many efforts to model catchment delivery of sediments and nutrients rely on correlations between flow, turbidity, suspended sediment and nutrient concentrations, it is useful to consider these correlations for the data from the Peel River at Taroona. The maximum turbidity that could be detected by the *in situ* sensor was 1000 NTU whereas the suspended sediment concentration from water samples collected on site was frequently of the order of grams per L with a maximum recorded value of 35.2 g L^{-1} on 2 Jan 1996. Of the 176 samples collected at Taroona, 53 had turbidities too high to measure.

Figure 8.15 shows a strong correlation ($r^2 = 0.85$, n = 28) between TSS and turbidity for all the available data pairs that were within range of the turbidity sensor. Three high outliers were eliminated prior to computing the regression and the data represent a small proportion of the 123 turbidity and 58 TSS measurements available. Nevertheless, turbidity appears to be a good surrogate indicator of suspended sediment in the Peel River for NTU < 1000.

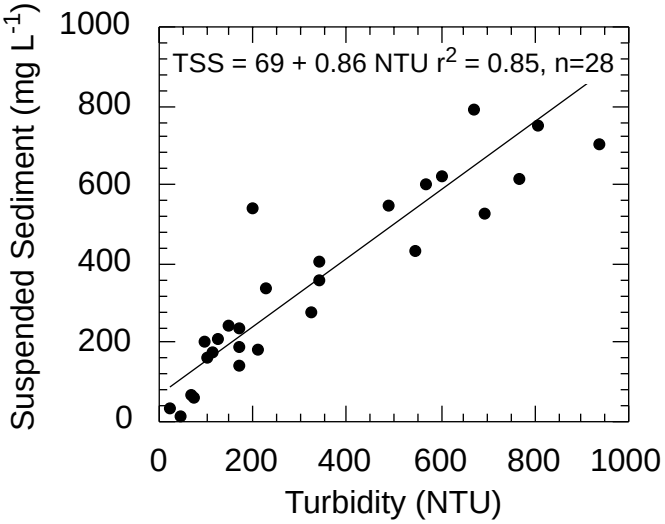

Figure 8.15 Correlation between suspended sediment and turbidity in samples collected from the Peel River at Taroona. 3 outliers have been eliminated from the correlation.

Correlations between nutrients and turbidity (Figure 8.16) and suspended solids (Figure 8.17) show significantly different behaviour for nitrogen and phosphorus. Correlations between phosphorus, both FRP and TP, and either turbidity or suspended sediment were poor ($r^2 < 0.09$). A more distinct trend is apparent in

both the NO_x , and TKN vs TSS data (r^2 ~ 0.14 , Figure 8.17) when the higher suspended sediment concentrations (> 1000 mg L^{-1}) are included – recall that the turbidity-based correlations are only valid to approximately 1000 mg L^{-1} of TSS. When individual inflow events were considered, the correlations were better (r^2 > 0.6) yet distinctly different for rising and falling stages of the hydrograph and between comparable stages for different inflow events with the slopes of the regressions differing by at least a factor of 1.6.

The variable nature of Peel River chemistry suggests that the external nutrient load to Chaffey Reservoir depends on which sub-catchments upstream of Taroona provide most of the runoff. This conclusion is based on the observation of good correlations for specific inflow events - which imply a consistent sediment source for each event - but a wide range of regression slopes which imply different sediment sources for different events. The Peel River exhibits remarkably high FRP concentrations (Figure 8.16). Identification of the source of this FRP would require detailed monitoring of the tributaries to the Peel River above Taroona.

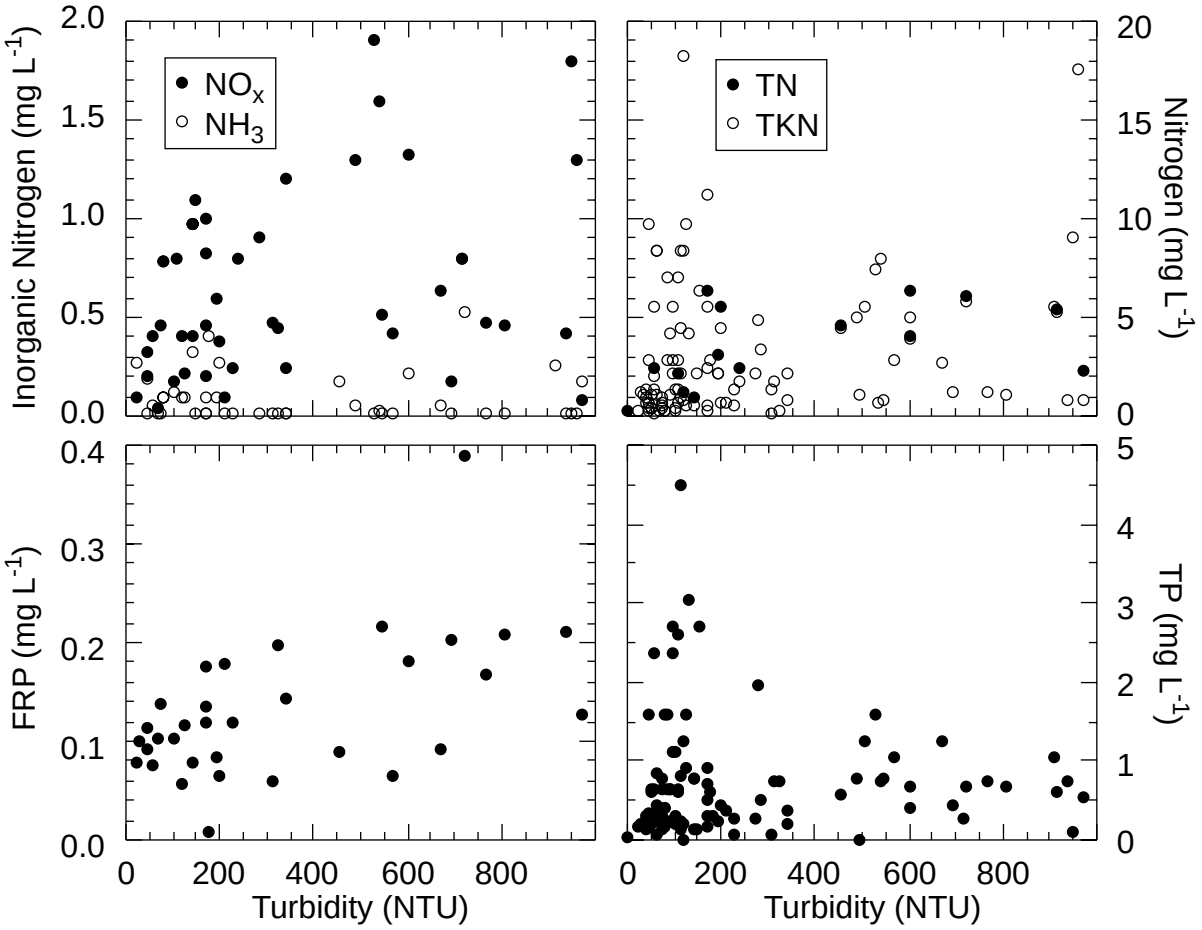

Figure 8.16 Correlations between turbidity and NOx, NH_4, TKN, TN, FRP, and TP for all data where the turbidity was within detection limits (< 1000 NTU).

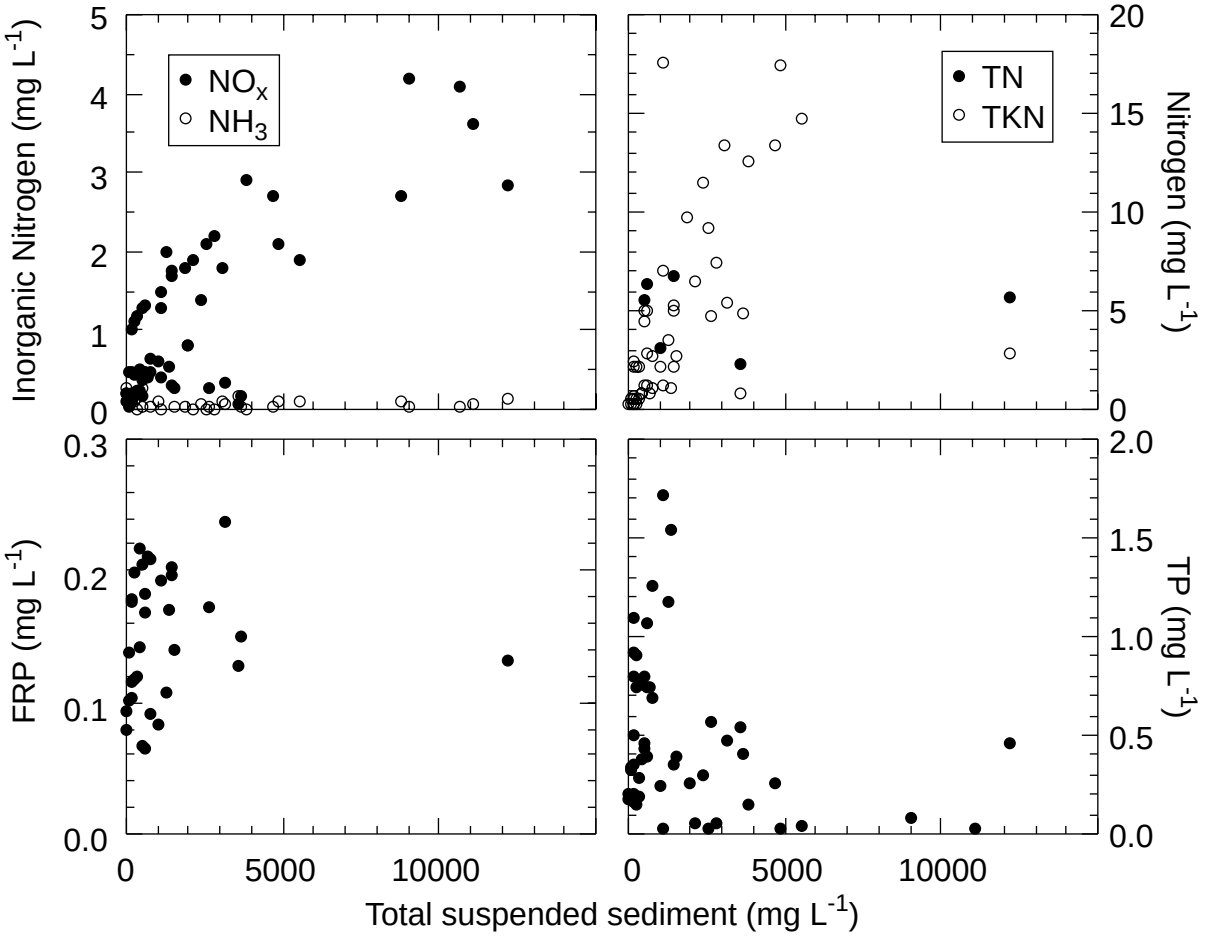

Figure 8.17 Correlations between total suspended sediment and NOx, NH_4, TKN, TN, FRP, and TP for the Peel River at Taroona.

8.5 Nutrient budget

Nutrients are delivered to the water column from external (catchment) and internal (sediment) sources. In addition, nutrients are lost from the water column by sedimentation and by the release of outflows. The nett change in the mass of nutrient (e.g. TN, TP, FRP) in the water column, ΔWC_{mass}, is

$$\Delta WC_{mass} = Load_{external} + Load_{internal} - Load_{outflow}$$

Simple rearrangement of this equation allows one to compute the internal nutrient load provided all of the other terms are known. The external and outflow loads are always positive whereas the internal load may be either positive or negative depending on the relative magnitudes of sediment nutrient release and sedimentation from the water column. When sediment release exceeds sedimentation losses the internal load is positive. Using this approach it is possible for the internal load of dissolved nutrients such as FRP to be positive at the same time that the internal load of total nutrient (i.e. TP), which includes particulate matter, is negative. This can occur when sediment release is occurring and at the same time algal cells, suspended sediment, etc. are sinking out of the water column. Here we compute the relative magnitudes of the internal and external loads using a mass balance approach and then compare the computed internal load to direct measurements of nutrient release from the sediments.

When the inflow and outflow concentrations vary over time, the nett internal load of a nutrient during a time interval, Δt, can be computed as

$$Load_{internal} = \int_{0'}^{H} C(z)A(z)dz \Big|_{t}^{t+\Delta t} - \int_{t}^{t+\Delta t} \left(Q_i C_i - Q_o C_o\right)dt$$

Here Q_i, Q_o, C_i, C_o are the inflow and outflow discharges and concentrations, respectively, H is the depth of the water column, $A(z)$ is the surface area at height z, $C(z)$ is the concentration at height z, and t is the time. The first term on the right-hand side is simply ΔWC_{mass} and the second term gives the net delivery or loss of nutrient due to inflows and release. A negative value for the internal load represents a loss of nutrient to the sediments of the reservoir.

The calculations use both historical and contemporary data. Water column chemical profiles collected at Stn 1 were assumed to be representative of the reservoir as a whole and inflow loads were computed from data collected from the Peel River at Taroona, 6.7 km upstream of the reservoir, but downstream of all major tributaries but one.

The total Peel River nutrient load consists of base flow and 'event' flow components. An inflow event is defined to occur whenever the water level at the Taroona gauging station exceeds 0.7 m (= 540 ML d^{-1}), which is the threshold required to trigger the automated sampler. To determine the nutrient load of an inflow event, a curve (typically a cubic spline) was fitted to the concentration data time series from samples taken throughout the inflow event. The curve was then used to interpolate in time between measured values to produce a concentration time series that matched the 15-minute resolution of the flow data. Finally, the product of the concentration and the flow rate was integrated over time for the duration of the inflow event to calculate the total mass of nutrient associated with the event.

Estimates of the amount of phosphorus and nitrogen exported downstream of the reservoir were made by muliplying the volume of water released by the average concentrations of TN, TP, and FRP in the water column at the depth of the outlet (Figure 4.4).

The basis for each mass balance has been defined as the period just after winter overturn until the first complete mixing event the next year. This method provides a realistic description of the annual cycling of nutrients and a more accurate basis for comparison of the nutrient status of the water body from year to year. The amount of nutrient present in dissolved form in the water column during summer is highly variable due to the unpredictability of the onset, and magnitude, of permanent stratification in years when the destratifier has been operated. By contrast, the annual winter overturn is relatively consistent and the system, in terms of the nutrient dynamics, is essentially returned to its equilibrium state or initial condition at this time.

8.5.1 Peel River event flow nutrient loads

The Peel River is subject to very large (e.g., 42820 ML d^{-1} peak discharge on 25 Jan 96) episodic inflow events that supply the bulk of the external nutrient load. Of the total inflow to Chaffey Reservoir during 1993-1997, 55% was delivered by inflow 'events'. Table 8.8 shows the volume, maximum flowrate and associated nutrient load for each inflow event during 1993-1997. On 25 January 1996, 14311 kg of TP entered the reservoir, five times more than the amount present in the water column prior to the inflow.

The inflow depth is the depth in the reservoir where the temperature matched the average inflow temperature at Taroona and neglects temperature changes between Taroona and the reservoir and entrainment of surface layer water where the inflow enters the reservoir. It represents the bottom of the intrusion. Entrainment of reservoir water where the river enters the storage will tend to raise the temperature of the inflowing water and therefore the intrusion depth will be somewhat above that listed in Table 8.8. For example, the February 1997 inflow intrusion was centred about 8.5 m and was approximately 6 m wide (Figure 7.1). Inflows warmer than the surface layer will always flow over the top of the reservoir. Over the study period fewer than 50% of the inflows entered directly into or very close to the surface layer. The remaining inflows, particularly larger ones and those occuring in the cooler months, intruded well below the surface layer.

Table 8.8 External loading at Chaffey Reservoir, 1993 – 1997. An asterisk (*) denotes TN loads inferred from TKN, NH_4, and NO_3 data as no TN data were available.

Date	Inflow Volume (ML)	Max Flowrate (ML d^{-1})	Inflow Depth (m)	Inflow TN load (kg)	TN in Reservoir (kg)	Inflow TP load (kg)	TP in Reservoir (kg)
25 Jul 93	432	2450	>20	-	40030	107	3161
02 Aug 93	1101	2187	>20	-	37993	171	2712
10 Sep 93	880	2999	7.4	-	39738	320	2161
14 Sep 93	-	1491	>20	-	31086	-	1994
04 Oct 93	1171	2462	5.6	-	29657	131	1596
16 Oct 93	3353	28000	-	-	35784	1899	2103
14 Nov 93	662	4980	-	-	33430	222	3445
06 Dec 93	2433	4609	-	-	28366	534	2869
26 Sep 95	1714	1000	-	955	20658	1788	427
03 Oct 95	657	803	1.5	258*	20852	115	638
01 Dec 95	573	2132	6.5	3446*	14494	382	765
06 Dec 95	1539	1100	-	1079*	14268	131	703
10 Dec 95	2876	15862	8.5	48164*	14268	5233	703
02 Jan 96	2269	12626	8.5	7702	18434	688	1202
25 Jan 96	9841	42820	>16	126101	24662	14311	2830
29 Jul 96	1517	865	>18	418*	35946	181	1301
30 Aug 96	3313	7228	>17	-	41472	-	1438
01 Sep 96	2831	2629	>17	-	41472	-	1438
06 Oct 96	1825	7723	3.0	-	54533	-	1879
08 Dec 96	1541	1367	3.8	-	19722	-	1373
13 Feb 97	9905	14123	12	7332*	56603	4098	1670
15 Feb 97	2805	12911	12	4478*	56603	855	1670

8.5.2 Peel River base flow nutrient loads

Because a significant portion (45%) of the inflow to the reservoir occurs under base flow conditions which are not automatically sampled we need to assess the significance of the nutrients entering the reservoir under these conditions. We can estimate limits for the nutrient loads during unsampled base flows by multiplying an assumed base flow concentration by the volume of unsampled flow. Base load concentrations were determined from manually collected grab samples taken during 1991-1997 when the flow was too small to trigger the automated sampler (< 540 ML d^{-1}). Typical concentrations and the estimated loads of nutrients during base flow conditions are shown in Table 8.9. The event sampling most likely accounted for 95% of the TP load and 93% of the TN load.

Table 8.9 Estimated nutrient loads from Peel River during base flow (unsampled) periods from 19 June 1995 to 16 February 1997. Base flow concentrations are for grab samples collected during 1991-1997. Event load is the total load during sampled inflow events. Event loads for NO_3 and NH_4 were not computed.

	Mean Conc (mg/L)	Median Conc (mg/L)	Conc std dev (mg/L)	Flow (ML)	Event Load	Base load (kg)
NO_3^-	0.297	0.300	0.143	23604		7010
NH_4^+	0.050	0.030	0.035	23604		1180
TP	0.058	0.045	0.038	23604	32032	1369
TN	0.263	0.200	0.122	23604	199933	6208

8.5.3 Mass balance results

The results of mass balances calculated for total nitrogen (TN) and total phosphorus (TP) are given in Table 8.10 for the period 1993 - 1997. These values reflect the nett annual change in water column TN and TP and are not absolute rates. No nitrogen data was available for inflows during 1993/1994. The majority of the external nutrient load entering the reservoir is transported to the sediment. Only a fraction leaves the reservoir, particularly in drier years when releases are restricted. In 1995/1996 when the reservoir was beginning to fill after the drought, 97% of the phosphorus and 91% of the nitrogen that was imported from the catchment was eventually lost from the water column, either to the sediments or by denitrification. Even during years with no major inflow such as 1994/1995, there was a net flux was from the water column to the sediment.

The effects of a severe two year drought beginning in late 1994 are evident in the results, particularly in the 1994/1995 data, where inflows and outflows are negligible and large net decreases (2884 kg of TP and 18739 kg of TN) in the mass of nutrients in the water column are apparent. During 1995/1996 most of the TN and TP entering the reservoir from the catchment was lost to the sediments. In other years, outflow loads were more important.

Table 8.10 N and P mass balances for Chaffey Reservoir from 1993 to 1997. ΔWC_{mass} is the net observed change during the year of water column nutrient mass. Sedimentation = - (ΔWC_{mass} – Inflow load + Outflow load). Negative sedimentation values indicate a net release of nutrient from the sediment to the water column.

	Inflow load (kg)	Outflow load (kg)	ΔWC_{mass} (kg)	Sedimentation (kg)
Total P				
1993/1994	3384	1671	1163	550
1994/1995	~0	1831	-2884	1053
1995/1996	27079	335	605	26139
1996/1997*	4953	293	3049	1611
Total N				
1994/1995	~0	27781	-18379	-9402
1995/1996	187705	4574	14427	168704
1996/1997*	12228	4737	21701	-14210

Changes in the mass of TP and FRP within the water column are compared to their external loads from the Peel River in Figure 8.18. This figure includes estimates of the base flow loads. Just the FRP load from the Peel R. generally exceeds the observed change in water column FRP and indeed accounts for more than half of the observed change in water column TP! When the external TP load is factored in, we see that the external phosphorus load during periods with inflow injects much more phosphorus into the reservoir than actually appears in the water column profiles. Clearly much of this external load is comprised of coarser particulates that are rapidly lost to the sediments (Section 8.2.2). From 26 Mar - 16 Apr 1996 there was actually a small (~50 kg) decrease in the water column TP due to sedimentation concurrent with the observed increase (~220 kg) in water column FRP.

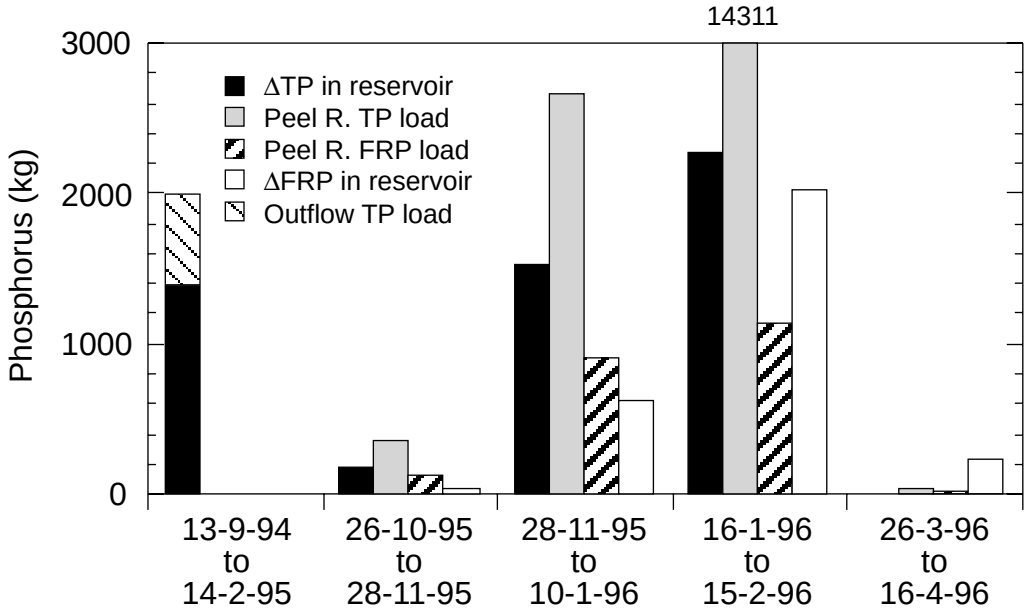

Figure 8.18 External loads of TP and FRP from the Peel River and the observed change in the total mass of TP (ΔTP) and FRP (ΔFRP) in the water column of

Chaffey Reservoir for the periods indicated. The destratifier was operated 4 – 28 Oct 1995 and 11 Jan – 13 Feb 1996.

8.5.3.1 Internal nutrient loads

We can use the mass balance data to compute internal nutrient loading rates as well. Although FRP was not measured prior to October 1995, the near absence of inflows from 13 Sep 94 to 14 Feb 95 kept the external TP load to less than 100 kg during this period so we can assume that most of the observed change in water column TP (ΔTP) reflects phosphorus released from the sediments. The outflow TP load was released from 5-12 m depth from 13 Sep 94 to 14 Dec 94 and from < 5 m from 14 Dec 94 to 14 Feb 95 and, based on Table 8.3, we assume most of this was particulate phosphorus rather than FRP which was accumulating in the hypolimnion. Neglecting the outflow TP gives a lower limit for the sediment phosphorus release rate of 8.9 kg d^{-1}; its inclusion increases the rate to 13 kg d^{-1}.

The reduction in sediment phosphorus release rate due to operation of the destratifier can be inferred from the data for the period 26 Oct 95 to 28 Nov 95. The destratifier was turned on with anoxic conditions in the hypolimnion on 4 October 95 and operated until 28 October. During this period dissolved oxygen concentrations rose to about 5 mg L^{-1} and concentrations remained above 2 mg L^{-1} through 28 November (Figure 8.7). If the small increase in water column TP (184 kg, Figure 8.18) is assumed to be due solely to FRP released from the sediment and supplied by the Peel R. and we subtract the Peel R. component (120 kg) we are left with a sediment release rate of 1.9 kg d^{-1}. Destratification reduced the internal phosphorus load by 79-85 %.

8.5.4 Benthic chamber measurements of internal nutrient loads from sediments

Benthic chamber deployments were made at various sites within the dam and at different times to explore benthic nutrient fluxes under permutations of high and low water temperatures and varying degrees of oxia/anoxia. The sites were selected to represent the range of organic carbon content found in the reservoir's sediments.

Table 8.11 shows oxygen consumption rates in the surface waters at sites in the southern basin that were located within the SML. There are marked differences between sites. Pelican Point (south eastern shore) is subject to erosion and is predominantly gravel with very little fine sediment, while the southern basin is a deposition zone for fine sediment. The measurements at the Fishing Club (southern shore at river mouth) were made shortly after a significant inflow which had deposited considerable organic matter at the site.

Table 8.11 Benthic chamber fluxes at shallow sites in southern basin of Chaffey Reservoir.

Location	T (°C)	pH	O_2 (mMol m^{-2} d^{-1})
Southern basin (1m)	28	9.8	84
Fishing club (1.2m)	22	9.4	82
Pelican Point (1m)	21	9.5	36

The results of benthic chamber deployments in the main basin (100 m south of Stn 2, Figure 5.1) are given in Table 8.12. Chambers 71, 75, and 78 were deployed

within 3 m of one another to examine small-scale variability in sediment fluxes. Blank values in the oxygen column indicate that the water was anoxic at the start of the experiment. Under both oxic and anoxic conditions (except for 1 occasion) there was a net flux of ammonia into the water column. Phosphorus fluxes were predominantly into the water column with the largest value occurring under oxic conditions. A flux of 1 mg P m^{-2} d^{-1} over the entire reservoir when full is equivalent to an internal load of roughly 5.3 kg d^{-1}. Recall that mass balances determined an average internal phosphorus flux of 9 – 11 kg d^{-1} (Section 8.5.3). The results for nitrate are more varied indicating both fluxes into and out of the sediments and may reflect local heterogeneities. The overall nutrient dynamics of the water column (Section 8.3, Figure 8.7) show a similar variability with the system dominated by ammonia one year, and by nitrate the next.

Table 8.12 Benthic chamber fluxes in main basin of Chaffey Reservoir.

Month	NH_4 mg N m^{-2} d^{-1}	PO_4 mg P m^{-2} d^{-1}	NO_x mg N m^{-2} d^{-1}	O_2 mg O_2 m^{-2} d^{-1}
March '97				
71	2.2	6.9	-0.09	94
75	5.8	2.2	0.00	116
Sept '97				
71	0.99	0.00	0.86	
78	0.44	-0.34	0.62	
Nov '97				
71	3.3	0.91	-0.22	
75	0.34	0.03	-0.47	
78	2.2	0.61	-0.57	
Jan '98				
71	4.4	0.04	-0.11	
75	2.1	0.06	2.1	
78	1.5	-0.93	0.68	
April '98				
71	-0.49	0.022	19	19
75	2.4	0.025	0.12	
78	2.8	0.30	-0.12	

Peeper measurements of sediment chemical profiles showed concentration gradients of ammonia and phosphorus towards the sediment-water interface which implies fluxes of both species into the water column. The spatial resolution of these measurements is limited (about 1 cm), however, and it is possible for surface processes in the thin oxic layer to go undetected. There was no evidence for nitrate fluxes into the water column suggesting that denitrification is occurring in the sediments and that the nitrate is formed at the sediment-water interface and in oxygenated waters.

8.6 Conclusions

Water column and sediment chemistry are closely coupled in Chaffey Reservoir. Sediment is delivered primarily by the Peel River and is accumulating at about 1 cm per annum based on silt pad measurements. When oxygen is depleted in the hypolimnion, nutrients once bound to the sediments are released to the water column at an accelerated rate. Phosphorus was released from the sediment at

roughly 10 kg d^{-1}(~ 4.5-5 mg P m^{-2} d^{-1}) and was mostly orthophosphate. Operation of the destratifier reduced the internal phosphorus load by 80%.

When the water column is anoxic, iron and manganese are present predominantly in colloidal form as FeS and MnS. Neither species has a high capacity for binding phosphate. These colloids slowly settle out of the water column resulting in a loss of Fe and Mn to the sediments.

Operation of the destratifier oxidises the bottom waters and Fe formerly present as FeS is converted to FeOOH which subsequently scavenges phosphate. The scavenging of phosphate is relatively rapid but incomplete (63%) with most of the removal due to the oxidised Fe species. Manganese oxides appear to be relatively ineffectual in adsorbing P. There is insufficient Fe^{2+} to provide sufficient iron oxide to completely scavenge all the available P in the anoxic bottom waters of the dam. Consequently, operation of the destratification system once anoxia has been established can raise – and not lower – concentrations of bioavailable (ortho-) phosphate at the surface.

The effectiveness of the destratification system in controlling surface concentrations of P would be enhanced by the provision of additional Fe^{3+} to the surface layers or by reduction of SO_4 so that Fe is not removed in the hypolimnion as FeS.

Destratification increases the temperature of the hypolimnion which in turn increases O_2 demand. Sediment P release may subsequently increase if anoxic conditions are reestablished.

9 Trophic dynamics - algal species succession

The growth of phytoplankton requires light for photosynthesis and nutrients for the manufacture of cell constituents. The biomass supporting capacity of a water body is likely to be the lower of the 'ceilings' imposed by the availability of these resources (Reynolds 1997). It is important to distinguish between the cell replication rate and the net rate of growth of the algal population; cell replication can occur at near maximal rates even if biomass is not accumulating provided nutrients are recycled quickly within the euphotic zone. The cell replication rate depends most strongly on light availability and temperature as the time scale associated with nutrient uptake is much shorter than that for photosynthetic fixation of CO_2 (Reynolds and Irish 1997). Phytoplankton biomass also depends on loss factors such as death, grazing by zooplankton, sedimentation and hydraulic washout as well as on the overall availability of nutrients.

Nutrient availability can vary temporally and spatially in the water column with strong vertical gradients in N and P forming during periods of thermal stratification (Section 8.3). Biological consumption can lead to very low inorganic nutrient concentrations in the SML at the same time as inorganic nutrients are accumulating in the hypolimnion as the result of sediment diagenesis. Re-supply of nutrients to the SML often requires deepening of the layer to entrain relatively nutrient-rich water from below (Section 7.1, Figure 7.1).

The amount of light available for photosynthesis depends on the attenuation of light in the water column, the depth of the SML and the amount of turbulence in the surface layer, q^*. In a weakly mixed environment (low q^*), migratory or buoyant phytoplankton can alter their position in the water column to optimise light availability. As q^* increases and the SML deepens, the mean light intensity is reduced providing an advantage to phytoplankton adapted to low-light conditions. Increasing q^* also reduces the rate at which sinking phytoplankton such as diatoms are lost from the surface layer.

In this section we analyse the 11 year record of chemical, physical and algal abundance data and describe the annual and interannual trends in biomass and community succession. We also consider the long term affects of destratification. In addition, we present the results of an intensive study of the algal and zooplankton communities between 1995 and 1997 that included measuring the light and nutrient requirements of the major algal taxa at Chaffey Dam and their adaptations to acquisition of these resources.

9.1 Methodology

Water samples were collected between 1987 and 1997 at a number of sites around the reservoir and enumerated to genera by DLWC staff at the Arncliffe Laboratories. Sampling was undertaken at least monthly, but for most of the period weekly data were available. The samples were collected using an elbow grab from about 0.25 m depth; therefore, the samples only represent phytoplankton from the surface of the reservoir. Cell abundance for each taxa has been converted to algal volume using mean cell dimensions and the appropriate shape formula. Cell dimensions were measured at MDFRC for the common taxa between 1995 and 1997 and previous years were assumed to be equivalent. Dimensions for the less common taxa were taken as the mean of the range for

that taxa reported in the literature (eg, Prescott 1982, Entwisle et al. 1997). Data used in the following analysis represent pooled data from all the sites within the dam and are reported as either weekly or monthly averages.

9.1.1 Elbow grabs vs 5 m-integrated sampling

The high prevalence of buoyant and motile species in the reservoir raises the question as to whether or not elbow-grab sampling biases the abundance estimates for the SML. The abundance of species that accumulate near the surface such as *Anabaena*, *Microcystis* and *Botryococcus* may be overestimated whereas those taxa that actively migrate to avoid the surface such as *Ceratium* may be underestimated. Between 1995 and 1997 DLWC surface samples from Stn1 were collected at the same time as the 5 m-integrated samples (enumerated by the MDFRC) were collected from the 5 sites shown in Figure 5.1. This allows us to compare the two methods.

In general the two sampling techniques compared well; both showed the same general trends in algal abundance and species composition. The elbow-grab technique, on most occasions, provided higher estimates of phytoplankton abundance relative to the 5 m-integrated sample. This was caused by the SML being shallower than 5 m and the uneven vertical distribution of the phytoplankton; virtually all of the phytoplankton were within the SML.

When buoyant algae such as *Botryococcus* or *Anabaena* were present, the elbow-grab method exhibited greater week to week variability than did the 5 m-integrated samples. Site-to-site variability between the 5 m-integrated samples increased and significant differences between the DLWC sample and the mean of the 5 MDFRC samples occurred when wind-driven surface-layer motions caused buoyant surface blooms to accumulate at the downwind end of the reservoir (Figure 9.1). Jones (1997) observed a similar degree of variation in 3 SE Queensland reservoirs and recommended pooling samples from a number of sites to overcome the problems of cross-reservoir variability. Our experience at Chaffey Dam indicates that this would be a cost effective method of increasing the reliability of blue-green algal counts.

Comparison of DLWC and MDFRC data indicated also that the DLWC data set underestimated the colonial green algae, *Volvox* and that the ciliate, *Stentor*, was not included in DLWC plankton counts. At various periods *Volvox* and the zoochlorella symbiont of *Stentor* contained a significant proportion of the chlorophyll in the reservoir.

9.1.2 Biovolume vs chlorophyll-*a*

Chlorophyll-a determinations were performed on aliquots from each of the weekly 5 m-integrated samples from September 1995 to November 1997. The mean concentration of Chl-*a* during this period was 21.5 $\mu g\ L^{-1} \pm 42$ (SD). The high variability reflected the ooccurrence of extreme algal blooms (Figure 9.1). For example, the spring 1996 bloom of *Botryococcus* exceeded 300 $\mu g\ L^{-1}$ of Chl-*a*. Blooms such as this significantly increased the mean Chl-*a* concentration above the median Chl-*a* of 9.2 $\mu g\ L^{-1}$.

A regression of the Chl-*a* against cell volume predicts a mean Chl-*a*:cell volume ratio of 3.8 (SE 0.24) µg Chl-*a* mm^{-3} which is at the lower end of the range (1.5 to 19.7 µg Chl-*a* mm^{-3}) reported by Reynolds (1984). This ratio is an average for a number of algal groups over two years at Chaffey Reservoir and should be used with caution as it will vary depending on the dominant algae.

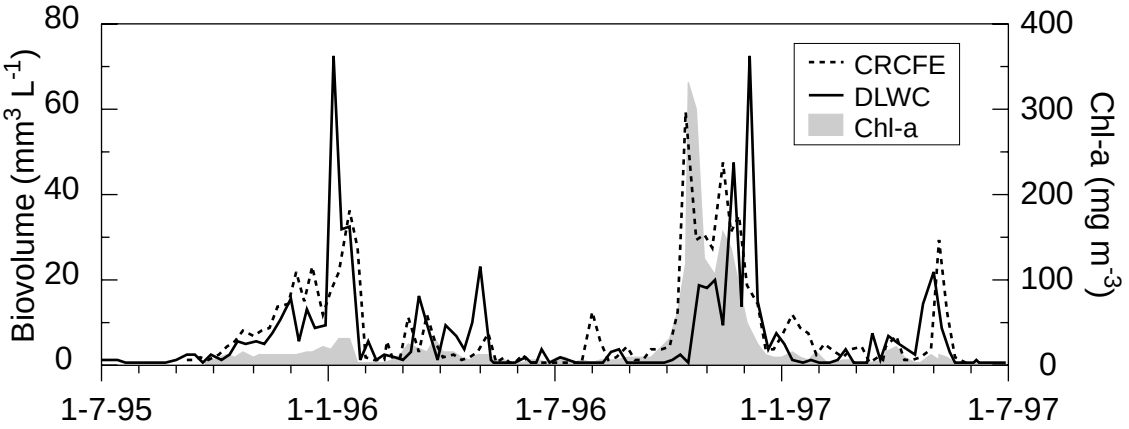

Figure 9.1 Weekly total algal biovolume as reported by DLWC and CRCFE and chlorophyll-a concentration during the project. DLWC data are from single samples collected from 0.25 m depth at Stn 1. CRCFE and chlorophyll data are averages of 5-m integrated samples collected at 5 sites around the reservoir.

9.2 Trends in algal abundance

9.2.1 Species composition

A total of 58 taxa of phytoplankton were recorded from Chaffey Reservoir between 1987 and 1997 (Table 9.1). This compares with 43 taxa recorded during the initial filling of the reservoir from 1979 to 1981 by May and Powell (1986) who reported also that the number of taxa increased as the reservoir filled. The most abundant taxa (by cell volume) were: *Ceratium* 37%, *Anabaena* 22%, *Botryococcus* 10%, *Peridinium* 8%, *Cryptomonas* 4%, *Microcystis* 4% and *Oocystis* 4%; and together accounted for 89% of the algal cell volume. Each of these 7 taxa were recorded in more than 50% of the months between 1987-1997 with *Anabaena* and *Ceratium* recorded in 82% of all months. *Peridinium* and *Cryptomonas* were not recorded by May and Powell (1986). The diatom *Aulacoseria* accounted for just 1% of total algal volume and was present 66% of the time.

Table 9.1 Phytoplankton species observed at Chaffey Reservoir during 1987-1997 as percentage of total biovolume and frequency of occurrence.

	% biovolume *	% occurrence **		% biovolume *	% occurrence **
Dinophyta (Dinoflagellates)			**Cryptophyta (Crytomonads)**		
Ceratium	37.13	82	*Cryptomonas*	3.55	97
Peridinium	7.71	56	*Rhodomonas*	0.59	82
			Chroomonas	0.08	8
Chlorophyta (Green Algae)					
Botryococcus	9.53	51	**Bacillariophyta (Diatoms)**		
Oocystis	3.59	98	*Aulacoseira*	1.03	66
Volvox	1.49	25	*Amphora*	0.45	13
Golenkinia	1.44	42	*Synedra*	0.36	69
Chodatella	0.96	58	*Gomphonema*	0.25	18
Staurastrum	0.79	44	*Cyclotella*	0.22	82
Chlorella	0.70	61	*Nitzschia*	0.05	42
Quadrigula	0.68	6	*Navicula*	0.04	50
Sphaerocystis	0.38	66	*Fragilaria*	0.03	35
Closterium	0.35	69	*Rhoicosphenia*	<0.01	19
Pandorina	0.27	11	*Kirchneriella*	<0.01	4
Chlamydomonas	0.19	65	*Cymbella*	<0.01	12
Carteria	0.18	20	*Surirella*	<0.01	5
Schroederia	0.17	54	*Cocconeis*	<0.01	15
Chlamydomonus	0.15	31			
Ankistrodesmus	0.15	75	**Euglenophyta (Eugleniods)**		
Nephrocytium	0.13	12	*Euglena*	0.48	35
Elakatothrix	0.12	69	*Trachelomonas*	0.39	70
Crucigenia	0.06	26	*Lepocinclis*	0.28	5
Scenedesmus	0.05	47			
Closteriopsis	0.05	5	**Chrysophyta (Golden-brown algae)**		
Coelastrum	0.02	26	*Synura*	0.03	6
Characium	0.01	8	*Mallomonas*	<0.01	27
Actinastrum	0.01	5			
Eudorina	0.01	3	**Cyanobacteria (Blue-green algae)**		
Lagerheimia	<0.01	1	*Anabaena*	21.98	82
Dictyosphaerium	<0.01	8	*Microcystis*	3.56	60
Micractinium	<0.01	4	*Aphanizomenon*	0.26	12
Schizochlamys	<0.01	2	*Oscillatoria*	0.01	22
			Merismopedia	0.01	5
			Pseudanabaena	<0.01	6
			Lyngbya	<0.01	8

* % biovolume = the contribution of that genera to the total cell volume for the period 1987-1997
** % occurence = the percentage of months between 1987 - 1997 in which that taxa was recorded

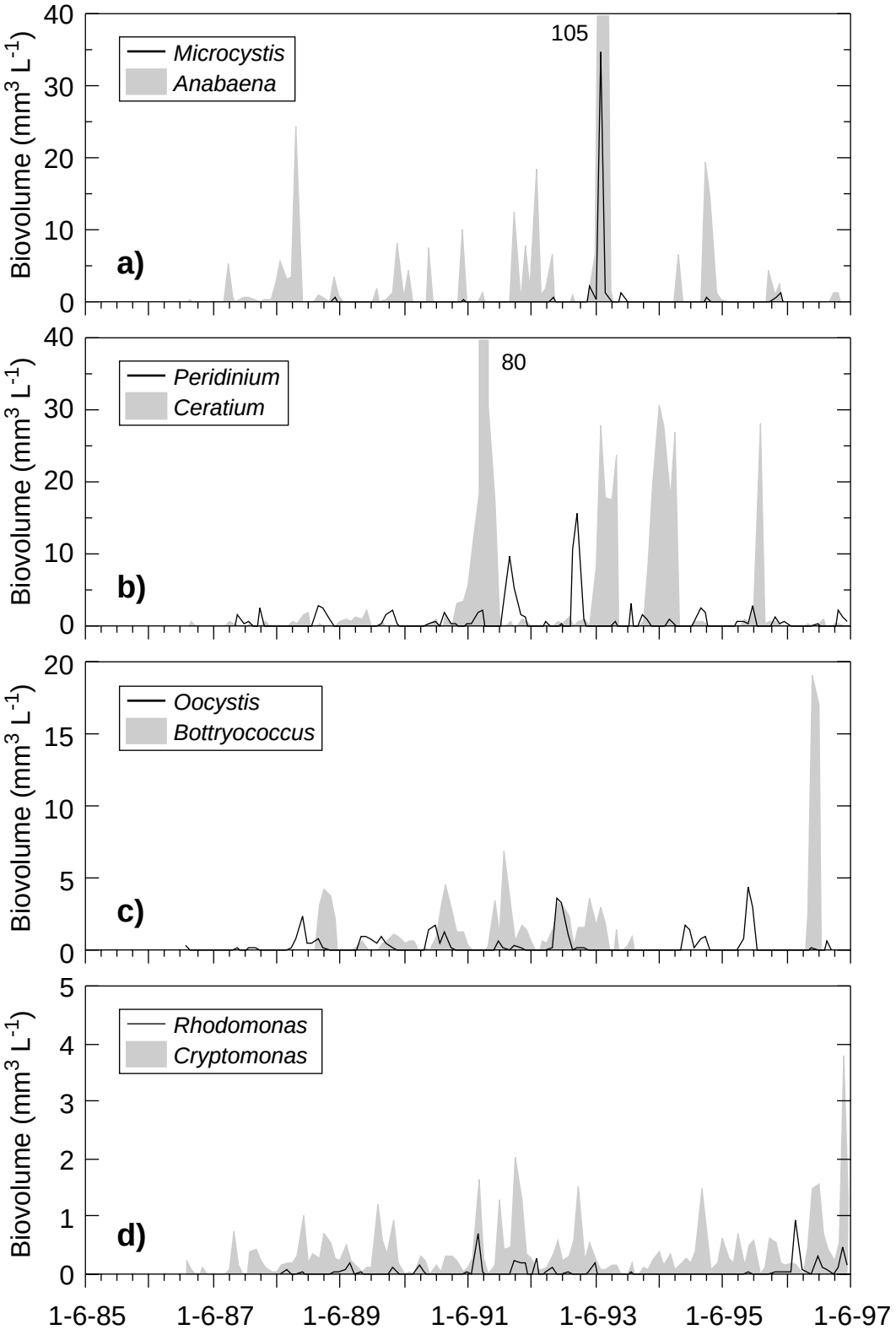

Figure 9.2 Algal cell volume ($mm^3 L^{-1}$), averaged monthly, for the major species of algae at Chaffey Dam. a) Cyanobacteria, b) Dinoflagellates, c) Chlorophycaea, d) Cryptomonads. These 8 species comprise 88% of the total phytoplankton population. Numbers indicate maximum biomass for peaks that extend beyond the limits of the y-axis. Data collected by DLWC.

9.2.2 Interannual biovolume variability

During 1987-1997 total algal cell volume underwent periods of high and low abundance with transitions between the two occurring on time scales of weeks to years (Figure 9.2). There were no distinct seasonal trends; total algal abundance ranged from very low to high in each month of the year. The years with the highest algal abundance generally had high algal abundance throughout the year, but in particular they had large, persistent blue-green algal and/or dinoflagellate blooms during the winter months. In contrast, years with low algal abundance did not have blue-green algal or dinoflagellate blooms during the winter months. Algal abundance did not correlate with changes in dam capacity (Figure 6.4), unlike North Pine Dam in SE Queensland (Harris and Baxter, 1996).

The average annual algal volume was calculated for the period between turnover[4] of the water column in one year with the corresponding period in the following year. It includes contributions from mid-winter, spring and summer blooms and ranged from 3.5 $mm^3 L^{-1}$ in 1987-88, a period of almost continual operation of the destratifier, to 28.5 $mm^3 L^{-1}$ in 1993-94.

The three largest blooms occurred during the winters of 1991, 1993, and 1994; with large populations of *Ceratium*, which dominated in 1991 and 1994, while *Anabaena* and *Microcystis* dominated in 1993. The large winter blooms of algal species that thrive in stratified conditions is consistent with the observation that the daily and maximum SML depths can be quite shallow even in winter (Figure 7.3) provided an adequate supply of nutrients was available. Large blooms of *Ceratium*, *Anabaena*, and *Botryococcus* also occurred in spring, summer and autumn.

Of the 11 years of algal abundance data, just 2 years (1991-1992 and 1993-1994) contributed 46% of the total algal volume. These two years witnessed the largest winter blooms since the dam filled and in both cases there were significant inflows to the reservoir prior to the development of the blooms (Figure 6.3). The very high winter biomasses may reflect high external nutrient loads at these times. Similarly, the large summer bloom of Ceratium in January 1996 followed significant external nutrient loading in the Peel R. during the previous month (Figure 8.18).

The response of the algal population to external nutrient loading events depends critically on the level at which the inflow intrudes into the reservoir. This level is determined by the ambient stratification and local climatic conditions at the time of the inflow (Section 7.1). The algal population is unlikely to respond in the short term to inflows that intrude below the euphotic zone.

9.2.3 Seasonal biovolume trends

Although the mean monthly biomass at Chaffey Dam did not show a seasonal pattern, analysis of the mean cell abundance and the rate of biomass increase (calculated for monthly averaged cell counts) for major taxa did show some

[4] Turnover is assumed to have occurred on the first day of the calendar year when there was a rapid increase in hypolimnetic O_2 accompanied by a decrease in hypolimnetic P. This process usually occurs between April and June, but can occur earlier in summer if artificial destratification is undertaken.

general intra-annual trends. In the rest of this section the term 'growth' refers to a *net* change in biomass of a species and includes losses such as respiration, grazing and sedimentation. It must not be confused with the *specific* growth rate which refers to the cell replication rate. A positive specific growth rate may apply to a declining population if the loss rates exceed it.

9.2.3.1 Blue-green algae

Between 1987 and 1997 blue-green algae were observed in all months of the year at least once (Figure 9.2a). Net positive increase of *Anabaena* biomass has occurred in all months of the year, but most frequently in February, March, May, July and September. The fastest increases occurred during March - May as the surface layer deepened. Rapid biomass accumulation during autumn often resulted in a high cell abundance which sometimes persisted, albeit increasing at a slower rate, through winter. If *Anabaena* was present during November and December it was usually declining in abundance and *Anabaena* were least abundant in December, January and February.

Microcystis biomass increased most rapidly during late summer and autumn. With the exception of November, which has 3 years in which biomass increased, the remaining months generally have low *Microcystis* abundance and negative growth rates.

9.2.3.2 Green algae

The growth of the *Botryococcus* population was positive during October for 6 of the 11 years, resulting in blooms during spring and summer in 4 of the 11 years (Figure 9.2c). High cell abundance may persist through autumn. *Botryococcus* biomass increased slowly in autumn and winter, especially June when any persistent blooms generally disappeared.

Oocystis exhibited a clear annual trend in cell abundance with relatively high abundance during late spring and summer and low abundance during winter months. *Oocystis* biomass increased the fastest during October and November. The rate of increase usually declined in December and January. Occasionally biomass increased during autumn and winter, however, this was relatively slow and did not result in high algal abundance.

The major green algal taxa had their highest net growth rates and maximum biomass between August and November, coincident with the strengthening of water column stability, increasing surface mixed layer temperature and increasing solar insolation.

9.2.3.3 Dinoflagellates

The biomass of *Ceratium* could increase in all months of the year, however, mean abundance was much greater during the winter months with the exception of one large bloom occurring during December 1995 and January 1996 (Figure 9.2b). *Peridinium* biomass generally increased during February, leading to a high abundance during autumn which declined by winter. There were large interannual differences in abundance of the dinoflagellates.

In temperate water bodies the dinoflagellates *Peridinium* and *Ceratium* are generally observed in high abundance during the later stages of stratification, where their relatively low surface-to volume ratios, large size and poor growth capacity are offset by the ability to avoid grazing and to self regulate vertical position in the water column to gain access to light and nutrient (e.g., Reynolds 1997). In Chaffey Dam, their ability to flourish year round suggests that mixed layer turbulence, at least in some years (e.g., 1991 and 1993) is low enough through winter for *Ceratium* to be advantaged.

9.2.3.4 Cryptomonads

Cryptomonas and *Rhodomonas* were ubiquitous in the surface water throughout the year with *Cryptomonas* occurring in 97% of the months between 1987-1997 (Table 9.1, Figure 9.2d). During periods of low algal abundance, crytomonads may dominate algal cell volume but do not reach a high biomass. The biomass of cryptomonads may increase in any month of the year, but this was most likely during spring as the temperature in the surface layer increased along with increases in solar insolation.

Cryptomonads are almost ubiquitous in surface waters and are relatively more abundant in moderately enriched waters. Their motility means they are not solely dependant on stratification or mixing for access to light and nutrient. They are considered to be a favourite food of many zooplankton and are thus susceptible to grazing pressure (Reynolds 1997).

9.2.3.5 Diatoms

Generally, there was very low abundance of diatoms at Chaffey Dam with *Aulacoseria*, at 1% of the total biovolume, being the most abundant (Table 9.1). *Aulacoseria* biomass is likely to increase in late summer (February to April, 5 of 11 years) with another period in August (4 of 11 years).

A large epiphytic diatom population, which included *Aulacoseria*, *Gomphomena, Fragillaria* and *Cyclotella*, developed in association with a *Cladophera* dominated benthic mat during the spring of 1997. This population was not planktonic, and so did not appear in the water column samples.

In temperate water bodies diatoms are generally found relatively early in the stratification sequence, relying on water column turbulence to maintain their position in the surface mixed layer. At Chaffey Dam, they appear in late summer and autumn as the surface layer begins to deepen and occasionally in August. There is sufficient nutrient, including Si, in Chaffey Dam to support large diatom populations and diatoms are almost always present in the record, though at very low abundance. This suggests that diatom abundance is limited by either the availability of light or, more likely, by high loss rates due to the strong persistent stratification.

9.2.3.6 Is there a generalised annual successional sequence at Chaffey Dam?

No clear successional sequence of phytoplankton was observed at Chaffey Dam, however, there was a periodicity of occurrence. During spring and early summer the biomass of many of the major taxa increased but it was green algae such as

Oocystis and *Botryococcus* that most often achieved a high biomass. The green algae sometimes declined in early summer (eg. 1987, 96, 97) or persisted into autumn (eg 1989, 90, 91 and 93). *Ceratium* abundance was low during spring and summer apart from the occurrence of a single bloom in 1996. During autumn a number of the major taxa show increased growth including *Microcystis*, *Anabaena*, *Ceratium* and *Aulacoseria*. In most years cyanobacteria achieve their highest biomass during this period (eg 1989, 90, 92, 95, 96 and 97) followed by dinoflagellates (eg 1991, 93, 94). The winter months can either have a low algal abundance (eg 1987, 89, 90, 95, 96, 97) or can have very high dinoflagellate (1991, 94) or blue-green algal (1988, 92) or both dinoflagellate and blue-green algal biomass (1993).

9.2.4 Nutrients and algal growth

Figure 9.3 shows time series of total algal biovolume and surface layer concentrations of FRP, NH_4, and NO_x from 1995 to 1997. FRP and inorganic N both decreased rapidly to relatively low concentrations during spring as stratification intensified and high algal biomass developed in the surface layer. Biomass reached a plateau when inorganic nitrogen was depleted in Dec 1995 despite increasing FRP concentrations and in Oct 1996. In both cases the FRP concentration was also small. The lowest nutrient concentrations in the SML occurred during the summer months except for Jan 1996 when the destratifier was operated and biovolume increased presumably due to the transport of nutrients from the hypolimnion into the surface layer.

During 1995 the ratio of NH_4 to NO_3 was 2:1 whilst in 1996 the inorganic N was predominantly NO_3. The TN to TP ratio varied annually, but was generally in excess of the Redfield ratio, particularly during the winter months with TN:TP approaching the Redfield ratio in spring and summer.

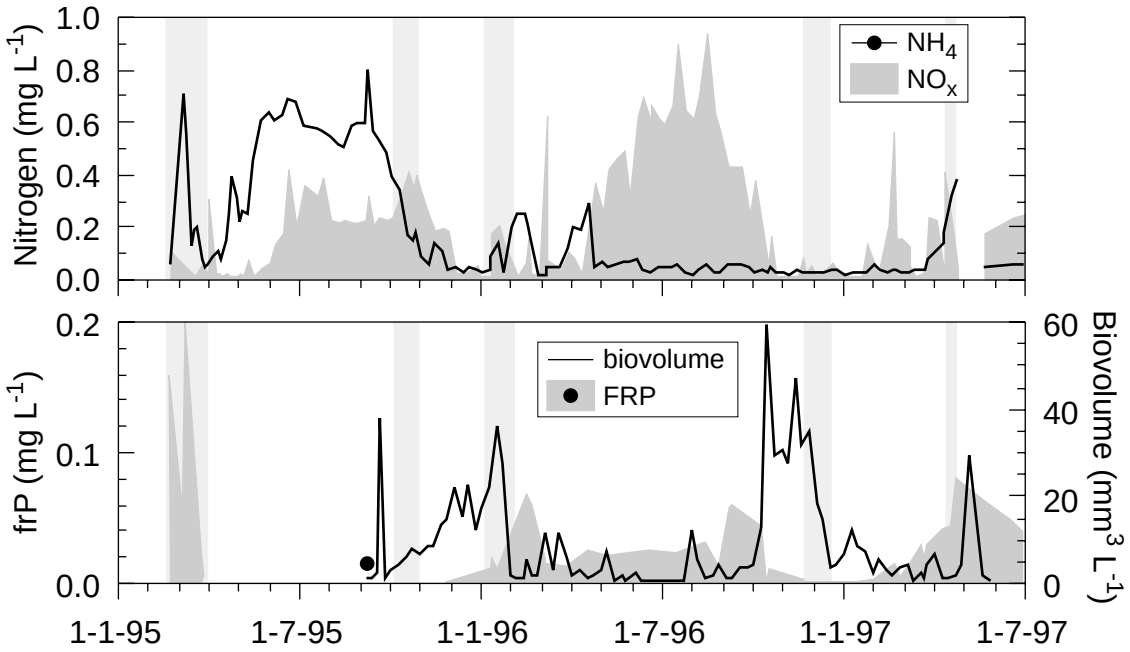

Figure 9.3 Algal biovolume and surface layer (0 – 5 m) FRP, NH4, and NOx concentrations during 1995-1997. Light shaded vertical bars denote operation of the destratifier. Algal data collected by CRCFE.

9.2.4.1 Algal growth 'events'

Prior to the commencement of artificial destratification in late February 1995 the reservoir was strongly stratified with low concentrations of inorganic N (<0.02 mgL-1) and FRP (0.004 mgL-1) in the surface layer and very high concentrations of FRP (0.415 mgL-1) and NH4 (1.1 mgL-1) in the anoxic hypolimnion. Chlorophyll concentration in the surface layer was 20 _g L-1 and the algal community was comprised of Oocystis sp. and Cryptomonas sp. with low numbers of Anabaena and Microcystis. Whilst there was a low concentration of FRP in the surface water, algal bioassays and *in situ* physiological assays (Section 9.2.4.3, Wood and Oliver 1995) indicated algal growth to be N-limited. Since, however, *Anabaena* has the capacity to fix N_2, its biomass would probably be limited by the availability of P. Destratification resulted in a rapid increase in the concentration of FRP and NH_4 in the mixed layer with FRP concentration in the SML at the end of the period of artificial destratification (28 Mar 95) being 0.01 mg L^{-1}. and NH_4 rising to 0.18 mg L^{-1} during the period of artificial destratification. During this period chlorophyll concentration doubled and the algal community became dominated by *Anabaena* and *Microcystis* .

In early January 1996 the SML FRP concentration was < 0.01 mg L^{-1} and inorganic-N was 0.035 mg L^{-1}. An algal bioassay (10-1-96) indicated that algal biomass, dominated by *Ceratium* (Figure 9.2b), was limited by the availability of P (Table 9.2). *Anabaena* and *Microcystis* were not present in the samples collected during this time. In late January, heavy grazing by *Asplanchna* (Section 9.4) reduced the Ceratium population, which may have suffered also from poorer light availability caused by increased turbidity due to a large inflow from the Peel R. (25-1-96) and a signficant deepening of the SML (10 Feb 96 to 17 Feb 96). Operation of the destratifier (11-1-96 to 15 Feb 96) in addition to the inflow and SML deepening increased surface layer FRP to 0.095 mg L^{-1} and NH_4 to 0.23 mg L^{-1}. Following this large increase in FRP and NH_4 *Microcystis* and *Anabaena* first appeared on 6 Feb 96 and 20 Feb 96 respectively, and cell number increased rapidly until late March (Figure 9.4). Notice that the *Microcystis* responded two weeks earlier than did the *Anabaena*, presumably due to the pulse of NH_4 in early February. *Anabaena* growth appears to have responded to the pulse of NO_x in early March.

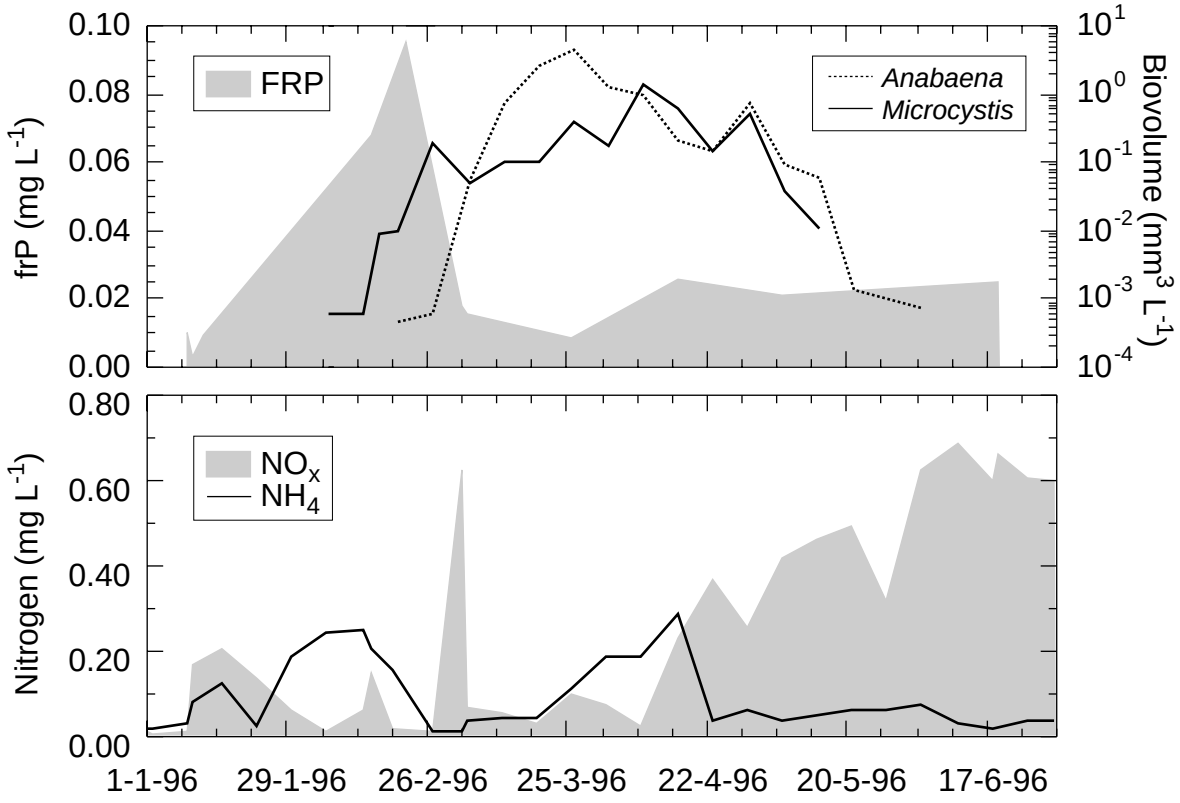

Figure 9.4 Response of *Anabaena* and *Microcystis* populations to changes in surface layer concentrations of FRP, NO_x and NH_4 during January – June 1996.

The *Botryococcus* bloom of in the spring of 1996 demonstrates how the growth of algae that occurs after the dam stratifies in mid-August can consume most of the bioavailable nutrient in the SML. Between September and November 1996 chlorophyll concentration in the surface layer increased steadily from 5 µg L^{-1} to 145 µg L^{-1} whilst TP and TN remained relatively constant (Figure 8.7). During this bloom, however, there was a dramatic reduction in FRP (from ~60 µg L^{-1} to 3 µg L^{-1}) and inorganic N (~550 µg L^{-1} to 40 µg L^{-1}) (Figure 9.3). The reduction in inorganic N and FRP was in a ratio of ~9:1 by weight suggesting that most of the FRP and inorganic N in the water column prior to the development of the *Botryococcus* bloom was converted into *Botryococcus* biomass. A bioassay undertaken in November 1996, prior to the rapid decline in chlorophyll, indicated that growth of *Botryococcus* was limited by the availability of N (Table 9.2). With the loss of *Botryococcus* from the surface layer during December 1996, TP and TN in the surface layer declined whilst FRP and inorganic N remained low, implying that the nutrients associated with the *Botryococcus* biomass were lost to the hypolimnion.

From mid-December 1996 through the end of February 1997 low numbers of *Anabaena* and *Microcystis* were present in the SML and the SML concentrations of FRP and inorganic N were < 0.003 mg L^{-1} and <0.03 mg L^{-1}, respectively. An algal bioassay undertaken on 22 Nov 96 indicated that algal biomass was limited by the availability of N (Table 9.2). *Anabaena* has the capacity to fix N_2, therefore, as in the summer of 1995, its biomass would probably be limited by the availability of P. Between 13-15 Feb 97 two large inflow events delivered ca. 5000 kg TP and 11800 kg TN to the reservoir below the SML (Section 7.1, Figure 7.1). The SML concentration of FRP remained <= 0.010 mg L^{-1} until surface layer

deepening during 4-11 Mar 97 began to entrain FRP delivered by the inflow into the SML. Relatively small increases in *Anabaena* and *Microcystis* biovolumes accompanied the pulses of NO_3 (0.63 mg L^{-1}) and FRP (0.13 mg L^{-1}) to the surface layer in mid-February, but immediately decreased in concert with the surface layer FRP (Figure 9.5). Throughout March there was a steady increase in surface layer FRP as the SML began to deepen and entrain FRP from the intrusion. At the same time inorganic nitrogen decreased to extremely low levels.*Anabaena* biovolume increased with the increasing supply of FRP to the surface layer. Unlike the previous two blooms, *Microcystis* biovolume remained low presumably due to the extremely low inorganic nitrogen concentration. An algal bioassay undertaken on the 13 Apr 97 indicated that there was sufficient nutrients to support algal growth.

The collapse in biomass in late April may be related to significant deepenening of the SML to more than 20 m that occurred on several occassions. Operation of the destratifier from 13-23 Apr made the water column more susceptible to deep mixing events that would have produced a much more dynamic light environment.

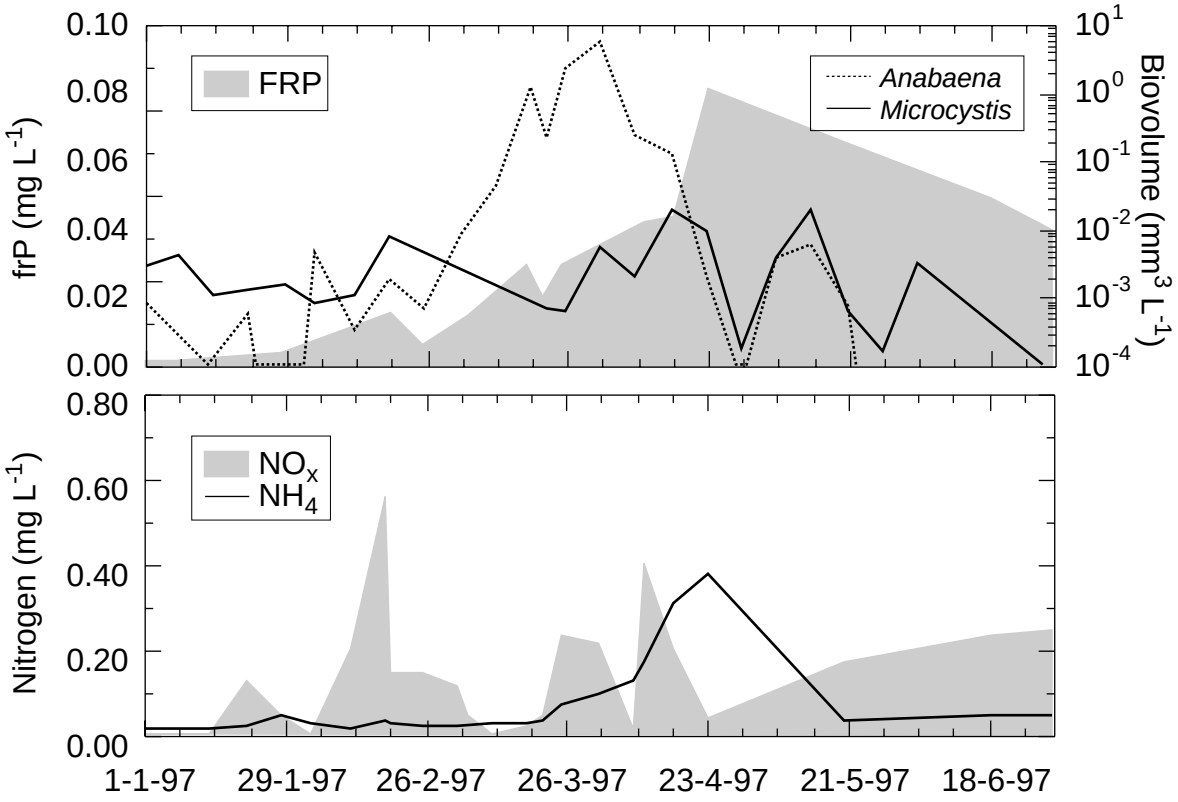

Figure 9.5 Response of *Anabaena* and *Microcystis* populations to changes in surface layer concentrations of FRP, NO_x and NH_4 during January – June 1997.

These data suggest that *Anabaena* and *Microcystis* growth is initiated following periods of extended stratification when there is an injection of nutrient into a nutrient depleted SML. *Anabaena* growth was stimulated by an increase in FRP which, in this study, was always associated with an increase in NO_3 or NH_4. *Microcystis* growth was also stimulated by an increase in FRP, but only if it was associated with an increase in NH_4. This accords with the hypothesis of Blomqvist et al (1994) which suggests that non N-fixing blue-green algae, such as *Microcystis*, require FRP and NH_4, rather than NO_3 for rapid growth in the field.

9.2.4.2 Hypolimnetic P and algal biomass

Average annual algal cell volume ranged from a low of 3.5 $mm^3 L^{-1}$ in 1987-88 to 28.5 $mm^3 L^{-1}$ in 1993-94. The years with the highest algal abundance generally had high algal abundance throughout the year, but in particular they had large, persistent blue-green algal and dinoflagellate blooms during the winter months. In contrast, years with low algal abundance did not have blue-green algal or dinoflagellate blooms during the winter months.

The onset of the large winter blooms of *Ceratium* and *Anabaena* co-occurred with the breakdown in stratification of the water column after summers which had the highest hypolimnetic P concentrations (eg 1990-91 and 1992-93). This suggested that hypolimnetic P concentrations played an important role in stimulating increases in algal biomass.

The maximum hypolimnetic P concentration (measured 1 m above sediment) prior to the breakdown in stratification of the water column varied interannually from a low of 230 $\mu g L^{-1}$ in 1995-96 to a high of 800 $\mu g L^{-1}$ in 1990-91. The longer the hypolimnion remained anoxic the higher the hypolimnetic P concentration became. Years where artificial destratification was attempted had the shortest period of anoxia and consequently accounted for 4 of the 5 lowest years of hypolimnetic P.

A linear relationship was found between the maximum hypolimnetic P concentration during the summer months and algal abundance in the following year with 88% of the variation in algal abundance. being explained by the maximum hypolimnetic P concentration measured during the previous period of intense stratification (Figure 9.6). Summers in which artificial destratification was attempted (even for relatively short periods) had lower than average hypolimnetic P concentrations and also lower algal abundance in the following year (open circles, Figure 9.6).

These data suggest that P which accumulates in the hypolimnion during anoxic conditions is a strong determinant of the algal biovolume in the following year. Artificial destratification, by reducing the period of anoxia in the hypolimnion, reduces the hypolimnetic P concentrations and thereby reduces algal biovolume in the next year.

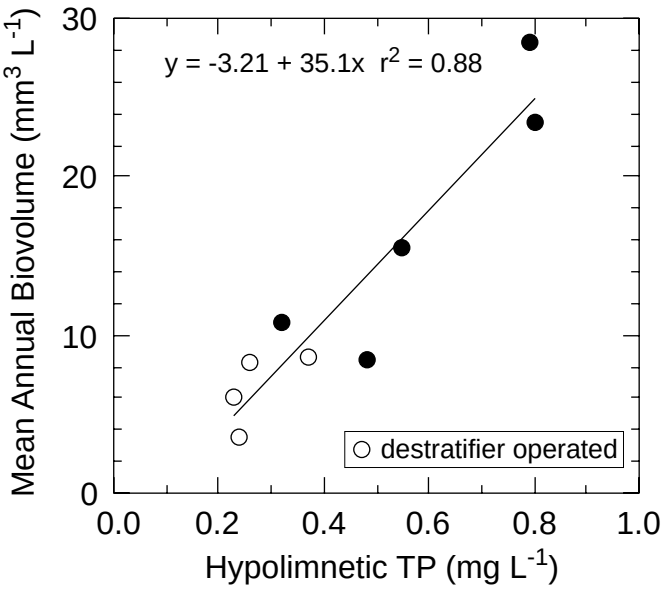

Figure 9.6 Mean annual algal biovolume vs hypolimnetic TP just prior to turnover at the start of the algal growing year. Open circles denote years that the destratifier was operated.

9.2.4.3 Algal physiology and bioassays

A number of algal bioassays and *in situ* physiological assays (NIFT, ΔΦ measurement; Wood and Oliver 1995, Oliver and Whittington 1998) were undertaken on samples of algae from the surface layer of Chaffey Dam (Table 9.2). Of the ten algal bioassays undertaken 3 indicated that algal growth was limited by the availability of nutrient, twice by N and once by P (Feb 1995 - N, Jan 1996 - P, Nov 1996 - N). On one occassion the NIFT assay indicated that phytoplankton were limited by the availability of N (Feb 1995), which was in agreement with the algal bioassay. On the other 2 occasions that bioassays indicated potential nutrient limitation of growth the phytoplankton did not show any physiological symptoms of nutrient limitation. Measurements of ΔΦ did not clearly indicate nutrient limitation of the phytoplankton community[5]. On each of the occasions when bioassays indicated nutrients were potentially limiting algal growth the water column was strongly stratified.

Table 9.2 Summary of algal bioassays conducted on 0-3 m integrated water samples from Chaffey Dam. Nutrient concentrations are of the initial water sample. NIFT refers to a positive result upon the addition of a nutrient (N or P). Bioassay control refers to the percentage increase in fluorescence in the control flask during the time interval listed. Zero indicates that the control flask did not grow. Limit nut. is the nutrient most likely to limit algal biomass. Ooc = *Oocystis,* Chod= *Chodatella,* Ana = *Anabaena,* Mer = *Merismopedia,* Mic = *Microcystis,* Cer = *Ceratium,* Sten = *Stentor,* Volv = *Volvox,* Bot = *Botryococcus*.

[5] Severe nutrient limitation has been shown to reduce ΔΦ in laboratory cultured algae (Kolber et al., 1988). Other factors, including the previous light history of the phytoplankton can also decrease ΔΦ. For the 6 experimental periods ΔΦ was measured to exclude the effects of light, there was no evidence of nutrient-limited reductions in ΔΦ.

Trip	Date	TN mg L^{-1}	NO_3 mg L^{-1}	NH_4 mg L^{-1}	TP mg L^{-1}	FRP mg L^{-1}	Chl*a* µg L^{-1}	NIFT	Bioassay	Limit nut	Major species
	<0.01	0.041		<0.01	0.041	0.004	19	N	**0**	N	Ooc Chod Ana Mer Mic
2	28 Mar 95	0.98	0.003	0.03	0.069	0.011	59	-	+ 40% 24h	-	Ana Mic
3	065	1.6	0.2	0.6	0.035	0.012	6	-	+ 250%	P	Coel
4	27 Oct 95	0.9	0.4	0.15	0.06	<0.01	23	-	+ 50% 70h	P	Ooc
5	28 Nov 95	2	0.2	0.01	0.02	<0.01	26	-	+ 20% 24h	P	Ooc
6	10 Jan 96	1.1	0.005	0.03	0.095	0.003	34	-	**0**	P	Cer
7	13 Feb 96	1.13	0.017	0.31	0.58	0.073	8	-	+ 300% 78h	N	Cer Mic Sten Volv
8	26 Mar 96	0.9	0.1	0.14	0.15	0.009	40	-	+ 80% 48h	P	Ana
9	22 Nov 96	0.6	0.01	0.02	0.073	0.003	138	-	**0**	N	Bot
10	13 Apr 97	0.8	0.03	0.13	0.06	0.03	60	-	+ 230%	-	Ana Mic

9.2.4.4 Summary

Blue-green algal abundance exceeded the DLWC Alert Level 3 (>15,000 cells / mL) for three periods between January 1995 and November 1997. The blooms occurred in mid to late summer and extended into autumn. During the period of bloom formation the seasonal thermocline was between 4 and 5 m with the SML shoaling diurnally to the surface. On each occasion the rapid increase in blue-green algae followed an increase in FRP and inorganic-N. The increase in nutrients resulted from entrainment of relatively nutrient-rich deeper waters into the SML.

The general nutrient picture that emerges is typical of a meso-eutrophic monomictic dam. Epilimnetic deepening in autumn and eventual turnover in winter redistributed nutrients throughout the water column. During early spring the dam stratified and significant populations of phytoplankton developed above the seasonal thermocline[6]. Both FRP and inorganic N concentrations declined as these nutrients were incorporated into phytoplankton biomass. TP and TN in the SML declined as phytoplankton biomass declines in the SML. Late spring and summer have the lowest concentrations of both inorganic N and FRP in the surface layer either of which may limit algal biomass until epilimnetic deepening, operation of the compressor or inflows from the Peel R. resupply nutrient to the surface layer during summer and autumn. During the three years of this study, algal biomass, particularly blue-green algae, increased after one of these events.

[6] In some years dinoflagellate and cyanobacterial blooms are present throughout the winter months.

9.3 Light limitation

9.3.1 The underwater light environment

The average light intensity experienced by phytoplankton is dependant upon the incident irradiance, the attenuation of light in the water column and the depth in the water column of the phytoplankton. In this section we examine the role that light may play in regulating algal growth in Chaffey reservoir.

The vertical attenuation coefficient of downwelling radiation (k_d) in the water column was measured at Chaffey reservoir on a number of occasions using a LiCor cosine corrected underwater Quantum Sensor (Li-192B). Secchi depths (z_{SD}) were measured weekly at two sites in the dam between 1995 and 1997. There were two distinct relationships between attenuation coefficient and secchi depth; one prior to the dam refilling in late January 1996 and the other from February 1996 till April 1997:

$k_d = 0.239 + 1.20/z_{SD}$ ($r^2 = 0.59$) Feb 1995 to Jan 1996

$k_d = 0.016 + 2.45/z_{SD}$ ($r^2 = 0.997$) Feb 1996 to Apr 1997

Calibrating the secchi depth data with k_d indicates that the euphotic depth,z_{eu}, where 1% of surface light remains ranged from about 1.0 m to 9.5 m with a mean of 3.9 m between 1995 and 1997. During periods when there was a high chlorophyll concentration in the water column the euphotic depth was shallow.

9.3.2 Light dose in the surface mixed layer

Vertical profiles of chlorophyll, *in situ* fluorescence and cell number have shown that under most conditions, more than 90% of the phytoplankton resided above the seasonal thermocline (Figure 7.2). This suggests that access to light is a significant determinant of the phytoplankton community structure. To examine the role of light, it is necessary to compute the typical light dose experienced by the phytoplankton at different times of years. This is assumed to be directly proportional to the average daily light intensity in the SML.

Because the SML depth has a strong diurnal variation, the average light intensity experienced by the phytoplankton has been calculated in two ways. The first method was to calculate the average light intensity over 24 hours using the deepest SML depth recorded (typically at dawn) in that 24 hour period. This approximates the light climate experienced by an evenly distributed population of neutrally buoyant algae in the diurnal mixed layer, taking account of the portion of the population that will be stranded at depth as the SML shoals during the day. The second method was to calculate the light intensity averaged over 24 hours within the SML (using 10 minute data). This is the light intensity that buoyant and motile algae would experience by remaining in the SML. The results of these calculations are shown in (Figure 9.7).

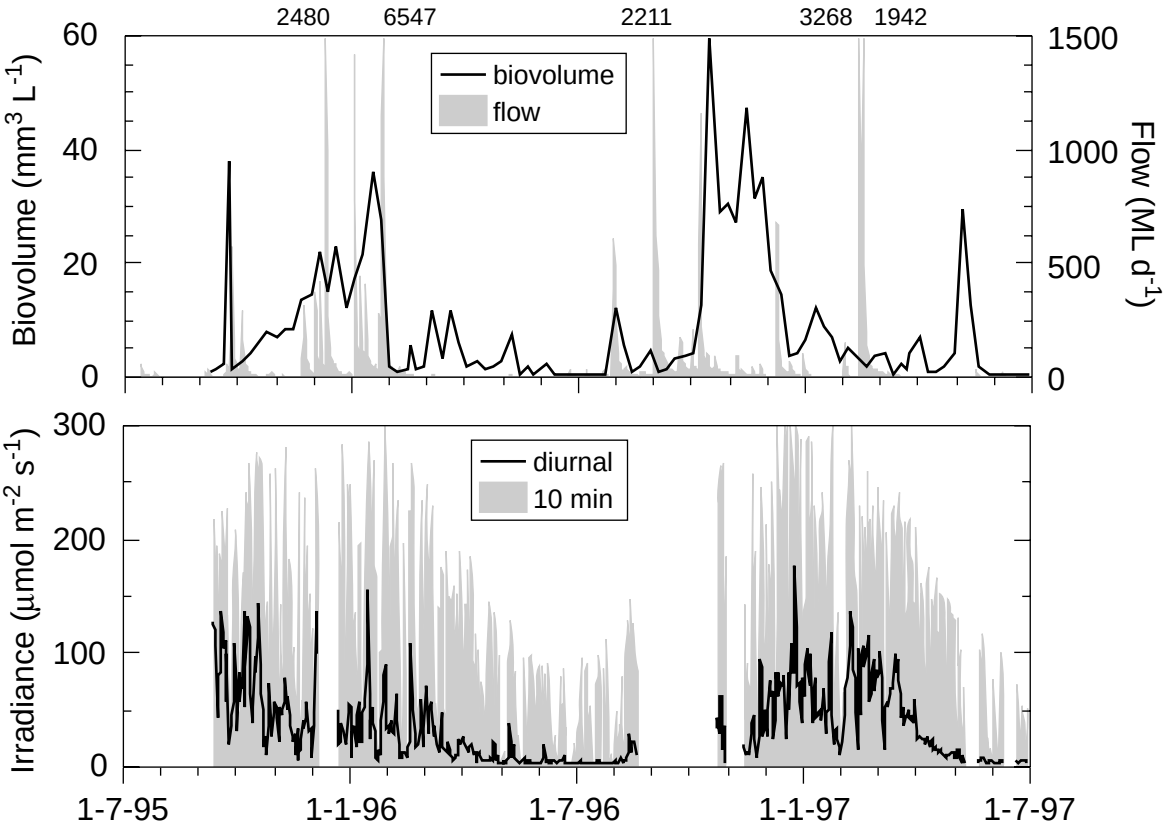

Figure 9.7 Top) Algal biovolume and Peel River discharge during the project. Numbers indicate daily mean discharge when data extend beyond the limit of the y-axis. Bottom) Average daily irradiance experienced by algae in the surface layer using the 10-minute surface layer depth data from the thermistor chains (grey shaded region) and the maximum diurnal SML depth (solid line).

As expected, the average daily light intensity experienced by the algae is higher if the algae remain in the SML as it shoals. This is particularly important during the winter months when the maximum diurnal SML depth may exceed 10 m each night but shoals to the surface during the daylight period. The average irradiance in the SML during winter 1996 was 4.7 µmol m^{-2} s^{-1} using the diurnal maximum SML, compared with 17.3 µmol m^{-2} s^{-1} using the instantaneous SML depth. Buoyant and motile algae that remained in the SML would be significantly advantaged under these conditions.

The rapid declines in biovolume measured during January 1996 and December 1996 were not associated with a reduction in average light intensity in the surface mixed layer (Figure 9.7). The average light intensity in the SML during January of 1996 was 54 (SD=30) µmol m^{-2} s^{-1} and during January 1997 was 62 (SD=23) µmol m^{-2} s^{-1}. These light intensities are similar or higher to periods when maximum growth rates for the common taxa in Chaffey Dam have been recorded. To further investigate the light requirements of various taxa in Chaffey Dam a series of experiments were conducted.

9.3.3 Light intensity vs net phytoplankton growth rate

9.3.3.1 Methods

To determine the effect of light on the growth of natural phytoplankton populations a series of *in situ* algal growth experiments were completed between November 1995 and March 1996. In each experiment a depth-integrated sample from the SML was subsampled into 1.25 litre PET bottles which were subsequently laid horizontally in 'cradles' suspended at various depths (dark to 66% surface irradiance) within the water column. The net growth rates of phytoplankton were measured by determining the change in biovolume of each species from the beginning to the end of the experimental period. The net growth rate therefore includes losses arising from respiration, mortality, etc. Bottles were shaken and opened to the atmosphere regularly to allow for gas exchange during the experiments. The experiments were terminated after 2 or 3 days depending upon net growth rate.

These data allow us to determine several important parameters related to the light environment in the reservoir. A conceptual diagram of the parameters is shown in Figure 9.8. From a management perspective the most important is the compensation point irradiance, $I_{\mu comp}$, which is the irradiance below which algal biomass does not increase or may even decline. The net growth rate begins to saturate at I_{knet} and has its maximum at $I_{\mu max}$. Some algal species are sensitive to strong light and μ may decrease as I increases beyond $I_{\mu max}$.

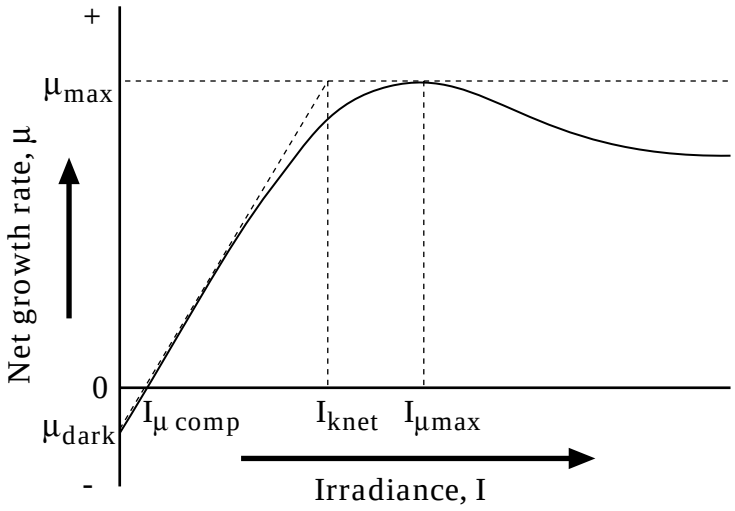

Figure 9.8 Conceptual diagram of the parameters measured in the light-growth experiments.

9.3.3.2 Results

Within each experiment the net growth rate response to light varied between phytoplankton taxa. In some experiments this resulted in a change in the species composition within 3 days. The data in Table 9.3 show the light intensities for the growth compensation point, $I_{\mu comp}$, the onset of light saturation, I_{knet}, and the maximum net growth rate, $I_{\mu max}$. During the summers of 1996 and 1997 the light intensity in the SML was higher than both $I_{\mu comp}$ and I_{knet} for each of the taxa measured. Three generalised responses of growth rate to light intensity were observed.

Table 9.3 Summary of net phytoplankton growth-irradiance relationships. Net growth rates, d^{-1}, μ_{MAX} = maximum for bottled plankton, μ_{dark} = dark treatment, μ_{field} = natural poulation (calculated from weekly cell counts) and light intensities, µmol m^{-2} s^{-1}, $I_{\mu MAX}$, I_{knet}, and $I_{\mu comp}$ (see text for description).

	Date	μ_{MAX}	μ_{dark}	μ_{field}	$I_{\mu max}$	I_{knet}	$I_{\mu comp}$
Oocystis	25 Nov 1996	0.18	-0.2	0.008	118	37.7	24
Ceratium	9 Jan 1996	0.064	-0.05	0.081	24	11.3	6
Volvox	13 Feb 1996	0.45	-1.38		113	39.9	24
Anabaena	26 Mar 1996	0.28	-0.91	0.119	31	10.3	11
Anabaena	9 Apr 1997	0.03	-0.76	-0.102	135	42.8	90

The first response, which included the blue-green alga *Anabaena* and the motile green alga *Volvox* exhibited relatively high growth under high light conditions and strongly negative growth at very low light and in the dark. For these taxa a three day shift to low light dramatically reduced their biomass and caused a shift to species with reduced loss rates at low light (Table 9.3). This data supports observations from the long term monitoring data which records a reduction in *Anabaena* growth during deep mixing events (> 9 m). The second group of algae also had relatively high growth rates at high light but were relatively unaffected by exposure to periods of low light. This group includes *Oocystis* and other green algae such *Chlamydomonas* and *Sphaerocystis*, the blue green alga *Microcystis*, and the cilliate *Stentor*. The third response was shown by the dinoflagellate *Ceratium*. This alga has a growth rate that is maximum at moderate light intensities while growth was reduced at high light intensities. The sensitivity of *Ceratium* growth to high light intensities suggests that this algae is best suited to a stable waterbody where it can utilise its motility to avoid photoinhibition of growth.

Phytoplankton growth was unlikely to be limited by light availability between spring and autumn provided the phytoplankton remained above the seasonal thermocline. Light availability would limit growth during the winter months, unless the phytoplankton remain within the SML as it shallows during the day. Phytoplankton will sediment out and be lost from the SML at an exponential rate which is determined by the thickness of the SML and the intrinsic settling rate of the plankton (Reynolds 1989). For a population to be maintained in the SML its replication rate must at least equal the loss rate. The shallow SML's frequently encountered at Chaffey Dam would require rapid replication rates or mechanisms to overcome settling, such as swimming or buoyancy.

9.3.4 Phytoplankton photophysiology

In the past detailed measurements of phytoplankton primary production rates have been restricted by the intensive labour and equipment requirements of the methods used to measure photosynthesis. These techniques also required long incubation times which reduced the reliability of transferring the measurements to natural populations. Traditional measurements of photosynthesis do not give an indiction of the processes of photosynthesis, variations in which are likely to give an insight into the relative abilities of the various taxa to being more successful under certain environmental conditions. Active fluorometry has the potential to overcome many of the problems of the conventional methods of measuring primary production as well as give insights into the major processes

of photosynthesis. A key outcome of this project has been to develop the use of active fluorometry for freshwater phytoplankton.

9.3.4.1 Methods

The technique of active fluorometry was used to provide information on the major processes involved in photosynthesis of the commonly occurring algae at Chaffey Reservoir including light capture and electron transport through the photosynthetic apparatus. It measures two parameters, the effective absorption cross section and the quantum yield of fluorescence. The effective absorption cross section, σ, is a measure of the size of the antennae (comprised of pigment molecules) that the algae use to capture light. The quantum yield of fluorescence, $\Delta\Phi$, provides a measure of the number of functional photosystem II reaction centres which is where the light captured by the antennae is converted to chemical energy. In combination these parameters give an estimate of the gross rate of photosynthesis (Kolber & Falkowski 1993, Oliver & Whittington 1998); respiratory losses are not included.

Differences in σ and changes in $\Delta\Phi$ reflect the conditions under which the algae are growing. Large σ is hypothesised to occur in algae that grow under low light conditions where more pigment improves the chances of capturing scarce photons for photosynthesis. Smaller σ is expected in brigher environments. Changes in σ occur on a time scale of several hours to days. In contrast, $\Delta\Phi$ changes rapidly (on the order of minutes) in response to changes in the ambient irradiance and more gradually as a result of stress such as chronic nutrient limitation. Exposure to irradiances above some threshold (roughly 100-120 µmol quanta m^{-2} s^{-1} for many terrestrial plants and algae) reduces $\Delta\Phi$ to below its maximum level, $\Delta\Phi_M$. The amount of reduction increases with increasing light intensity and duration of exposure. Non-light related stresses, such as nutrient limitation, that put the algae in a sub-optimal physiological state cause $\Delta\Phi < \Delta\Phi_M$ as well.

The photosynthetic rate of a number of the commonly occurring phytoplankton found at Chaffey Dam was estimated from the chlorophyll fluorescence measurements using the equation proposed by Kolber and Falkowski (1993). This relationship was tested using a number of laboratory cultures. Estimates of photosynthesis from fluoresence measurements were compared with direct measurements of photosynthesis using an oxygen electrode. There was a good agreement between the two methods (see Oliver and Whittington 1998). Actively fluorometry was then used to estimate photosynthetic parameters for a number of key algae in the reservoir.

9.3.4.2 Species-specific photosynthetic parameters

The bloom forming blue-green algae in Chaffey Reservoir generally had smaller cross sections than the eukaryotic algae. The exceptions were motile green algae, such as *Volvox* sp., which under stratified conditions could migrate toward the surface. Most of the algae measured at Chaffey Reservoir had relatively small absorption cross sections compared with estimates in the literature. This result supports the hypothesis relating cross section to light environment and indicates

that the algal population at Chaffey Reservoir was generally suited to the high light conditions.

Under optimal conditions the maximum quantum yield of fluorescence , $\Delta\Phi_M$, had an upper value of between 0.4 and 0.83 depending upon the algal group.

The photosynthetic parameters from the fluorescence measurements and the derived maximum rate of photosynthesis for a number of commonly occurring algae are given in Table 9.4. The data indicate a high temporal variability in maximum photosynthetic rate and the onset of light saturation for the same species. This suggests frequent measurement of these parameters will be required to model primary productivity.

Table 9.4 Photosynthetic parameters estimated from fluorescence measurements for commonly occurring algae at Chaffey Reservoir. Maximum rate of photosynthesis = P_{MAX}, and onset of light saturation of photosynthesis, I_k. ****Stentor* **is a ciliate which has a symbiotic relationship with zoochlorella. Measurements were made on live *Stentor* and therefore reflect the photosynthetic capacity of the associated zoochlorella.**

Species	date	$\Delta\Phi_{MAX}$	σ Å^2 quanta^{-1}	I_K µmol quanta m^{-2} s^{-1}	P_{MAX} mg O_2 mg chla^{-1} h^{-1}
Ceratium	15 Feb 96	0.50	57	421	4.7
Ceratium	10-11 Jan96	0.59	59	145	1.8
Microcystis	15 Feb 96	0.49	34	362	4.2
Volvox	15 Feb 96	0.81	24	656	5.9
Stentor	15 Feb 96	0.72	17	1101	4.5
Anabaena	29 Mar 96	0.56	34	748	11.7
*Anabaena**	29 Mar 96	0.50	34	769	10.4
Botryococcus	23 Nov 96	0.68	56	304	4.9
*Botryococcus**	28 Nov 96	0.29	61	393	4.3
Ankistrodesmus	9 Sep 95	0.66	74	531	11.5
*Ankistrodesmus**	8 Sep 95	0.50	67	429	6.7
Oocystis	29 Oct 95	0.64	71	673	13.2
*Oocystis**	28 Oct 95	0.38	75	125	2.5

9.3.4.3 Coupling between photosynthesis and surface layer dynamics

The impact of surface layer mixing dynamics on photosynthesis was investigated by monitoring changes in $\Delta\Phi$ of natural populations over a range of depths under stratified and mixed conditions. The time scales and light intensities for the onset and recovery of reductions in $\Delta\Phi$ were and found to be similar to those of mixing processes in the surface layer of the reservoir. An example is shown in Figure 9.9.

Before noon on 26 Nov 96, strong insolation and low wind speeds caused the lake to become strongly stratified. Vertical mixing was suppressed and the SML was just 0.2 m deep by 10.00 h. The maximum depression of $\Delta\Phi$ occurred in the near surface sample with progressively smaller changes in $\Delta\Phi$ until ca. 1.8 m, the mid-point of the euphotic zone (light intensity ca. 10% of the surface irradiance). Below this depth $\Delta\Phi$ did not change significantly. The reduction in $\Delta\Phi$ in the upper layers is consistent with the effects of photoinhibition. Just before noon the wind speed increased to 4 m s^{-1} causing the SML to deepen to 0.5 m. As irradiance decreased but before the wind reduced (~ 1600 h) the SML deepened again to just below 3 m depth. The convergence of $\Delta\Phi$ values at 0.25 and 0.55 m at 13.30 h

confirms that mixing occurred to a depth of ca. 0.55 m. The latter event saw a further convergence of $\Delta\Phi$ at all depths. This result highlights how changes in $\Delta\Phi$ can be useful for appraising the light environment experienced by the phytoplankton. From these data, phytoplankton mixing trajectories can be estimated which can be compared to mixing patterns derived from temperature changes in the reservoir. In general, mixing trajectories of the algae predicted from thermal changes in the reservoir accorded well with estimates made using changes in $\Delta\Phi$. This technique shows promise for assessing the effect of mixing processes such as artificial destratification on the trajectory of phytoplankton in the water column.

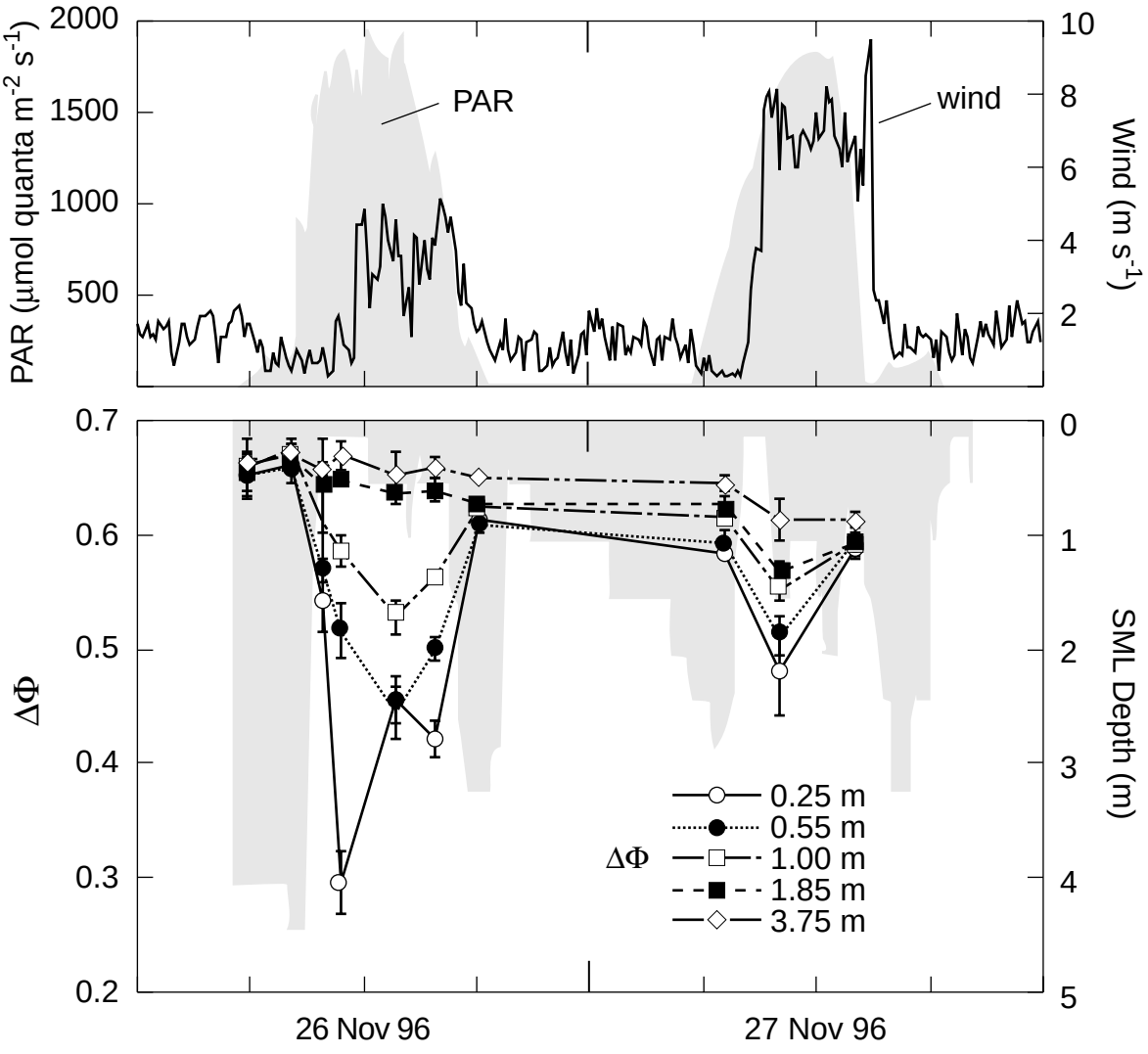

Figure 9.9 Top) PAR (grey shaded area) and wind speed (line) during 26-27 Nov 1996. Bottom) Surface mixed layer (SML) depth (grey shaded area) and ΔΦ at 5 depths for the same period. Measurements were made when the algal community was dominated by the green alga *Oocystis* sp..

9.3.5 Buoyancy and motility mechanisms to avoid sedimentation and optimise light capture

One of the striking features of the algal community at Chaffey Dam is the high abundance of algae that are either buoyant (*Botryococcus*) or have the ability to

migrate vertically in the water column by regulating buoyancy (*Anabaena, Microcytis*) or by swimming with the use of flagella (Cryptomonads, Dinoflagellates, *Stentor, Volvox*). These algae accounted for 88% of the total algal biovolume between 1987-97. Several possible advantages of vertical migration have been postulated. These include a reduction in sinking losses, overcoming nutrient limitation by obtaining access to deeper reserves of nutrient and optimisation of surface light intensity for growth (Harris et al. 1979, Ganf and Oliver 1982, Jones 1991).

The success of buoyant blue-green algae in nocturnally mixed waterbodies where the maximum diurnal SML depth is much greater than the euphotic depth depends on the ability of the filament or colony to position itself in a favourable light climate to satisfy its energy demands when stratification is re-established. The rate of flotation is therefore an important aspect governing the survival of blue-green algae.

9.3.5.1 Relationship between light, nutrients and buoyancy

Brookes et al. (1999) reported the results of experiments conducted during April 1997 at Chaffey Dam that examined the relationships between light, nutrients and cell buoyancy in *Anabaena*, the dominant blue-green alga in the reservoir. Integrated depth-samples of lake water from 0.2-0.6 m were suspended at dusk on 8 Apr 97 in PET bottles at various depths in the water column so that irradiance varied from 67, 30, 10, 3 and 1 % of the surface irradiance the following day. Some of the bottles also had nutrients added to them as 0.1 mg L^{-1} P as phosphate and 1 mg L^{-1} N as nitrate. At 08.00 h on 9 Apr 97, all of the *Anabaena* were positively buoyant in all of the samples. By sunset 39% and 9%, respectively, of the upper two samples (0.3 m and 0.9 m) which were exposed to high light no longer floated. At 08.00 h on 10 Apr 97 only 4% of the filaments in the 0.3 m bottle were not floating and by 17.00 h, 62% and 31% of the 0.3 and 0.9 m samples no longer floated. The addition of nutrients resulted in an increased resistance to buoyancy loss with only 12% of the 0.3 m sample losing buoyancy by 17.00 on 10 Apr 97. Six days later, 0.4 m depth-integrated samples of the natural population taken every 0.4 m were also uniformly buoyant at dawn with ca. 30% of the population in the top 2 m losing buoyancy by 13.00 h and 15% of the population non-buoyant by 16.00 h. Two days prior to the latter experiment, the destratifier was turned on and so the ambient conditions within the SML (i.e. nutrient concentrations, stratification, and circulation) in the reservoir had been modified slightly. Nevertheless, the 30% loss in buoyancy in the top 2 m was quite similar to the loss in buoyancy of the 0.9 m bottled sample on 10 Apr 97 (after 2 days).

The light-dependence of the flotation rate of the mixed *Anabaena* (87%) and *Microcystis* (13%) population was studied by suspending samples of lake water in PET bottles at depths corresponding to 70, 30, and 1% of surface irradiance at 10.30 h on 14 Apr 97 (Brookes et al. 1999, Table 9.5). The net population flotation velocity ranged from 0.04 m h^{-1} (many individual colonies were sinking) for nutrient replete cells held at high light to 2.01 m h^{-1} for nutrient replete cells held at very low light for 30 hours. The sinking rate for non-buoyant cells was not determined.

The flotation rate of *Anabaena* was dependent upon the colony size. By 08.00 h on 15 Apr 97 differences in carbohydrate content between treatments were not yet

significant, yet algae held at low light had formed the largest colonies and had the greatest flotation rates (Table 9.5). Curiously, all of the treatments had a lower velocity and a larger colony size than the original population at the start of the experiment. Carbohydrate content increased in cells held at high light which resulted in an increased cell density and therefore a reduced flotation rate. Gas vesicle volume, whilst not measured, would be expected to alter under the different light regimes (Oliver 1994, Oliver and Ganf 1999).

Table 9.5 Time dependence of greatest axial linear dimension (GALD), flotation rate and carbohydrate content of an algal suspension from Chaffey Reservoir containing 87% Anabaena and 13% Microcystis suspended at depths corresponding to 70, 30, and 1% of surface irradiance. From Brookes et al. (1999).

% surface light	Time	Mean GALD (µm)	Flotation rate (m h^{-1})	Carbohydrate (pg $cell^{-1}$)
Initial	14 Apr 97 10:30	90.3	0.39	
70	15 Apr 97 08:00	101.8	0.06	14.39 (2.7)
70	15 Apr 97 13:30	101.9	0.05	29.22 (0.65)
70	15 Apr 97 16:30	108.6	0.01	23.35 (1.38)
30	15 Apr 97 08:00	127.5	0.14	14.55 (4.44)
30	15 Apr 97 13:30	121.6	0.04	28.56 (2.35)
30	15 Apr 97 16:30	124.3	0.06	24.19 (0.4)
1	15 Apr 97 08:00	133.3	0.22	15.89 (2.5)
1	15 Apr 97 13:30	184.5	0.84	11.35 (4.67)
1	15 Apr 97 16:30	202.9	2.01	12.47 (0.66)

9.3.5.2 Algal migration by swimming

The dinoflagellate, *Ceratium*, is the dominant algal taxon in Chaffey Reservoir (in biovolume terms) and uses its ability to swim to maintain its location within the euphotic zone. Whittington et al. (submitted) studied the photophysiological and migratory characteristics of *Ceratium* during a large bloom in January 1996 when surface irradiance was high and thermal stratification intense. During periods of high incident irradiance *Ceratium* migrated downwards from the near-surface waters to avoid long term reductions in photosynthesis induced by high light. Under similar light and stratification conditions, populations of the non-motile algae, *Oocystis*, were trapped in the surface layer and exhibited photoinhibitory reductions in photosynthetic capacity (Oliver and Whittington 1998).

The swimming speed of *Ceratium* was computed from changes in the *in situ* distribution of chlorophyll fluorescence (Whittington et al., submitted). *Ceratium* migrated towards the near-surface from sub-optimal light intensities at a velocity of 0.58 - 0.97 m h^{-1}. Sub-surface accumulations formed between 0.4 and 0.8m (Figure 9.10) where light intensity was 210 to 552 µmol m^{-2} s^{-1} which was optimal for photosynthesis and growth. The formation of sub-surface accumulations by upward and downward migrations increased water column integral photosynthesis, compared to a uniform cell distribution in the mixed layer by 1.35 times.

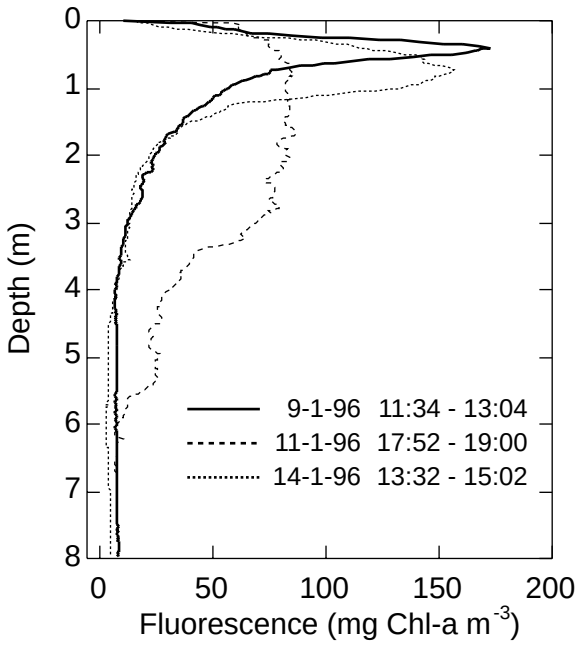

Figure 9.10 Averaged fluorescence profiles collected from Chaffey Reservoir. 11:34-13:04 9 Jan 1996 (solid line, mean q^* = 0.002 m s^{-1} during profiling), 17:52-19:00 11 Jan 1996 (long dashed line, mean q^* = 0.007 m s^{-1} during profiling) and 13:32-15:02 14 Jan 1996 (short dashed line, mean q^* = 0.004 m s^{-1} during profiling).

9.3.5.3 Algal migration in a turbulent environment

Buoyant and motile algae cannot control their location effectively if the turbulence in the water column is strong. Humphries and Imberger (1982) proposed the following expression to describe the balance between cell rising or sinking velocity and turbulence intensity in determining the vertical distribution of a plankton population in the mixed layer:

$$\Psi = \frac{|v|}{0.067 q^*}$$

where Ψ is a non dimensional variable which can also be defined as the time scale for diffusion in the mixed layer relative to that for sinking or rising over the depth of the mixed layer (Humphries and Lyne 1988), v is the sinking or rising velocity and q^* is the turbulent velocity scale in the mixed layer (Section 7.2, Figure 7.4). The value of Ψ gives a first order approximation of the relative importance of algal motion through swimming, buoyancy or sinking and water column turbulence in determining the vertical distribution of the population. When $\Psi < 1$ turbulent diffusion dominates cell distribution, and when $\Psi > 1$ sinking and rising dominates cell distribution.

The relationship for Ψ predicts that q^* would have to exceed 8.3 x 10^{-3} m s^{-1} for turbulence to overcome buoyancy in determining the distribution of *Anabaena* held in low light conditions for > 24 hours, i.e. with a flotation velocity of 2 m h^{-1}. During the April 1997 experiments, q^* exceeded this value for about 6 hours each day, mainly from midnight to 06.00 h due to convective mixing (Figure 9.11). The SML deepened to between 6 and 10 m nocturnally, but shoaled to < 1 m for at least 6 hours following sunrise every day. Despite the high flotation rate, *Anabaena* theoretically would be mixed throughout the SML at dawn each day

but by midday all of these colonies would reach the surface where they would be exposed to strong irradiance. Even at the slower flotation speed of 0.84 m h^{-1} (1% light for 27 hours) the entire population below 4.5 m should still rise fast enough to ensure an average exposure of ca. 10% of the surface irradiance each day. It appears unlikely that *Anabaena* could remain at low irradiances long enough to produce the higher flotation speeds observed in the bottle experiments at 1% light. This hypothesis is consistent with the natural population's measured rising speed of 0.39 m h^{-1} which suggests an average exposure to between 1 and 30% of the surface irradiance.

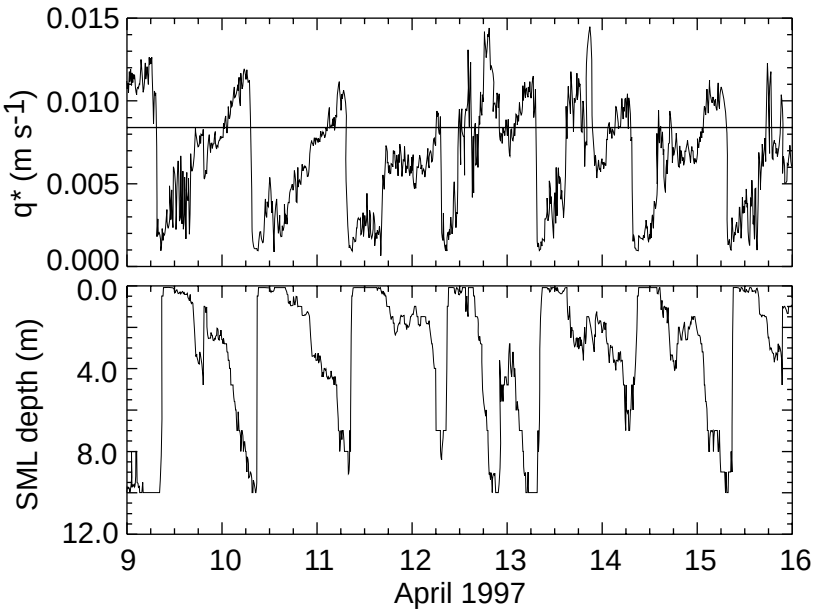

Figure 9.11 Turbulent velocity scale, *q, and SML depth during April 1997. The horizontal line in the upper plot is at $q^* = 8.3 \times 10^{-3}$ m s^{-1}.**

Ceratium were able to form sub-surface accumulations whenever $q^* < 0.008$ m s^{-1} within the SML. Figure 9.10 shows chlorophyll-fluorescence profiles horizontally averaged across the entire reservoir for three quite different meteorological conditions (Figure 9.12). On 9 Jan 1996 surface irradiance was low and winds were sufficiently light that q^* was just 0.002 m s^{-1} and the maximum *Ceratium* abundance was at 0.4 m. On 14 Jan, q^* was 0.004 m s^{-1}, winds were again light but surface irradiance was much stronger resulting in a deeper fluorescence peak as the *Ceratium* moved down to avoid inhibiting irradiances closer to the surface. *Ceratium* were not able to maintain their position during the afternoon of 11 Jan 1996 when a stronger southerly wind of up to 6 m s^{-1} caused the SML to deepen briefly to below 2.5 m and *Ceratium* to accumulate at the northern end of the reservoir. With $q^* = 0.007$ m s^{-1}, *Ceratium* were evenly distributed above 3 m (Figure 9.10). During the hour prior to profiling q^* averaged 0.010 m s^{-1}. The increase in fluorescence from 4.5 - 5.75 m depth shows the intrusion caused by the operation of the destratifier on 11 Jan 1996.

The relationship of Humphries and Lyne (1988) and our measurements of *Ceratium* swimming speed predict that *Ceratium* can successfully exploit the structured, stable epilimnia of the reservoir whilst q^* is less than ca. 0.004 m s^{-1}. Generally, the optimum light zone for *Ceratium* was deeper than 0.4 m, and so algae below this depth were able to optimize growth by forming aggregations below the SML regardless of q^* in the SML when the SML was less than 0.4 m, an

almost daily occurrence at Chaffey Dam. During the *Ceratium* bloom, the SML depth was < 0.4 m for 75% of the time that $q^* \leq 0.004$ m s^{-1}. Because of this, we cannot determine exactly the value of q^* required to mix *Ceratium* (because most of the population was not in the SML), but it appears from the results here that it is < 0.010 m s^{-1} and probably < 0.007 m s^{-1}.

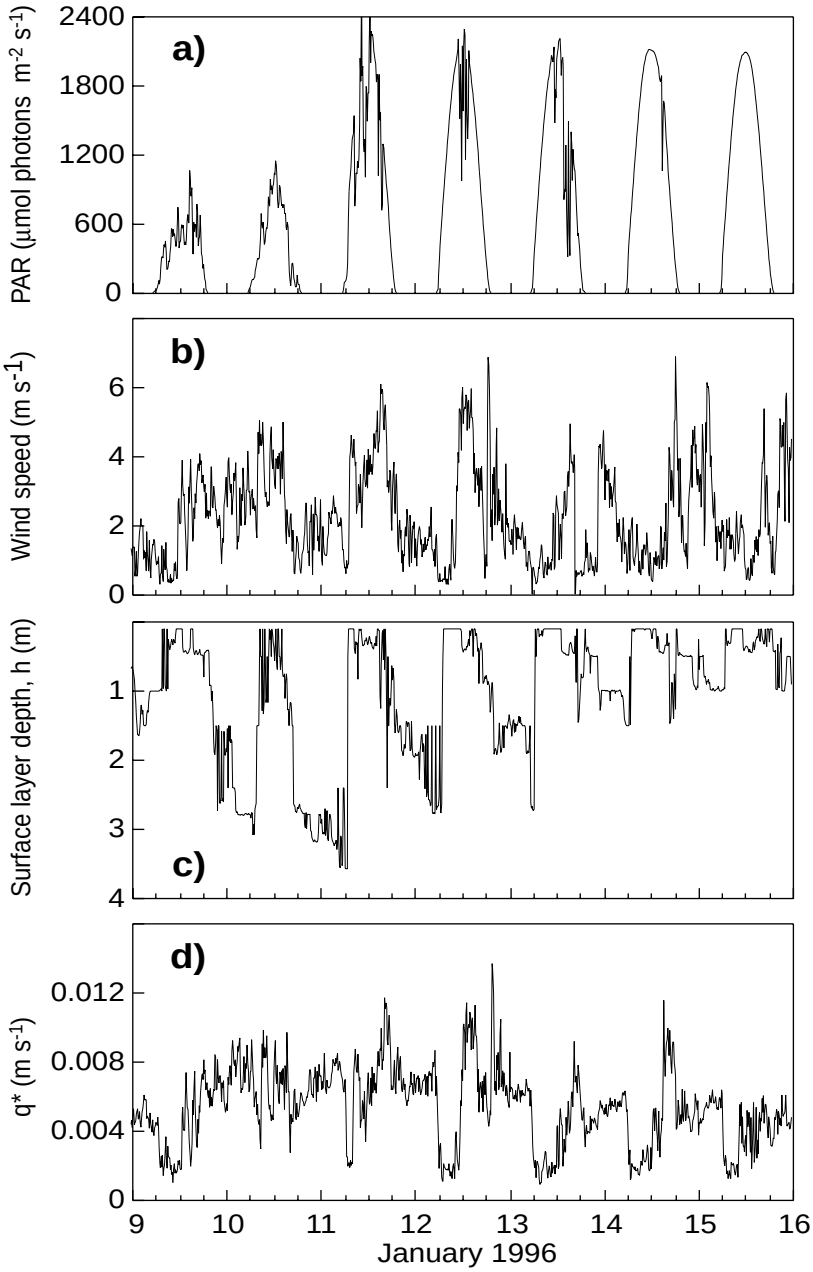

Figure 9.12 Meteorological and water column conditions measured at Chaffey Reservoir. 10 minute averaged data for a) incident irradiance, PAR, µmol photons m^{-2} s^{-1} ; b) wind speed, m s^{-1}; c) mixed-layer depth, h, m; d) turbulent velocity scale in the mixed-layer, *q, m s^{-1}, for the period 9 Jan 1996 to 15 Jan 1996.**

These examples reinforce the value of buoyancy and migration for algae in Chaffey Dam. The field data obtained at Chaffey dam provides experimental support for the relationship proposed by Humphries and Lyne (1988) and provides information on the lower limit of q^* required for turbulence to

overcome buoyancy or migration in determining the distribution of algae in the SML. This is critical information if the aim is to light limit the growth of these algae by artificial mixing.

9.3.6 Sedimentation

In sharp contrast to the high abundance of motile and buoyant algae there was generally a very low abundance of diatoms between 1987 and 1997. Although diatom biovolume was low, diatoms were nearly always present in the water column (Table 9.1). The observed growth of diatoms in unenriched algal bioassays and the growth of a large epiphytic diatom population in association with a *Cladophora* dominated benthic community during the spring (October) of 1997 indicates that the water chemistry was suitable for their growth.

That significant diatom populations do not develop except when physically supported in the light field indicates that sedimentation may be controlling the growth of diatoms at Chaffey Dam. The exponential rate of sinking loss per unit time, k_s, of plankton from a continuously mixed layer, h_m is given by:

$$k_s = v h_m^{-1}$$

where v is the sinking velocity. If a population is to be maintained in the mixed layer then loss through settling must be counteracted by growth rate r, such that $r - k_s$ remains positive. Settling rates for *Aulacoseria* and *Cyclotella* from Chaffey Dam were not calculated but values taken from the literature suggest settling rates for *Aulacoseria* in Maude Weir Pool on the Murumbidgee R. of 0.95 m d^{-1} (Sherman et. al, 1998) and for *Cyclotella* in Mt Bold Reservoir, SA, of 0.90 m d^{-1} (Oliver 1981). Given these settling rates and a mixed layer depth of 2 m, the growth rate would have to exceed 0.45 d^{-1} (~doubling every 1.5 days) for the population to increase. This is a high growth rate but should be achievable for nutrient replete populations in Chaffey Dam. This calculation makes the assumption that the diatoms are entrained in a well-mixed surface layer. For *Aulacoseria*, with a settling rate of 0.95 m d^{-1}, q^* would have to exceed 1.6×10^{-4} ms^{-1} for entrainment which it does. However, the SML shoals to the surface on most days and therefore cells in the euphotic zone but below the SML will clear at the settling rate, irrespective of the growth rate. If the SML shoaled to the surface there would be a loss of ca. 1/3 of the diatom population from the euphotic zone each day and replacement would require a growth rate of 1.1 d^{-1} (doubling time of ca. 0.6 d). This is close to the maximum growth rate under ideal conditions and not likely to be sustainable in the field.

9.3.7 Can artificial destratification light limit algal growth?

Artificial destratification using the existing equipment in Chaffey Dam is unable to significantly alter the depth of the SML (see section 7.3), however, it does significantly weaken the intensity of stratification. This increases the chances of a meteorologically induced deepening of the SML (eg Feb 1996) and probably leads to a more rapid breakdown in stratification during autumn. However, during the course of this study the average light intensity experienced by algae entrained in the SML was not significantly reduced by the operation of the current destratification system.

During periods when the artificial destratification system was operating there was evidence that algae from the SML were entrained in the bubble plume. These algae then moved horizontally away from the bubble plume in the intrusion below the SML. On one occasion that this was observed the dominant alga was *Ceratium*. The net upward migration rate of *Ceratium* was ca. $2x10^{-4}$ m s^{-1} and the intrusion entered at ca. 6 m below the surface. At this swimming velocity *Ceratium* initially located in the intrusion was able to re-enter the euphotic zone within 4 hours. In a similar fashion, buoyant blue-green algae would float from the intrusion back into the SML at a time scale in the order of hours. These examples show that motile and buoyant algae can rapidly re-enter the SML from the intrusion associated with bubble plume. Unless the SML is significantly deepened, entrainment of motile or buoyant algae in the intrusion will not significantly reduce the average light intensity experienced by the algal population. Furthermore, in the case of *Anabaena*, as light limitation is imposed the rising velocity increases and the minimum q^* required to entrain colonies in the mixed layer increases as well.

To determine the possible effect of artificial destratification on algal growth, the average light intensity in the SML was modelled assuming the SML to be held at 11 m (artificial mixing) and using meteorological data from September 1995 to November 1997. Note that an 11 m SML depth is approximately the mean depth of the reservoir when full and is also approximately 3 times greater than the mean euphotic depth of 3.9 m; the latter condition being associated with light-limited growth of *Anabaena* (Sherman et al. 1998). The mean SML depth cannot exceed the mean reservoir depth so the minimum light exposure of a uniformly distributed phytoplankton is constrained by the mean reservoir depth. The average light intensities in an 11 m SML during 1996 and 1997 would have been 9.4 ± 6.7 µmol m^{-2} s^{-1} and 23.6 ± 16.5 µmol m^{-2} s^{-1}, respectively, compared to 112 ± 88 µmol m^{-2} s^{-1} and 134 ± 79 µmol m^{-2} s^{-1} calculated using the actual SML depths. The model results imply that if artificial destratification was able to maintain an SML depth of at least 11 m and entrain the phytoplankton then the average light intensity in the SML would be low enough to limit the growth of algae in Chaffey Reservoir year round (Table 9.3).

9.4 Zooplankton

To investigate the role of grazers in controlling algal abundance in the reservoir zooplankton abundance was determined from 10 m-integrated water samples collected at 3 sites (A1, A2, A4, Figure 5.1) at the same time as the 5 m-integrated samples were collected for phytolankton enumeration. A hose was lowered slowly through the top 10 m of the water column while lake water was continuously pumped into a bucket. The contents of the bucket were then passed through a zooplankton net with a 37 µm filter and preserved in alcohol. Samples were collected on 118 dates.

The following observations refer to net zooplankton, consisting of rotifers and microcrustacea (cladocerans and copepods). Sampling methods did not permit enumeration or evaluation of the protist component of the Chaffey zooplankton.

9.4.1 Summary & overview

Over the 1995-97 sampling period, 48 taxa of microfauna were recorded from the Chaffey Dam zooplankton (30 Rotifera, 12 cladocerans, 5 copepods, 1 ostracod). In Australia there are few published studies of similar resolution to provide comparison. However, from available data on Australian reservoir zooplankton, the Chaffey assemblage would seem to be at the lower end of the known reservoir species richness. In comparison, from only 18 collections over a three year period in L. Mulwala (Yarrawonga Weir, Murray R., NSW), Shiel (1981) reported 98 taxa of microfauna (67 of rotifers, 21 cladocerans, 8 copepods), from 29 collections in Dartmouth Dam over a comparable period, 61 taxa (38 rotifers, 15 cladocerans, 7 copepods and 1 ostracod), from eleven collections in Eildon Dam over the same period 48 zooplankton taxa (22 rotifers, 13 cladocerans, 11 copepods and 2 ostracods), from 26 collections from Hume Dam over the same period 44 taxa (26 rotifers, 10 cladocerans, 8 copepods). Collections from Lyell Reservoir reported by Kobayashi (1992b) are not readily comparable in view of the 250 µm mesh size used in his 12 mo. study, nevertheless he recorded 10 rotifer taxa, 12 cladocerans and 5 copepods. Similarly, only the microcrustacean zooplankton in Wallerawang Reservoir were reported by Kobayashi (1992a), where he recorded 12 cladoceran and 3 copepod species.

The same species dominants in the Chaffey assemblage are reported from other Murray-Darling Basin storages, and appear to be ubiquitous in south-eastern Australia. *Bosmina, Ceriodaphnia, Daphnia* and *Diaphanosoma* species are the most common cladocerans, *Calamoecia* and *Boeckella* species the common copepods. Their population dynamics and seasonal events in Chaffey are broadly similar to those reported from other south-eastern Australian reservoirs given the constraints imposed by drawdown and catchment-specific human activities (see below).

Zooplankton population densities in Chaffey reservoir are within ranges reported from the above studies, if on the low side for the microcrustacean component. e.g. Kobayashi (1992a) reported a mean of 27.2 ind l^{-1} for microcrustacea from Wallerawang, Geddes (1984) reported a range of 35-123 microcrustacea l^{-1} (mean 66 l^{-1}) from L. Alexandrina, Walker & Hillman (1977) a range of 10-60 microcrustacea l^{-1} from L. Hume. *Asplanchna priodonta* (Figure 9.13) was the most numerous rotifer in the reservoir but there are few published records of rotifer population densities in Australian reservoirs with which to compare. Shiel *et al.* (1987) reported ranges generally less than 200 ind. l^{-1} in Murray-Darling Basin storages, with occasional pulses of several thousand ind. l^{-1}, and one recorded pulse of 24,000 ind. *Synchaeta* l^{-1} in Mt Bold Reservoir, S.A., apparently in response to a *Carteria* bloom.

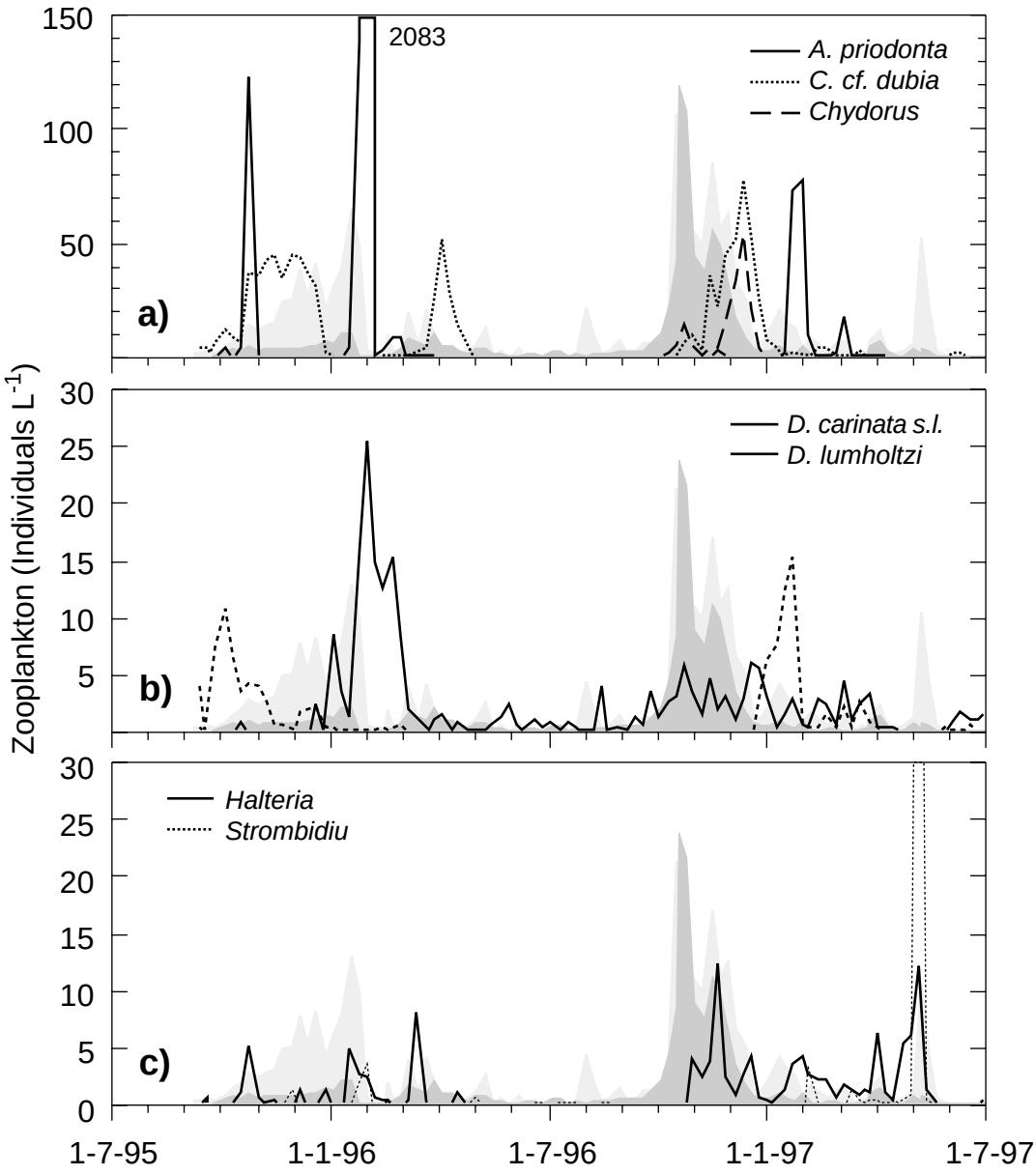

Figure 9.13 Population densities of the most numerous zooplankton species found in Chaffey Reservoir relative to the timing of algal growth. Dark shading is the 5 site mean chlorophyll-a in the top 5 m and the light shading is the corresponding biovolume. a) *Asplanchna priodonta, Ceriodaphnia* cf. *dubia* and *Chydorus* sp. b) *Daphnia carinata* and *Daphnia lumholtzi* . c) The ciliates *Halteria* and *Strombidiu* .

The timing of zooplankton growth vis a vis changes in the phytoplankton population is shown in Figure 9.13. Interpretation of grazing and predatory interactions within the Chaffey plankton community must be largely speculative. In general, zooplankton densities increased in response to growth of the phytoplankton population. Only the *Asplanchna priodonta/Ceratium* interaction (e.g. Jan 96) was demonstrable and quantifiable from the relatively small zooplankton sample volumes collected. The rotifer was selectively and intensively grazing the dinoflagellate, the first such record for Australia but known to occur in other countries. Other specific grazing associations are likely, given the dietary preferences of some of the resident zooplankton. *Ascomorphella volvocicola,* for example is a specific herbivore of *Volvox*

colonies. It was present in the Chaffey zooplankton only when *Volvox* was present. Some rotifers (e.g. *Gastropus, Synchaeta*), selectively prey on monads and were present in the Chaffey zooplankton when the preferred food item was abundant. Bacteriovores, e.g. *Conochilus, Filinia, Hexarthra, Pompholyx, et al.* although generally in low numbers, provide evidence of bacteriovory in the plankton community.

The microcrustacean assemblage in Chaffey is problematic in that only small species were abundant; larger-bodied zooplankton such as *Daphnia* and *Boeckella,* which predominate in other reservoirs, were not present in large numbers, or were markedly seasonal. Fish predation was invoked by Kobayashi (1992b) to explain a similar size shift in both Lyell and Wallerawang reservoirs. Both reservoirs were stocked with planktivorous fish, such as brown and rainbow trout. Possibly, some food chain effect is operating on the Chaffey zooplankton community, but in the absence of fish species information, density, stocking, etc. data, it is not possible at this point to determine if fish are depleting the larger herbivorous zooplankton.

Circumstantial evidence points also to invertebrate predation structuring the Chaffey zooplankton - large numbers of juvenile shrimp, which are planktivorous, were noted in settling trap samples. These may be seasonal or perennial predators of larger zooplankton. Notonectids and other carnivorous aquatic stages of insects may also structure zooplankton communities, however evidence for their activities in Chaffey is lacking.

Intuitively, it is likely that the smaller (rotifer) component of the Chaffey zooplankton is structured by the numerically dominant nauplii/copepodite stages of *Thermocyclops,* the size preference and food item choice of which changes with maturity. The calanoid *Calamoecia,* notably one of the smallest centropagids, probably is omnivorous in juvenile stages, preying on ciliates, rotifers, and smaller instars. High mortality of copepods in Chaffey, as suggested by low density of adults, despite juveniles usually being the most abundant zooplankters present, implies predation by a visual predator(s). Larger zooplankters in Chaffey also appear to be depleted by predation, possibly as a result of the fish stocking that occurs at the dam.

9.5 Summary

During the springs of 1994, 95 and 96 biological consumption of FRP and inorganic-N in the SML reduced the concentration of these nutrients to levels limiting algal biomass. At the same time, nutrients were accumulating in the hypolimnion. When commenced in summer, the short-term effect of artificial destratification was to inject nutrients into the SML which then led to an increase in algal biomass, particularly *Anabaena* and *Microcystis.*

In the long term, oxygenation of the hypolimnion by artificial destratification reduced the internal release of P from the sediments. There is clear evidence that the years in which artificial destratification was attempted had the shortest periods of anoxia in the hypolimnion and the lowest concentrations of hypolimnetic P. Since the hypolimnetic P concentration strongly determines the following year's algal biomass, operation of the destratification system does

reduce the average annual algal biomass. However, blooms of blue-green algae still occurred even in the years with the lowest hypolimnetic-P.

The inability of the destratifier to deepen the SML prevented it from reducing the availability of light sufficiently to stop blooms of blue-green algae. Theoretical calculations using the growth-irradiance curves for the phytoplankton in the reservoir suggest that for light to become limiting an SML depth of 11 m must be maintained. This is close to the average depth of the reservoir when full. Because of the broad expanses of shallow water in the southern part of the reservoir, it seems unlikely that light limitation will be an effective strategy to control blue-green algal blooms in Chaffey Dam.

Furthermore, because the flotation speed of Anabaena increases with light limitation, the q^* required to distribute them throughout the SML increases as well. Climatic conditions may not be capable of maintaining a sufficient level of turbulence in the water column.

10 Management implications

The strong correlation between hypolimnetic TP and the following year's average annual algal biovolume suggests that algal control strategies focusing on reducing the supply of phosphorus to the water column are most likely to provide short term benefits. Being similar in magnitude, both external and internal sources need to be addressed as reduced external loading will not improve the algal bloom problem during drought years. Conversely, reduced internal loads may provide only a small improvement during normal-to-wet years when the catchment delivers very high quantities of FRP.

Although the algal physiological data suggest that light limitation of algal growth is theoretically possible, destratification within the time scale required to deepen the surface mixing layer sufficiently to achieve this is likely to prove very costly. Using a conventional bubble plume destratifier, the air flow rate would probably need to be increased from 100 L s^{-1} to at least 1300 L $s^{-1}$and probably more (Section 4.2.2). The pipe network would have to increase in size vastly as the number of individual plumes increases from 10 to more than 100, ideally with at least 30 m separation between plumes.

A rough idea of the cost of a new bubble-plume destratification system can be extrapolated from the experience of the South East Queensland Water Corporation who in the late 1990's installed a state-of-the-art system with an airflow rate of 400 L/s at North Pine Dam. This system had a capital cost of $400,000 and currently costs approximately $100,000 per annum to operate. The cost of a new system should scale roughly linearly as the ratio of airflow rates between the new and North Pine systems, i.e. a 1300 L s^{-1} system would have a capital cost of roughly $1.2m and and operating cost of $300,000 per annum.

Below, we describe briefly operational considerations regarding artificial destratification, nutrient reduction strategies, and a speculative method for light-limiting algal growth.

10.1 Operational considerations for artificial destratification

10.1.1 Effects of the destratification system on water column chemistry

Destratification provides an effective means of increasing hypolimnetic oxygen concentrations and thereby reducing sediment nutrient releases. The downward mixing of oxygenated waters into the hypolimnion rapidly reduces the concentrations of hydrogen sulphide and reduced iron and manganese and also facilitates scavenging of FRP by increasing the supply of Fe(OOH). Within the former hypolimnetic zone oxygen becomes the electron acceptor rather than sulphate at the sediment surface, and sulphate reduction will only occur in anoxic areas deeper within the sediment. Essentially, the exposure of the sediments to oxygen will change the bacterial population from anerobic to aerobic populations and thus stop the anerobic route for release of nutrients into the water column.

It is essential that operation of the destratifier commences before large concentrations of nutrients are allowed to accumulate in the hypolimnion. Otherwise, it provides an effective means of transporting these nutrients into the

surface layer where they can be utilized to fuel algal growth. If commencement of destratification is delayed until after significant quantities of reduced chemical species and organic carbon accumulate in the water column, the short-term effect may be to further exacerbate anoxia throughout the water column (Section 8.3.7). Furthermore, any reduction in the SML O_2 concentration may retard nitrification and denitrification, shifting the distribution of inorganic nitrogen species. This has implications for the balance of species in the euphotic zone.

Destratification clearly can reduce sediment nutrient release, but it also retards the loss of nutrients from the surface by sedimentation. The decision to destratify must weigh the benefits of decreased internal nutrient loading against potentially higher mean nutrient concentrations during the summer growing season.

10.1.2 Thermal effects of destratification

When the destratifier is operated the temperature of the hypolimnion is increased by about 10 °C. The increased temperature increases the rates of all of the biologically mediated reactions, especially the consumption of O_2 by the sediments and within the water column. Our measurments demonstrated that water column BOD increased by a factor of 2.7 for a 10 °C temperature increase. This has profound implications for the oxygen budget of the reservoir. The supply of oxygen across the air-water interface plus the *in situ* production by photosynthesis must meet the demand for oxygen in the warmer reservoir. If the supply of oxygen doesn't match the downward transport and consumption, then destratification can actually reduce the total amount of oxygen in the water column.

Once destratification commences it must continue throughout the stratification season as the increased hypolimnetic temperatures will accelerate the development of anoxia and the ensuing release of phosphorus from the sediments in the event of the destratifier being turned off.

10.2 In-reservoir phosphorus reduction strategies

10.2.1 Selective withdrawal from the hypolimnion

Selectively releasing water from the hypolimnion removes nutrients from the water column before they can reach the surface layer. The disadvantages include the smell of H_2S in the vicinity of the outlet and possible problems with manganese deposition for down stream users of water taken from the river.

The relatively small quantities of water released from the dam under normal conditions may limit the effectiveness of this option due to insufficient removal of accumulated nutrients from the hypolimnion.

10.2.2 Destratification

By reducing the internal nutrient load, continuous (August – May) operation of the destratification system is likely to reduce the average algal biomass in the dam because there will be less nutrient supplied to the SML from the hypolimnion during epilimnetic deepening. It is also likely to reduce the intensity and

duration of blue-green algal blooms because it brings forward the date of initial overturn of the water column.

Destratification will not completely eliminate the growth or formation of blue-green algae because the Peel R. can deliver quantities of nutrient to the reservoir sufficient to stimulate algal blooms (for example Feb 1997). These inflows are high in NO_3 relative to NH_4 and therefore likely to stimulate the growth of *Anabaena* rather than *Microcystis*. Because the major inflows typically intrude below the SML (section 7.1), the phytoplankton population will not respond to the associated nutrient load until the SML deepens enough to entrain water from such an intrusion.

Operation of the destratifier will likely increase transport of nutrients from an inflow intrusion to the SML thereby promoting algal growth. Discontinuing the operation of the destratifier in order to prevent this transport of nutrients will result in anoxia in the hypolimnion within 30-60 days and the resumption of the associated internal nutrient load. The internal nutrient load will increase the average algal biomass experienced during the following year. Clearly, operation of a destratifier during years with significant spring or summer inflows is a complicated issue that is particularly sensitive to the timing and chemistry of inflow events.

10.2.3 Hypolimnetic oxygenation

Hypolimnetic oxygenation involves directly injecting pure oxygen or compressed air into the hypolimnion. The latter method is often referred to as 'aeration'. Oxygen is dissolved directly into the hypolimnetic water to reduce the nutrient release from the sediments while at the same time not disturbing the thermal stratification. Preserving the stratification allows nutrients to be lost from the SML through particle sedimentation and slows the upwards transport of dissolved nutrients from the hypolimnion to the SML. The elevated oxygen concentration reduces sediment nutrient release.

Hypolimnetic oxygenation has the potential to decrease average annual biomass and summer-autumn biomass more than destratification. Allowing a spring phytoplankton bloom reduces SML nutrient concentrations to limiting levels when the bloom species subsequently sediments out of the SML. This will result in very low chl-a concentrations in summer and autumn. Hypolimnetic oxygenation will prevent the subsequent remobilization of sediment nutrients thereby reducing the resupply of nutrients to the SML during autumnal deepening.

There are several oxygen delivery systems used in different reservoirs around the world. Two main approaches are used: injection of pure oxygen gas through a diffuser (e.g. 'seeper hose system' developed by the Tennessee Valley Authority); and injection of water previously supersaturated with oxygen in a special mixing chamber (e.g. Speece Cone or Vitox™ systems). The appropriate system for a specific reservoir depends particularly on the reservoir's depth. Direct injection of oxygen gas performs best in deeper reservoirs where dissolution of the oxygen into hypolimnetic waters is maximised by longer contact times as the bubbles rise through the hypolimnion. In shallower reservoirs where bubble contact time is

limited, a Speece Cone or Vitox system may be required to efficiently deliver the oxygen.

Hypolimnetic aeration in which compressed air released through a diffuser in the hypolimnion provides the oxygen source may be an attractive option, especially for shallow reservoirs (depth < 10 m). A special chamber is used to confine the effect of the bubbles to the hypolimnion so that the thermocline is not disturbed. The city of Norfolk, Virginia, uses this technique to control iron and manganese in their water supply reservoirs.

We can provide a rough estimate of the cost to oxygenate Chaffey Reservoir using a seeper hose system using the oxygen demand figures from section 8.3.7. The seeper hose system is attractive in that it has no moving parts – it is powered entirely by the expansion of liquid oxygen to gaseous oxygen – and should offer greater reliability as compared to compressor-based systems. The capital and operating cost estimates have been extrapolated from a similar calculation made for the 167,000 ML Hinze Dam (Gold Coast, QLD) and are indicative only. The median areal oxygen demand in Chaffey Reservoir from 1992-1997 was 0.55×10^{-3} kg O_2 m^{-2} d^{-1}. Assuming the top of the anoxic region is at an elevation of 506 m (i.e. the reservoir is full) gives a sediment area of 248 ha and a hypolimnetic oxygen demand of 1364 kg d^{-1}. Assuming a factor of safety of 3x gives a design oxygen supply rate of roughly 4000 kg d^{-1}. The Hinze Dam system had a design oxygen supply rate of 15,000 kg d^{-1} with estimated capital cost of $1.5m and operating costs of $3000 d^{-1}. Assuming the cost scales linearly with oxygen supply rate and that the system operates 210 days per year gives for Chaffey Reservoir a capital cost of $500,000 and an annual operating cost of $168,000. Continuous operation for 210 days of the existing compressor at Chaffey Reservoir costs approximately $145,000 for power alone. These figures suggest that hypolimnetic oxygen may be a financially attractive alternative to conventional bubble-plume destratification.

10.2.4 Sediment remediation

Sediment remediation will greatly reduce the remobilisation of nutrients from the current dam sediments. Possible remediation strategies include: dredging; injection of the sediments with $CaNO_3$ (the Riplox method); and capping with an engineered clay such as Phoslock™. However, subsequent external loads of sediments to the dam via the Peel River will replace the treated sediments as the source of nutrients and require further remediation. This option is not viable unless a significant reduction in the external sediment load can be effected.

To cap with Phoslock the 240 ha of sediments regularly exposed to anoxic conditions would cost approximately $xxx,xxx.

10.2.5 Fe^{3+} dosing

Further reductions in water column FRP, and therefore average annual algal biomass, may be achieved by increasing the supply of amorphous FeOOH given that there is insufficient Fe^{2+} to scavenge all the FRP in the water column. This effect could be achieved by adding Fe^{3+} to the water column either through injection via the bubble plume or by distribution across the surface of the dam reservoir. Note that it is necessary to maintain oxic conditions throughout the

water column, by either destratification or hypolimnetic oxygenation, in order for this strategy to be effective. Iron dosing also may have to be repeated following the arrival of large external nutrient loads.

10.2.6 Sediment dessication and oxidation as control strategies for P release

As noted earlier (Section 8.2.7) this project has shown that sediments subject to prolonged exposure to air and drying suffer a decrease in the capacity to release P on rewetting and being subjected to anoxia. The duration of this effect will depend on the time required for bacteria to recolonize the sediments upon reinundation. This finding opens up opportunities to moderate P release in reservoir systems were there is scope to lower water levels and expose sediments.

Historically, Chaffey Reservoir has been operated to maintain the reservoir in a full or nearly full condition (Figure 6.4b). Assuming that only the sediments below 506 m (i.e. depth > 12 m) are regularly exposed to anoxic conditions and thereby provide a significant source of P (section 10.2.3), dessication of 50% of the sediment area below 506 m would require drawing the reservoir level down to 501.5 m, i.e. just 7% of capacity. Given that the average annual inflow to the reservoir is 22,200 ML, the reservoir may not fill again for several years posing an unacceptable risk to supply for downstream users.

10.3 Catchment management

Catchment delivery of nutrients, in particular FRP and SO_4, is a significant contributor to the algal growth problem at Chaffey Reservoir. Identification of the sources of inorganic nutrients, particularly FRP and SO_4 is essential prior to the implementation of any large scale catchment management changes. This will require monitoring of flows and in-stream chemistry using stage-dependent samplers on the major tributaries to the Peel River upstream of Taroona.

10.3.1 Control of sulphate entry into the Dam.

Considerable quantities of sulphate enter the dam during major flood events. Earlier work by Donnelly (1994) showed that the sulphate in the sediments had an $\delta^{34}S$ consistent with the source of sulphate being derived from the principal variety of fertiliser applied in the catchment. While some more recent work (Candace Martin, unpub.) supports this proposition, our work suggests that there may be an additional non-fertiliser source. The sulphate concentration in the Dam varies between 15 and 25 mg L^{-1} depending on the season and the antecedent inflows. While this concentration is not sufficient to cause a significant increase in the rate of nutrient generation (Caraco et al, 1993), it is a major electron acceptor. In terms of oxidising capacity it is equal to, or perhaps surpasses, the dissolved oxygen content of the dam, with 2 moles of organic matter (nominally CH_2O) broken down per mole of sulphate. The significant drawdown in sulphate concentration once the dam has stratified and its return to the original concentration after the autumnal overturn (Figure 8.6) are good evidence for its active involvement in the diagenic processes.

Lessening the sulphate concentration reduces the amount of sulphide produced under anoxic conditions in the water column. This would:

- reduce the chemical oxygen demand during overturn of the hypolimnion
- decrease sulphide reduction of FeOOH and the concomitant release of adsorbed phosphate

Donnelly (pers. com.) advocates the replacement of the gypsum in the standard fertiliser with elemental sulphur which would lead to a slower release of the phosphate in the fertiliser and a reduction in the external sulphate load to the reservoir. Sulphate reduction appears to "switch off" at a concentration of about 10 mg L^{-1} which seems to be a reasonable target to aim for in the storage.

10.4 Light limitation strategies

10.4.1 Surface impellers to light-limit algal growth

Using impellers to pump surface layer water down below the thermocline may provide an alternative strategy to light-limit algal growth. In this scenario, impellers are designed to pump a known proportion of the surface layer, say 20% of the top 5 m of the water column per day, down into or below the thermocline. The idea is to decrease the residence time within the surface layer significantly, thereby producing a more dynamic light regime less suitable for buoyant cyanobacteria. At present it is not known to what depth the surface-layer water must be delivered to prevent buoyant cells rising back into the SML in time to resume normal growth.

Low velocity impellers used in combination with a draft tube can move large quantities of water at a much lower cost than either bubble plume or conventional mixer systems. However, this method is highly speculative at present and unresolved issues include hardware reliability, public access, liability and the number of impellers required. The CRC for Water Quality and Treatment is currently undertaking a trial of surface impellers at both Myponga and Happy Valley reservoirs in South Australia.

11 Appendix A – Destratification experiments

11.1 The effect of Artificial mixing on phytoplankton abundance and community composition.

Between February 1995 and April 1997 the compressor at Chaffey Dam was operated for 5 periods of between 11 and 36 days. Artificial mixing was undertaken at different times of the year, with different water column chemistry and thermal structure and with different initial phytoplankton abundance and community structure. The changes in algal community structure and biomass occurring at the times when artificial destratification was attempted are summarised in Table 4 and described below.

11.2 Trial 1. 22 Feb 95 to 29 Mar 95

Prior to the commencement of artificial destratification in late February 1995 the reservoir was strongly stratified with low concentrations of inorganic N (<0.02 mgL^{-1}) and FRP (0.004 mgL^{-1}) in the surface layer and very high concentrations of FRP (0.415 mgL^{-1}) in the anoxic hypolimnion. Chlorophyll*a* concentration ([Chla]) in the surface layer was 20 $\mu g\ L^{-1}$ and the algal community was comprised of *Anabaena circinalis, Oocystis* sp. and *Cryptomonas* sp.. Whilst there was a low concentration of FRP in the surface water, algal bioassays and *in situ* physiological assays (Wood and Oliver 1995) both indicated algal growth to be limited by the availability of N. Destratification resulted in a rapid increase in the concentration of FRP in the mixed layer and over a 35 day period of destratification [Chla] doubled and the algal community became dominated by the N-fixing blue-green alga, *Anabaena circinalis*. *Anabaena* persisted at a high abundance for 4 weeks after aeration ceased. This trial reinforces the requirement to understand what is limiting the growth of algae prior to artificial mixing, since mixing is most likely to increase algal growth in nutrient limited water bodies.

11.3 Trial 2 4 Oct 95 to 28 Oct 95

During the 2 weeks leading to the commencement of artificial mixing the diurnal mixed layer was between 2 and 4m, there was sufficient N and P to support algal growth (check this statement!) and chla concentration was increasing. The phytoplankton community was dominated by the green algae, Oocystis. During the 25 days of compressor operation the chlorophyll concentration did not significantly alter (12.7 ±6.3 $\mu g\ L^{-1}$) and Oocystis remained the dominant phytoplankton. *Oocystis* concentration doubled in the month after the compressor was turned off.

11.4 Trial 3 11-1-96 to 13 Feb 96

Prior to the commencement of artificial mixing there was a large population of the migratory dinoflagellate, *Ceratium* in the relatively shallow mixed layer prior to operation of the destratifier. Within 12 days of compressor operation there was a dramatic decline in the abundance of *Ceratium* which was reflected in surface layer [Chla] declining from 38.7 ±31.8 $\mu g\ L^{-1}$ (SD n=5) on 16-1-96 to 1.9 ±1.0 $\mu g\ L^{-1}$ (SD n=5) on the 23-1-96. The very high CV was due to the extreme horizontal heterogeneity in Ceratium abundance. The spectacular decline in [Chla] was

coincident with the onset of artificial mixing. However, the decline in *Ceratium* abundance was the direct result of intensive grazing by the rotifer, *Asplanchna priodonta*. [Chla] remained low during the remaining period of destratification but did increase during February with the growth of *Cryptomonas* and the dinoflagellate *Peridinium*. During the last week of compressor operation *Microcystis aeruginosa* and *Anabaena circinalis* appeared in the mixed layer and became the dominant algae during March and April.

11.5 Trial 4 24 Nov 96 to 24 Dec 96

Artificial destratification was attempted in late November 1996. Chla concentration in the mixed layer was 139 ±46 μg L^{-1} and the phytoplankton was almost exclusively dominated by the buoyant, colonial green algae, *Botryococcus*. There was a strong thermocline at ca. 4m with an anoxic hypolimnion. Mixed layer inorganic N (0.03 mg L^{-1}) and FRP (0.003 mg L^{-1}) concentrations were low and bioassay results indicated that phytoplankton growth was potentially limited by the availability of N. During the period of artificial mixing Chla concentration declined steadily to less than 10 μg L^{-1} after 30 days. *Botryococcus* disappeared during the period of artificial mixing and was replaced by low numbers of *Ceratium* and *Oocystis*.

11.6 Trial 5 13 Apr 97 to 23 Apr 97

Artificial destratification was attempted in mid April as the epilimnion was deepening. Algal bioassay results indicated that prior to the commencement of artificial mixing there was sufficient nutrient (inorganic N 0.16 mg L^{-1} ; FRP 0.03 mg L^{-1}) in the mixed layer to support phytoplankton growth. A bloom of *Anabaena* which peaked between 1-8/4/97 at ca. 69000 cells mL^{-1} had declined by the commencement of destratification to ca. 3500 cell mL^{-1} and continued to decline during artificial mixing. Chl remained low but the *Anabaena* was replaced by crytomonads and *Peridinium*, which continued to increase after artificial mixing ceased.

11.7 Conclusions of short term mixing

The operation of the artificial mixing system at Chaffey Dam did not result in a systematic change in either phytoplankton abundance or composition. With the current compressor installed in Chaffey Dam the most likely short term outcome of its operation is to not affect phytoplankton abundance or community composition. However, if there is a nutrient limited phytoplankton population in the mixed layer and sufficient nutrient is transported from the hypolimnion to the mixed layer it is likely that this will result in an increase in algal growth. The increase in *Anabaena* and *Microcystis* abundance observed during the first trial is an example of this.

12 Appendix B - Zooplankton observations by year

12.1 12 Sep 95 – 26 Dec 95 (n=17 dates x 3 sites)

Rotifera were rare in the sampling period. Nine taxa of Rotifera were recorded. With the exception of the omnivorous *Asplanchna priodonta*, all were at low densities - one or a few individuals per litre, and of negligible significance in terms of numbers or biomass. *A. priodonta* pulsed briefly for two weeks coincident with it's preferred food item, the dinoflagellate *Ceratium*. A similarly small pulse of a bacteriovore, *Filinia longiseta*, occurred over two weeks in Oct.-Nov., however at a maximum density of ca. 22 ind. l^{-1} this represents negligible biomass. *Filinia* is <200 µm body size.

Nine taxa of planktonic cladocerans were recorded, only one of which, *Ceriodaphnia* cf. *dubia* was persistent in appreciable numbers at all three sites. *Daphnia lumholtzi* and *Diaphanosoma unguiculatum* probably were present throughout the sampling period, but were in such low numbers or patchily distributed that they were not collected on every sampling occasion, or at every site. When they were collected they were in low numbers, generally only one or a few individuals per litre. All three taxa are small, <1 mm. Larger herbivorous cladocerans, e.g. *Daphnia* were notably absent during this period.

Copepoda were numerically dominant during the 1995 sampling period, primarily as nauplii and copepodites of the small centropagid *Calamoecia lucasi*, or of the cyclopoid *Thermocyclops* sp. Notably, occasional pulses of egg hatching and nauplius production were not reflected by population increases in *Calamoecia/Thermocyclops* late instar copepodites or adults in succeeding weeks - the juveniles did not survive to maturity.

During the 1995 sampling period, mean zooplankton densities at the three sites were low: Site 1: 112 ind l^{-1}; site 2: 126 ind. l^{-1}, site 4: 178 ind. l^{-1}.

12.2 02 Jan 96 – 30 Dec 96 (n=52 dates x 3 sites)

Low diversity of Rotifera throughout 1996 was a feature of all three sites. Of 14 rotifer taxa identified, only one, *Asplanchna priodonta*, reached high densities (>4000 ind. l^{-1}) again coincident, or with a slight lag following, the dinoflagellate *Ceratium*. Gut content analysis of *A. priodonta* during the Jan.-Feb. pulse demonstrated that it was grazing primarily or exclusively on *Ceratium*. *Hexarthra mira*, a bacteriovore / detritivore, probably was persistent throughout summer-autumn, but was collected only intermittently, as one or a few individuals per litre, and rarely was concurrent at all three sites. Rotifers were notably absent from all three sites June-Dec.

Eleven taxa of cladocerans were recorded over the 12 mo. sampling period, none of them perennially. *C.* cf. *dubia* was again the most abundant cladoceran plankter, with late-summer / spring maxima. It was not recorded at all May-Nov. *Daphnia carinata* s.l. and *Diaphanosoma unguiculatum* probably overwintered in small numbers - individuals appeared sporadically in samples May-Sept. *D. carinata* s.l., the largest herbivore present, reached appreciable numbers for only

three weeks in Feb. (max. <20 l^{-1}). Also sporadic in low numbers were *Bosmina meridionalis* (Jan.-Apr.), *Ceriodaphnia cornuta* (Mar.-Apr.). *Chydorus* sp., a detritivore/bacteriovore, appeared Oct-Dec., was the second most abundant cladoceran during this period.

Of the four taxa of Copepoda recorded over the 12 mo. period, both *Calamoecia lucasi* and *Thermocyclops* sp. probably were perennial, again primarily as juveniles. They were present on most sampling dates, although not at all sites, and in low numbers May-Dec. With the exception of the pulse of *Asplanchna priodonta* in Jan., juvenile copepods were numerically abundant Jan-May. They persisted in low numbers over winter, but did not recover dominance in the Sept.-Dec. period, when the group of cladocerans *Ceriodaphnia/Daphnia/Chydorus* were numerically dominant. Again, the low numbers of adults of both *Calamoecia* and *Thermocyclops*, generally occurring as only a few individuals per litre, suggest that mortality of juvenile stages was high. Notable also was the infrequent occurrence of the larger centropagid calanoid grazers, *Boeckella fluvialis* and *B. triarticulata.* One or the other species was recorded intermittently as one or two individuals during Feb.-Dec., suggesting that *Boeckella* could well have been perennial over the study period, but in such low numbers or patchy distribution that it was not sampled.

During the 1996 sampling period, mean zooplankton densities at the three sites also were low, given that high population densities of *A. priodonta* were reached and dissipated in a short time frame: Site 1: 60 ind l^{-1}; site 2: 140 ind. l^{-1}, site 4: 75 ind. l^{-1}.

12.3 Jan 97 – 09 Dec 97 (n=49 dates x 3 sites)

Of nineteen taxa of Rotifera recorded during the 1997 sampling period, only *A. priodonta* again contributed significant numbers to the zooplankton, albeit at much lower densities than in the previous summer (max. <150 l^{-1}). *A. priodonta* persisted in small numbers through until April, again coinciding with population peaks in *Ceratium*. It did not appear in the zooplankton again until late Dec. *Hexarthra mira* again appeared in autumn, persisting in low numbers through Apr.-May. It probably was perennial, given the occasional individuals collected later in the year, but in very low numbers. *Keratella procurva* also appeared intermittently, with continuous presence at all sites for two weeks mid-May with a peak of ca. 40 l^{-1} at site 4. There was also a two-week pulse of *Pompholyx complanata* mid winter, ca. 57 ind. l^{-1}.

The bimodal summer-spring appearance of cladocerans was less pronounced in 1997 than in the previous year, and compositional differences were evident. *Ceriodaphnia* cf. *dubia* and *Daphnia carinata* s.l. probably both were perennial, but in low numbers and patchy distribution throughout the year. *Daphnia lumholtzi* was the most abundant cladoceran over the summer months, reaching 25 ind. l^{-1} in Jan. *Bosmina meridionalis* occurred in small numbers Jan.-Feb. Other cladocerans were rare, isolated occurrences.

Copepoda again predominated, primarily as copepodites and nauplii. *Calamoecia lucasi* and *Thermocyclops* sp. juveniles were the numerically dominant zooplankters in the reservoir, however adult *Calamoecia* were present only in

very low numbers (<5 l-1) and adult *Thermocyclops* largely present as occasional individuals. *Boeckella* spp. were recorded only as isolated individuals.

During the 1997 sampling period, mean zooplankton densities at the three sites were again low: Site 1: 24 ind l^{-1}; site 2: 29 ind. l^{-1}, site 4: 26 ind. l^{-1}.

13 References

Alperin, M.J., Blair, N.E., Albert, D.B., and Hoeler, T.M. 1993. The carbon isotope geochemistry of methane production in anoxic sediments: 2 a laboratory experiment. In: Biogeochemistry of global changer (Ed. R.G. Oremland) pp594 - 605. Chapman and hall. New York.

Asaeda, T. and Imberger, J. 1993. Structure of bubble plumes in linearly stratified environments. J. Fluid Mech. **249**:35-57.

Baldwin, D. S. 1996a. The phosphorus composition of a diverse series of Australian sediments. Hydrobiol. **335:**63-73.

Baldwin, D. S. 1996b. The effects of exposure to air and subsequent drying on the phosphate sorption characteristics of sediments from a eutrophic reservoir. Limnol. Oceanogr. **41:** 1725-1732.

Baldwin, D. S., Ford, P. and Nielsen, D. L., 1998. Resolution of the Spatial Variability in Sediment Composition Within and Between Water-Storage Reservoirs Using Non-parametric Statistical Techniques, Water Res, **32**:826-830.

Banens, R.J. 1987. The geochemical character of upland waters of northeast New South Wales. Limnol. Oceanogr. **32**:1291-1306.

Beecham, R. 1995. Significance of fertiliser phosphorus in the water quality of Chaffey Dam. Master of Engineering thesis, University of New South Wales.

Berner, R. A. 1984. Geochimica Cosmochimica Acta. **48**:605-615.

Berounsky, V.M. and Nixon, S.W. 1990. Temperature and seasonal cycle of nitrification in coastal marine waters. Limnol. Oceanog. **35**:1610-1617.

Blomqvist P., Petterson A., and Hyenstrand, P. 1994. Ammonium-nitrogen: A key regulatory factor causing dominance of non-nitrogen-fixing cyanobacteria in aquatic systems. Archiv fur Hydrobiologie. **132**:141-164.

Brookes, J.D., Ganf, G.G., Green, D. and Whittington,J. 1999. The influence of light and nutrients on buoyancy, filament aggregation and flotation of *Anabaena circinalis*. J. Plankton Res. **21**:327-341.

Caitcheon, G.G., Donnelly, T.H. and Murray, A.S. 1994. Sources of phosphorus and sediment in the catchment of Chaffey Reservoir, New South Wales. Technical Memorandum 94/16, October 1994, CSIRO Div. Water Resources, Canberra.

Caraco, N.F., Cole, J.J. and Likens, G.E. 1989. Evidence for sulfate-controlled phosphorus release from sediments of aquatic systems. Nature. **341:** 316-318.

Caraco, N.F., Cole, J.J. and Likens, G.E. 1993. Sulfate control of phosphorus availability in lakes. Hydrobiologia. **253:** 275-280

Davelaar, D. 1993. Ecological significance of bacterial polyphosphate metabolism in sediments. Hydrobiologia. **253:** 179-192

Donnelly, T.H. 1993. The major sources of phosphate in the Chaffey catchment, NSW. CSIRO Div. Water Resources Consultancy Report No. 92/20, March 1993, 37 pp.

Entwisle T.J., Sonneman, J.A. and Lewis, S.H. 1997. Freshwater Algae in Australia. Sainty and Associates, Australia.

Finnigan, T.D. and Ivey, G.N 1999. Sub-maximal exchange between a convectively forced basin and a large reservoir J. Fluid Mech. **378:** 357-378.

Ganf, G.G. 1981. Effects of destratification on phytoplankton. In, Destratificatiion of lakes and reservoirs to improve water quality. Eds Burns, F.L. and Powling, I.J. pp283-287.

Ganf, G.G. and Oliver, R.L. 1982. Vertical separation of light and available nutrients as a factor causing replacement of green algae by blue-green algae in the plankton of a stratified lake. J. Ecol. **70**:829-822.

Gächter, R and Meyer, J. S. 1993. The role of micro-organisms in mobilisation and fixation of phosphorus in sediments. Hydrobiologia. **253:** 103-121.

Gächter, R., Meyer, J. and Mares, A. 1988. Contribution of bacteria to the release and fixation of phosphorus in lake sediments. Limnol. Oceanogr. **33:** 1542-1558.

Geddes, M.C. 1984. Seasonal studies on the zooplankton of Lake Alexandrina, River Murray, South Australia, and the role fo turbidity in determining zooplankton community structure. *Aust. J. Mar. Freshwat. Res.* **35**, 417-426.

Harris, G.P., Heaney, S.I. and Talling, J.F. 1979. Physiological and environmental constraints in the ecology of the planktonic dinoflagellate *Ceratium hirundinella*. Freshwater Biology. **9**:413-428.

Harris, G.P. and Baxter, G. 1996. Interannual variability in phytoplankton biomass and species composition in North Pine Dam, Brisbane. Freshwater Biology. **35**: 545-560.

House, W.A., Denison, F.H. and Armitage, P.D. 1995. Comparison of the uptake of inorganic phosphorus to a suspended and stream-bed sediment. Water Res. **29:** 767-779.

Humphries, S.E. and Imberger, J. 1982. The influence of the internal structure and dynamics of Burrinjuck Reservoir on phytoplankton blooms. Univ. W. Aust., Environ. Dynam. Rep. ED-82-023.

Humphries, S.E. and Lyne, V.D. 1988. Cyanophyte blooms: the role of cell buoyancy. Limnol. Oceanogr. **33**:79-81.

Imberger, J. 1998. Flux Paths in a Stratified Lake: A Review. In J. Imberger [ed.], Physical Processes in Lakes and Oceans, American Geophysical Union. (Coastal and Estuarine Studies), p. 1–18.

ISO 1991. ISO / DIS 10260 – Water quality – measurement of biochemical parameters – spectrometric determination of the chlorophyll-a concentration. International Organization for Standardization, Geneva.

Jaworski, N.A., Lear Jr, D.A. and Villa Jr, O. 1972. Nutrient management in the Potomac estuary. Am. Soc. Limnol. Oceanog. Spec. Symp. **1**:246-273.

Jones, R.I. 1991. Advantages of diurnal vertical migrations to phytoplankton in sharply stratified, humic forest lakes. Arch. Hydrobiol. **120**:257-266.

Jones, G. 1997. Limnological study of cyanobacterial growth in three South-East Queensland reservoirs. In: Managing Algal Blooms, Ed. Davis, J.R., CSIRO Land & Water, Canberra, pp 51-66.

Kobayashi, T. 1992a. A study of physicochemical conditions, phytoplankton and microcrustacean zooplankton in Wallerwang Reservior, New South Wales. *Proc. Linn. Soc. N.S.W.* **113**, 27-41.

Kobayashi, T. 1992b. Plankton of Lyell Reservoir, New South Wales. Proc. Linn. Soc. N.S.W. **113**, 245-261.

Kolber, Z., Zehr, J. and Falkowski, P.G. 1988. Effects of growth irradiance and nitrogen limitation on photosynthetic energy conversion in photosystem II. Plant Physiology **88**: 923-929.

Kolber, Z. and Falkowski, P.G. 1993. Use of active fluorescence to estimate phytoplankton photosynthesis *in situ*. Limnol. Oceanogr. **38**: 1646-1665.

Kristjansson, J.K., Schonheit, P. and Schonheit, P. 1982. Different Ks values for hydrogen of methanogenic bacteria and sulfate reducing bacteria : an explanation for the apparent inhibition of methanogenesis by sulfate. Arch. Microbiol. **131**:278 -282.

Lemckert, C.J. and Imberger, J. 1993. Axisymmetric intrusive gravity currents in linearly stratified fluids. J. Hydraul. Eng. ASCE **119**:662-679.

Lemckert, C.J. and Imberger, J. 1993. Energetic bubble plumes in arbitrary stratification. J. Hydraul. Eng. ASCE **119**:680-703.

Lemckert, C.J., Schladow, G.S. and Imberger, J. 1993 Destratification. Some rational design rules. Report #ED-711-CL, Centre for Water Research, University of Western Australia. 8 pp.

Martin, V., Bowling, L. and Robinson, G. 1995. Chaffey Catchment Nutrient Study. New South Wales Dept. Land and Water Conservation Water Quality Service Unit Report No. TS 95.173, November 1995. 66 pp.

May, V. and Powell, J.M. 1986. Algae of the Peel River and the newly constructed Chaffey Dam, New South Wales, Australia. Cunninghamia **4**:503-536.

McAuliffe, T.F. and Rosich, R.S. 1989. Review of Artificial Destratification Of Water Storages in Australia. Research Report No. 9, December 1989, Urban Water Research Association of Australia, Melbourne.

McDougall, T.J. 1978. Bubble plumes in stratified environments. J. Fluid Mech. **85**:655-672.

Middelburg, J.J., Klaver, G., Nieuwenhuize J., Wielmaker, A., de Haas, W., Vlug, T. and van der Nat, J.F.W.A. 1996. Organic matter mineralization in intertidal sediments along an estuarine gradient. Mar. Ecol. Prog. Ser. **132**: 157 -168.

Mitchell, A. and Baldwin, D.S. 1998. The effects of desiccation/oxidation on the potential for bacterially mediated P release from sediments. Limnol. Oceanogr. **43**:481-487.

Mitchell, I. 1993. Chaffey Dam Siltation Report. New South Wales Dept. Land and Water Conservation, Dam Safety Unit, Technical Services Division Report No. TS 93.054. 26 pp.

Monismith, S.G., Imberger, J. and Morison, M.L. 1990. Convective motions in the sidearm of a small reservoir. Limnol. Oceanogr. **35**:1676-1702.

Muschal, M. 1995. A study of the biota of Chaffey storage. 1994. Report TS 95.116, Environmental Studies Unit, NSW Dept. of Land and Water Conservation. 38 pp.

Nowicki, B.L. 1994. The effect of temperature, oxygen, salinity, and nutrient enrichment on estuarine denitrification rates measured with a modified nitrogen gas flux technique. Estuarine, Coastal, and Shelf Science **38**: 137-156.

Oliver, R.L. 1981. Factors controlling phytoplankton seasonal succession in Mt. Bold Reservoir, South Australia. PhD thesis, University of Adelaide.

Oliver, R.L. 1994. Floating and sinking in gas-vacuolate cyanobacteria. J. Phycol. **30**:161-173.

Oliver, R.L. and Ganf, G.G. (in press). "Freshwater blooms". In Whitton, B.A. and Potts, M. (eds.), Ecology of cyanobacteria: Their diversity intime and space. Kluwer Academic Publishers.

Oliver, R.L. and Whittington, J. 1998. Using measurements of variable chlorophyll-a fluorescence to investigate the influence of water movement on the photochemistry of phytoplankton. In: Physical Processes in Lakes and Oceans, ed. Imberger, J., Coastal and Estuarine Series, AGU Monograph, 668 pp.

Prescott, G.W. 1982. Algae of the Western Great Lakes Area. Otto Koeltz Science Publishers. Koenigstein, Germany.

Reynolds, C.S. 1984. The ecology of freshwater phytoplankton. Cambridge University Press, Cambridge.

Reynolds, C.S. 1989. Physical determinants of phytoplankton succession. In Phytoplankton Ecology. Succession in Plankton Communities. Ed. U Sommer. Springer-Verlag, Berlin.

Reynolds, C.S. 1997. Vegetation Processes in the Pelagic: A model for Ecosystem Theory. Ecology Institute, Oldendorf, Germany.

Roden, E.E. and Edmonds, J.W. 1997. Phosphate mobilization in iron-rich anaerobic sediments: microbial Fe(III) oxide reduction versus iron-sulfide formation. Archiv. Hydrobiol. **139:** 347-378.

Ruttenberg, K. 1992. Development of a sequential extraction method for different P forms in marine sediments. Limnol. Oceanogr. **37**:1460-1482.

Schladow, S.G. 1992. Bubble plume dynamics in a stratified medium and the implications for water quality amelioration in lakes. Water Resour. Res. **28**:313-321.

Schladow, S.G. 1993. Lake destratification by bubble-plume systems: design methodology. J. Hydraul. Eng. ASCE. **119**:350-368.

Schladow, S.G. and Fisher, I.H. 1995. The physical response of temperature lakes to artificial destratification. Limnol. Oceanogr. **40**:359-373.

Schonheit, P., Kristjansson, J.K. and Schonheit, P. 1982. Kinetic mechanism for the ability of sulfate reducers to out-compete methanogens for acetate. Arch. Microbiol. **1432**: 285 - 288.

Sherman, B.S., Whittington, J. and Oliver, R.L. 1999. The impact of artificial destratification on water quality in Chaffey Reservoir. *Arch. Hydrobiol*. (accepted).

Sherman, B.S., I.T. Webster, G.J. Jones and Oliver, R.L. 1998. Transitions between *Aulacoseira* and *Anabaena* dominance in a turbid river weir pool. Limnol. Oceanog*r*. **43**:1902-1915.

Shiel, R.J. 1981. Plankton of the Murray-Darling river system, with particular reference to the zooplankton. Ph.D. Thesis, University of Adelaide. 287 pp.

Shiel, R.J., C.J. Merrick and Ganf, G.G. 1987. The Rotifera of impoundments in southeastern Australia. Hydrobiologia **147**, 23-29.

Stumm, W. and Morgan, J.J. 1981. Aquatic Chemistry: an introduction emphasizing chemical equilibria in natural waters.p 468. Wiley, New York.

Sturman,J.J., Ivey.G.N. and Taylor J.R. 1996. Convection in a long box driven by heating and cooling on the horizontal boundaries J. Fluid Mech. **310**:61-87.

Sturman.J.J, Oldham.C.E. and Ivey,.G.N. 1999. Steady convective exchange flows down slopes. Aquatic Sciences **61**:1-19.van Berkel, J. and Beckett, R. 1997. Estimating the effect of particle surface coatings on the adsorption of orthophosphate using sedimentation field-flow fractionation. J. Liq. Chrom. & Rel. Technol. **20**:2647-2667.

Vincent, W.F. and Downes, M.T. 1998. Nitrate accumulation in aerobic hypolimnia: relative importance of benthic and planktonic nitrifiers in an oligotrophic lake. App. Envir. Microbiol. **42**, 565 - 573.

Walker, K.F. and Hillman, T.J. 1977. *Limnological survey of the River Murray in relation to Albury Wodonga*. A. W. D. C. Albury 256 pp.

Webster, I.T., Jones, G.J., Oliver, R.J, Bormans, M., and Sherman, B.S. 1996. Control strategies for cyanobacterial blooms in weir pools. Final report to the

National Resource Management Strategy Grant No. M3116. Centre for Environmental Mechanics Technical Report No. 119, 75 pp.

Wells, M.G., Griffiths, R.W. and Turner, J.S. 1999. Competition between distributed and localized buoyancy fluxes in a confined region J. Fluid Mech. **391**:319-336.

Whiticar, M.J., Faber, E., and Schoell, M. 1986. Biogenic methane formation in marine and freshwater environments: CO_2 reduction vs acetate fermentation - isotopic evidence. Geochim. Cosmochim. Acta, **50**: 693 - 709.

Whittington, J., Sherman, B.S., Green, D., and Oliver, R.L. submitted. Is vertical migration in Ceratium a strategy to optimise photosynthetic production or to avoid photoinhibition? (submitted to J. Plankton Res.)

Wood, M.D. and Oliver, R.L. 1995. Fluorescence transients in response to nutrient enrichment of nitrogen- and phosphorus- limited *Microcystis aeruginosa* cultures and natural phytoplankton populations: A measure of nutrient limitation. Australian J. Plant Physiol. **22**:331-340.

Wüest A., and Gloor, M. 1998. Bottom Boundary Mixing: The Role of Near-Sediment Density Stratification. In J. Imberger [ed.], Physical Processes in Lakes and Oceans, American Geophysical Union. (Coastal and Estuarine Studies), p. 485–502.

Young, C.G. 1993. Issues in the formulation of a water quality management plan for Chaffey Reservoir and its catchment. B.N.R. thesis, University of New England, Armidale, NSW. 102 pp.

Zic, K., Stefan, H.G. and Ellis, C. 1992. Laboratory study of water destratification by a bubble plume. J. Hydraul. Res. **30**:7-26.